UNIVERSITY OF CALIFORNIA, SAN DIEGO

Mesozooplankton trophic variability in a changing ocean

A dissertation submitted in partial satisfaction of the

requirements for the degree Doctor of Philosophy

in

Oceanography

by

Moira Décima

Committee in Charge:

Professor Michael R. Landry, Chair
Professor Lihini I. Aluwihare
Professor Ron S. Burton
Professor Don MacLeod
Professor Mark D. Ohman

2011

The Dissertation of Moira Décima is approved, and is acceptable in quality and form for publication on microfilm and electronically:

_____

_____

_____

_____

_____

Chair

University of California, San Diego

2011

DEDICATION

I dedicate this dissertation to my mother for her constant, unconditional love and support. I also dedicate it to the memory of my father, who would have been happy to see me follow in his steps as a fellow scientist.

TABLE OF CONTENTS

LIST OF ABBREVIATIONS

AA – Amino Acid

C - Carbon

CalCOFI – California Cooperative Oceanic Fisheries Investigations

CCE – California Current Ecosystem

Chl *a* – Chlorophyll *a*

CSIA – Compound-Specific Isotope Analysis

CV – copepodid V

$\delta^{15}N$ (‰) – Isotope delta notation: $[(^{15}N/^{14}N)_{sample} - (^{15}N/^{14}N)_{std}] * (^{15}N/^{14}N)_{std}{}^{-1} * 1000$

DW – Dry weight (mesozooplankton)

EEP – eastern equatorial Pacific

ENSO – El Niño Southern Oscillation

GGE – gross gross efficiency

HNLC – High Nutrient Low Chlorophyll

LME – Linear mixed-effect

LTER – Long Term Ecological Research

N – Nitrogen

PDO – Pacific Decadal Oscillation

PP – Primary Production

Phaeo – Phaeopigments

TEF – Trophic enrichment factor

TIW – Tropical Instability Wave

TP – Trophic position

US JGOFS - US Joint Global Ocean Flux Study

LIST OF FIGURES

Chapter 1

Chapter 2

Chapter 3

Chapter 4

LIST OF TABLES

Chapter 1

Chapter 2

Chapter 3

Chapter 4

ACKNOWLEDGEMENTS

I came to Scripps at a very bizarre and hard time in my life. The recent death of my father had set me on a new path towards myself, one that I continue to travel. I began graduate school with the added difficulty of this search, and I am positive that had I not encountered the few amazing people that I did, it would have never been possible for me to finish this dissertation.

The first person I am indebted to is my amazing adviser Mike Landry. It goes without saying that the most important person in shaping the scientific abilities of a young graduate student is her adviser, and to have an amazing scientist such as Mike as been a true honor and privilege. I am repeatedly amazed at the breadth of his knowledge and the preciseness of his mind. The new angles he can bring to any problem, the flexibility from which to view an ecological problem, the far reaching implications of results, the 'big picture' as he so often reminds me, are qualities of a scientific genius I have only encountered a handful of times. His patience to continuously bring this awareness back to my scientific perspective, back from when I was nothing but a dumb graduate student until now (when I am at least less dumb), has been invaluable to my formation. He has influenced my interests, my views of oceanography, trophic dynamics and general ecology. His guidance and teaching have been instrumental in my formation as a sea-going oceanographer. But beyond scientific training, the personal attention and care that Mike gives is what makes the difference between a good and a great adviser. I know he has not always particularly understood the reasons why I had to do certain things, but he has always, regardless, respected, cared and observed them. I am certain

that any other thesis adviser would not have seen me through. It is not an exaggeration to say he has truly changed my life.

I am also very grateful to Mark Ohman, my other important source of scientific instruction throughout my graduate years. His passion for science is both admirable and contagious, as is his love for mesozooplankton. Mark has pushed me to understand and practice rigorous scientific thinking, a task I found challenging within the discipline of Ecology. He has been an invaluable teacher in scientific concepts, at-sea work, zooplankton ecology, and the game 'name that plankton'. I hold with great pride the moment I was able to identify the zooplankter that stumped him (well, a piece of one: it was the swimming bell of a siphonophore).

The rest of my committee has been invaluable through their support and feedback, throughout these years. Lihini Aluwihare, in particular, has assisted with isotope chemistry, offering as much feedback, advice and support as she ever could. My two other committee members, Ron Burton and Don Macleod, have patiently endured and offered whatever feedback was possible, during meetings concerning material that clearly was out of their field of expertise. Finally, I wish to acknowledge Brian Popp, from the University of Hawaii, in whose lab I was able to run samples for the CSIA-AA method which constitute my final chapter.

I also wish to acknowledge my lab, which despite our sometimes inner chaos has been amazing during all our sea-going projects. Mike Landry, Stukel, Ally and Darcy: Stukel put it right when he said: 'we have all bled together at sea'. Those were times of hard work, extreme exhaustion, never ending at-sea tasks, and still … those were some of the best experiences of my life. Andres, last member to join the lab and work with me,

your humor, lightness, good nature made it possible to happily pull those endless 12 hour lab days. I also wish to thank the remaining people from my lab: Dan, John, Andrew, Emy, Kate and Mary.

I need to especially acknowledge the CCE LTER research program, which has funded and given me the opportunity to carry out my research within the California Current. I cannot possibly give enough thanks to all the technicians and graduate students that have participated in this program: Ralf Goericke, Shonna Dovel, Megan Roadman, Ryan Rykaczewski, Jesse Powell, Travis Meader, Andrew King, Brian Hopkinson…I cannot list all the invaluable people that have accompanied us out at sea, but I am highly grateful to them all. I also must acknowledge the Scripps Pelagic Invertebrates collection and the help of both Annie Townsend and Linsey Sala.

My funding has been provided by the Alliance for Graduate Education and the Professoriate (AGEP), a fellowship through SIO (the Stout Fellowship), the GK-12 Program by the National Science Foundation (NSF) and two NSF grants: Hawaii Ocean Time-series (HOT) and Comparative Analysis of Marine Research Organization (CAMEO). My research has been funded by the CCE LTER Program and the Equatorial Biocomplexity grant.

Of course, nothing that I have every achieved was without the moral support of the few close to me, my family and friends. My family has always been the pillar of security in my life - the ones I know will always be there. My mother, her kind words and accepting support … I could achieve nothing without her always being there for me, (even when I resent advice and disappear for weeks) her unconditional love,

perseverance, connection and openness sustain me in this harsh world, and I owe her my determination and resilience in life.

My sister Lujan. We left our family together, our home, our culture and our friends, to find whatever it was that we were each looking for. We did this together, and I could not have done it alone. And it was once we left our home that I really got to know her. We learned to rely on each other. I found out that regardless of what the world thought of my actions, if I could count on her and she on me, all was good. She has seen me struggle on and off throughout these seven years of graduate school, and she has been there every step of the way. She has come to see me, listened to me, offered whatever I might need. She has been my source of close, true, constant support. My brothers: Juan and Agustin. With Juan I have shared the struggles of being vocationally pulled in different directions, and the challenge of having to make true change in life. We succeeded together. And last but not least, the youngest, Agustin, with whom I share the love for research existential debates. We have shared late night conversations where I was surprised to be trumped by this, albeit young, philosopher in training. The physical distance has made the presence of all my siblings, especially my brothers, sporadic, but by no means unimportant. My yearly trips home would not have been as truly energizing as they were without the one or two nights when the four of us would stay up, drink wine and share our most recent thoughts and feelings on life. Thousands of miles separating our daily struggles, but retouching back to our roots on those yearly occasions wiped out the potential permanent effect of distance. And they have helped keep me the person that I am and was. Finally my aunt Dorsie, I have loved our periodic bar-b-q's in LA, conversations of life and shared love for careers, family and friends.

Finally, while he is no longer with me, I owe a debt of gratitude to my father. He could not support me through this endeavor because he left before I began. But I know he would be truly ecstatic to see me here today. He wanted me to be a scientist, he saw himself in me in many ways (not just in research), and I know he would be sincerely proud to see me finish this process.

Life has also blessed me with the most amazing friends. It was in graduate school that I found a small group of four, constituting a rock-solid support group for two of the most challenging years of my life. Mike, Jenny and Brendan, I will forever cherish the together, the lunches in our office, the times out, the shared summer's nights of pong. Life was especially hard for me at those times, and your continued understanding, support, time and affection made all the difference. Mike… there are so many places to acknowledge my other half in graduate school. As part of my lab, as my sea-going buddy, as part of the core group the supported me in my first years, as my best friend who was with me through the entirety of these years. My twin, husband, and best friend. I am at a loss to find the right words to thank the person who has walked the closest and farthest along this trail, by my side. The good times, the drunken shenanigans, the conferences and trips, the sleepless nights of cruise preparation and cruise work, and every hoop we had to jump though during grad school. I could not have done this without him, and I am forever grateful we happened to coincide in time in space. Brendan and Jenny, the other two that made my first years so special, remain in my life until today. Brendan, how can two friends have so much in common and never be able to adequately express it to each other? We might of finally found communication during our last months, when the others had left. Jenny, my friend in crime and in plots to abandon

grad school, we never did construe that pyramid scheme. I will always cherish our chats of science and its shortcomings, and the other venues of happiness in life. However, we seem to have found our place within it.

A myriad of other friends have accompanied me during different portions of my journey, and I apologize I cannot give everyone their truly deserved space. Michelle, I met you upon arrival in San Diego. You showed me this new city, new people and new ways of life. It was through you that I was able to value the non-intellectual aspects of life, and that is an ability I now truly cherish, and I hold tight to my heart when I get carried away in this career choice of mine. Adam, my inverse or my negative (or positive if I am the photographic negative). Another scientist and lover of science, tempted by the arts, searching for ways to accommodate both modalities that are supposedly at odds with each other. You have been a companion of my soul, and I can't ask for more than that from a friend. Nadia, amiga del alma, ni puedo agradecerte en Ingles porque no es apropiado. Las noches que compartimos el primer año, donde recordamos lo que queríamos de la vida: ciencia y trabajo, amigos y momentos profundos compartidos, y mucho de los dos. Me ha alegrado enormemente que hayas vuelto a mi vida, y que seas hoy con quien puedo contar por estos pagos para descargarme, enojarme, y también sentirme contenida. Amigas como vos no he tenido desde la secundaria, y te llevo en el corazón. Rosa and Kait, my band members, you have given me so much happiness in the last months prior to my dissertation writing. My life was reduced to the basic necessities, and within that was our once or twice a week of music playing – bringing me happiness and warming my soul. Even if the phDivas only have one performance in their history, they live forever in my heart. CJ, I met you late in my graduate career, but your support

with sample processing, laboratory issues, isotope advice and moral support has been invaluable. My friends in the art world have been instrumental in balancing my scientific life with my creative impulses, and I have to thank Juliana Snapper, who brought me new life perspective through her views, classes and Tuesday night conversations. Thanks are due to my other friends who have shared my time here: Patricia Montoya, Hannah Price, Christina Lambert, Danny Shapira, Ami Jones, Kim Tucker, Julie Lee, and so many others.

Mis amigas de Argentina, tengo que mencionar a mi amiga del alma Wanda. Necesito agradecerte tu comprensión siempre, conexión de esencia, y ayuda emocional con mis características locuras de toda la vida. Laura, me has acompañado en cada viaje a Tucumán, cuando he necesitado cargar pilas y reconectarme con los míos. Sole, noches de birra y tardes de pileta, te quiero con el alma. Nidia y Cris, el futbol nos juntó y luego de 10 años, sin futbol y con nuevas vidas y familias, seguimos siendo parte de nuestras vidas. A todas mis otras amigas, las que una vez fueron las 30, y quien sabe cuántas somos ahora, las adoro. En las noches cálidas de Tucumán, donde nos juntamos y compartimos historias de vida, vuelvo a mí y a quien una vez fui.

I thank all those that made this accomplishment possible. Finally, I must thank the ocean for being big, beautiful and blue. I pray that she always remains that way.

Chapter 1, in full, has been published in Deep-Sea Research II: Topical Studies in Oceanography: Décima, M, Landry, M. R., Rykaczewski, R. R., 2011. " Broad scale patterns in mesozooplankton biomass and grazing in the eastern equatorial Pacific". Deep-Sea Res II **58**: 387-399. The dissertation author was the primary investigator and author of this paper.

Chapter 2, in full, has been published in Limnology and Oceanography: Décima, M, Ohman, M. D., DeRobertis, A. "Body size dependence of euphausiid spatial patchiness". Limnol. Oceanogr. **55**: 777-788. The dissertation author was the primary investigator and author of this paper.

Chapter 3, in full, is currently in preparation for submission: Décima, M.R., Landry, M. R., Ohman, M.D., "Zooplankton Trophic Variability in the California Current Ecosystem". The dissertation author was the primary investigator and author on this paper.

Chapter 4, in full, is currently in preparation for submission: Décima, M.R., Landry, M. R., Popp, B. N., "The 1998/1999 El Niño Southern Oscillation event and the isotopic content of amino acids in California Current zooplankton: effects on baseline ^{15}N and trophic structure". The dissertation author was the primary investigator and author on this paper.

VITA AND PUBLICATIONS

EDUCATION

2011 Doctor of Philosophy, University of California, San Diego

2003 Bachelor of Science, University of California at Santa Cruz

Bachelor of Arts, University of California at Santa Cruz

CRUISE EXPERIENCE

CRD – 2010 – Mesozooplankton biomass and grazing estimates, experimental grazing incubations

CCE – P0810 - Mesozooplankton biomass and grazing estimates, experimental grazing incubations

CCE – P0704 - Mesozooplankton biomass and grazing estimates, experimental grazing incubations

CCE – P00605 - Mesozooplankton biomass and grazing estimates, experimental egg production incubations

EB05 - Mesozooplankton biomass and grazing estimates

CalCOFI 0404 – Chlorophyll and nutrient analysis

NMFS Rockfish cruise – Euphausiid abundance estimation

CIMT monthly cruises (2003-2004) – Mesozooplankton biomass estimates

CONFERENCES

2010 Ocean Sciences Talk Trophic Structure Variability in the California Current: Independent Methods to Assess Trophic Relationships in Dominant Zooplankton".

2009 Society for the Advancement of Chicanos and Native Americans in Science (SACNAS). Talk Use of amino acid nitrogen stable isotopes to determine trophic positions in the California Current, during and after a major ENSO event

2009 LTER ASM Poster Trophic relationships in two plankton species during and after a major ENSO event, in the California Current

2009 LTER ASM Workshop Comparisons of top-down controls on autotrophic biomass in aquatic and terrestrial ecosystems

2009 GLOBEC Talk Body size-dependence of euphausiid spatial patchiness

2008 CalCOFI	Talk	Spatial patchiness as a function of life history: the case of euphausiids
2008 Ocean Sciences	Poster	Prey selectivity and carbon ingestion of two dominant species in California Current Ecosystem: *Euphausia pacifica and Calanus pacificus"*.
2006 LTER ASM	Poster	Brood Size variability in California Current populations of *Euphausia pacifica*
2006 Ocean Sciences	Poster	Zooplankton Trophic Dynamics in the Central Pacific

TEACHING AND OUTREACH EXPERIENCE

2009 Scripps GK-12 graduate fellow

2008 Assisted in the production of the LTER children's book "Sea Secrets". Moonlight Publishing

2008 Teacher's assistant (UCSD), SIO 101, California Coast Oceanography

2006 Teacher's assistant (UCSD), Academic Connections "Beneath the Sea: Concepts in Biological Oceanography"

2005 Volunteer for Aquatic Adventures, Summer camp

2005 Volunteer for Aquatic Adventures, Sea Series program

PUBLICATIONS

Décima, M, M.R. Landry and R. Rykaczewski, 2011. "Broad scale patterns in mesozooplankton biomass and grazing in the Eastern Equatorial Pacific". Deep-Sea Res. II **58** 387-399

Landry, M.R.; K. E. Selph, A. G. Taylor, M. Décima, 2011, W. M. Balch, R. R. Bidigare. "Phytoplankton growth, grazing and production balances in the HNLC equatorial Pacific". Deep-Sea Res. II **58** 524-535

Décima, M, Mark D. Ohman and Alex De Robertis, 2010. "Body size- dependence of euphausiid spatial patchiness". Limnology and Oceanography vol **55:** 777–788

Landry, M.R., M. Décima, M. P. Simmons, C.C.S.Hannides and E. Daniels, 2008. Mesozooplankton biomass and grazing responses to Cyclone Opal, a subtropical mesoscale eddy. Deep-Sea Res. II **55** 1378-1388.

ABSTRACT OF THE DISSERTATION

Mesozooplankton trophic variability in a changing ocean

by

Moira Décima

Doctor of Philosophy in Oceanography

University of California, San Diego, 2011

Professor Michael R. Landry, Chair

Mesozooplankton (animals >200-μm) are critical components of the marine food web, sensitive to climate change via bottom-up and top-down forcing. Trophic structure is a key determinant of energy flow to mesozooplankton, influencing species composition and total biomass yield. In my dissertation, I investigate mesozooplankton trophic flexibility in response to spatiotemporal variations in environmental conditions. I begin by investigating patterns in mesozooplankton biomass and grazing in the Eastern Equatorial Pacific. Strong relationships were not apparent between mesozoo- and microplankton standing stocks or physical flows. The lone significant correlation between mesozooplankton nighttime biomass and peak microplankton concentrations

suggests that aggregation can be an important factor influencing plankton trophic coupling. Biomass comparisons with the 1992 US JGOFS EqPac study show an 80% decadal increase, which is not reflected in contemporaneous primary production (PP) estimates, and parallels a trend documented in the North Pacific Subtropical Gyre, suggesting a large-scale forcing mechanism. A shift in mesozooplankton average trophic position (TP) could explain the disproportionate effect on zooplankton relative to phytoplankton.

The rest of my dissertation focuses on processes in the California Current Ecosystem. I investigate aggregation patterns in 8 euphausiid species and establish that patchiness is dependent upon body size, likely induced by predators, and secondarily modified by environmental factors.

I then conducted experimental studies to investigate mesozooplankton trophic flexibility. Feeding behaviors of two regionally important species, *Calanus pacificus* and *Euphausia pacifica*, differed, but TPs of both increased as PP decreased. For the total mesozooplankton community, trophic structure was inferred from phytoplankton grazing estimates and energetic requirements for metabolism and growth. In water parcels only 50km from the coastline, herbivorous grazing could not support metabolic requirements. Lastly, I investigate trophic flexibility of *C. pacificus* and *E. pacifica* during the 1998/1999 ENSO event. Compound-Specific Isotope Analysis of Amino Acids allowed me to differentiate between changes in bulk tissue ^{15}N due to baseline and trophic enrichment. Using linear mixed-effects models, I show altered baseline ^{15}N in both zooplankton species, and a trophic shift between years for *E. pacifica*. This trophic shift could be due to the more generalist feeding behavior of *E. pacifica.*

INTRODUCTION

The marine planktonic food web

Trophic pathways determine the flows of energy and nutrient flux within pelagic ecosystems. In theory, the structure of planktonic food webs is determined ultimately by the rate of nutrient delivery. High nitrate delivery favors phytoplankton communities dominated by large cells, while smaller cells with higher uptake capacities are favored when nutrient are scarce. Complex plankton food webs comprise a continuum of trophic pathways (Legendre and Rassoulzadegan 1995), which can be temporally variable due to nutrient regeneration feedbacks and trophic cascades.

Mesozooplankton (animals > 200 μm) are critical to the functioning of the pelagic food web. They constitute the main trophic link from microscopic phyto- and microzooplankton to higher trophic levels such as fish, marine mammals and birds (e.g. Ainley and Boekelheide 1990; Croll et al. 2005; Field et al. 2006). They are key mediators in the 'biological pump', producing large fecal pellets sinking rapidly to depth (Emerson and Roff 1987; Landry et al. 1994; Stukel et al. 2011) and actively transporting carbon below the euphotic zone by diel vertical migration (Longhurst et al. 1990). Ecological paradigms suggest that the size composition of the phytoplankton community should be a major determinant of the production yield of herbivorous mesozooplankton, since the smallest size classes of phytoplankton are not directly usable as a food resource (Cushing 1989). In the traditional 'herbivorous' food chain (large phytoplankton → mesozooplankton → fish) the mesozooplankton trophic position is 2.0 and the production yield of mesozooplankton is maximum. If small phytoplankton dominate the community, however, the main food resource for mesozooplankton will likely be the protozoans that

feed on small phytoplankton (Stoecker and Capuzzo 1990; Fessenden and Cowles 1994; Ohman and Runge 1994; Calbet and Landry 1999). If mesozooplankters that were feeding exclusively on phytoplankton shift to a diet composed mainly of protozoans and other heterotrophs, their maximum biomass yield will decrease by about three-fold, reflecting the energy lost in the energy transfer through the added trophic level (based on assumed gross growth efficiencies, GGE, of 0.3, Straile 1997). Consequently, the amount of carbon transferred to mesozooplankton and thus potentially available to higher trophic levels depends critically on the mean number of steps in the trophic pathway.

Despite our theoretical understanding of the underlying processes in marine food webs, trophic transfers in the ocean are poorly resolved. Studies using correlations between regional mesozooplankton grazing and Chl *a* and primary production (PP) (e.g. Dam et al. 1995), global grazing estimates and PP (Calbet 2001), patterns in population structure (Martin et al. 2006) and model simulations (Stromberg et al. 2009) all arrive at different conclusions regarding the relationship between trophic efficiency and nutrient loading of an ecosystem. Multiple processes can blur the mechanisms that link phytoplankton production to zooplankton biomass. Temporal mismatches in generation times can lead to imbalances in the biomass of phyto- and mesozooplankton biomass, such as those observed during the succession of spring blooms, or in advective systems (e.g. Roman et al. 2002). Aggregations of mesozooplankton have also been found to be not only uncorrelated with phytoplankton biomass or PP but to exert strong top-down controls over the community and its production rates (Landry et al. 2009). While PP ultimately limits secondary production, the complexity of this relationship due to time

lags in biological responses, advection, and complex feedback mechanisms is a common feature of marine ecosystems.

Mesozooplankton in a changing ocean

The ocean has been changing at a dramatic rate for the past century (IPCC 2007). The North Pacific Ocean basin is affected by forcing on different time scales. These include long-term global warming (IPCC 2007), decadal-scale forcing such as the Pacific Decadal Oscillation (PDO, Mantua and Hare 2002) and the North Pacific Gyre Oscillation (NPGO, Di Lorenzo et al. 2008), and interannual events such as the El Niño Southern Oscillation (ENSO). While plankton responses to a given source of climate variability are neither synchronous nor ubiquitous in marine ecosystems (with perhaps the exception of ENSO conditions, Overland et al. 2010), there is ample evidence for global-scale teleconnections (e.g. Perry et al. 2004; Richardson 2008; Mackas and Beaugrand 2010; Schwing et al. 2010). Recently documented changes in zooplankton standing stock in the North Pacific include a decadal increase in the oligotrophic subtropical north Pacific (Sheridan and Landry 2004), a long-term decrease in zooplankton biovolume in the California Current System (Roemmich and McGowan 1995a; Roemmich and McGowan 1995b) attributed to a change in the pelagic tunicate community (Lavaniegos and Ohman 2003; Lavaniegos and Ohman 2007), and decadal increases in zooplankton and copepods in the Japan and East China seas (Rebstock and Kang 2003), to name a few.

Our present understanding of how climate forcing affects the marine ecosystem is limited. Changes in any one climate index may result in multiple effects on the regional

physical oceanography of an ecosystem, including advective patterns and nutrient delivery. To be able to predict the future directions of pelagic ecosystems, we must understand the mechanisms by which alterations in physical forcing translate into changes in the structure and functioning of biological communities. Large marine ecosystems within the Pacific ocean show a persistent warming over the past century (Schwing et al. 2010), which can lead to increased upper-water column stratification, documented in various ecosystems (Bograd and Lynn 2003; Sarmiento et al. 2004; Kim and Miller 2007). Nutrient delivery to the euphotic zone is highly dependent on the degree of thermal stratification (Roemmich and McGowan 1995a), and it is hypothesized that increased stratification will lead to decreased PP and/or shifts in phytoplankton community structure. Net PP in low-latitude stratified oceans have been observed to decrease, presumably in response to changes in upper ocean temperature and stratification (Behrenfeld et al. 2006). The response of mesozooplankton communities inhabiting these ecosystems will depend critically on their ability to exploit alternate trophic pathways in response to decreasing production or changes in the size structure of the phytoplankton community.

Finally, it is important to understand the effect of climate change on mesozooplankton for two very different reasons. On the one hand, changes in trophic structure, with consequent effects on standing stocks, are likely to alter patterns of energy and nutrient cycling dramatically through processes mediated by mesozooplankton. These changes can affect energy transfer to higher trophic levels, as well as the sequestering of CO_2 to the deep ocean by the 'biological pump'. On the other hand, because most are not commercially exploited, and generation times are usually < 1 year,

they are important indicators of climate change (Mackas and Beaugrand 2010). Understanding patterns of mesozooplankton community variability can both help us elucidate the complexities of ecosystem forcing, through the biological amplification of physical signals (e.g. Taylor et al. 2002), as well as begin to understand the ultimate long-term effects on this component of the marine pelagic ecosystem.

Dissertation outline

The overarching goal of this thesis is to elucidate mesozooplankton trophic flexibility in response to variable environmental conditions. When I use the term trophic flexibility I am referring to the ability of an organism or groups of organisms to alter their trophic position by shifting, at least partially, their food resources. However, there is a difference between trophic changes in whole mesozooplankton communities, i.e. a change in *average* mesozooplankton trophic level, and the ability of a single species to shift its trophic position. While both changes can result in important differences in community or population biomass yield, their ecological implications are quite different. For example, a community that shifts in relative composition of herbivores and carnivores (resulting in a change in average trophic position) can have significant consequences for specialist predators that largely exploit one species or type of prey (e.g. whales that feed mainly on krill). If individual species are able to modulate their trophic positions in response to environmental conditions, they may demonstrate greater resilience to climatic perturbations.

In this dissertation, I investigate trophic flexibility of both mesozooplankton communities and individual species in response to environmental conditions varying in

space and time, in the eastern equatorial Pacific (EEP) and the California Current Ecosystem (CCE).

In Chapter one, entitled "Broad scale patterns in mesozooplankton biomass and grazing in the eastern equatorial Pacific", I investigated spatial patterns in biomass, grazing and community size structure in relation to the dominant physical flows of the region with respect to the microplankton community biomass (their prey). Significant correlation with lower trophic levels was only found between peak water-column microplankton concentrations and mesozooplankton nighttime standing stock. This result suggests that mesozooplankton can allocate and exploit prey maxima. That prey patchiness can influence predator biomass patterns, raising the question about possible responses to changes in trophic structure local biomass patches are diminished by grazing.

An interesting and unexpected finding also arose in comparing mesozooplankton biomass with the US JGOFS EqPac study conducted 12 years earlier in the same area. This comparison suggested a decadal increase in mesozooplankton biomass of ~80%, paralleling the magnitude and direction of the observed increase in the adjacent North Pacific Subtropical Gyre (Sheridan and Landry 2004). Because no significant differences in primary production were detected between the studies, a shift down in mesozooplankton trophic position emerged as a possible explanatory mechanism. These were the initial observations and hypothesis that focused the more experimental portion of my dissertation research (Chapters 3 and 4) on the issue of trophic flexibility.

The paper based on this chapter has been published in Deep Sea Research II: Topical Studies in Oceanography (Décima, M, M. R. Landry and R. Rykaczewski, 2011)

In Chapter two, entitled "Body size dependence of euphausiid spatial patchiness", I investigated patterns of euphausiid patchiness with size in the California Current System (CCS). Euphausiids are critical components of the mesozooplankton community, second to copepods in their biomass contribution to the CCS (Lavaniegos and Ohman 2007), and constitute a major link to all higher predators in the CCS (Dorman et al. 2011).

To better understand the environment and size constraints on euphausiid aggregation behavior, I determined the patterns of differential aggregation with body size for the 8 dominant CCS species. I found a "U shaped" pattern of patchiness with euphausiid size. I interpreted the initial descending limb of the "U shape", a decrease in patchiness with increasing size, as consistent with the effects of turbulent diffusion on small larvae (too small to swim), and the increase in patchiness at the larger size classes consistent with biological processes, most probably predator induced. I found no difference associated with seasons or the one ENSO year sampled, but higher patchiness was noted for most species during one year of early and intense upwelling. Additionally, patchiness was usually greater in the inshore CCS region, characterized by higher Chl *a* concentrations. More productive conditions resulted in higher aggregation, which could have important top-down consequences for the phytoplankton community, when imbalances in phyto- and mesozooplankton biomass occur.

Although not formally a motivation for the study, the results raise the question of how temporal shifts in trophic position, specifically the trophic flexibility of individual euphausiid species in response to changes in prey assemblages, may occur in natural systems when aggregations of animals have the potential to strongly impact local prey resources.

The paper based on this chapter has been published in Limnology and Oceanography (Décima, M, M. D. Ohman and A. DeRobertis, 2010).

In Chapter three, entitled "Zooplankton trophic variability in the California Current Ecosystem", the relationship between the mesozooplankton and the microplankton community is further investigated in the California Current System (CCS). For this study, I established mesozooplankton community patterns in biomass, grazing, and nutritional requirements across a broad environmental gradient within the CCS. The nutritional requirements of the mesozooplankton community suggested high consumption of autotrophic carbon in the very nearshore region, but heterotrophic prey were necessary to satisfy daily carbon community requirements of zooplankton in the offshore environment. A community varying in trophic structure with environmental conditions was inferred from these results.

Potential shifts in trophic position (TP) of individual species were further investigated experimentally for two regionally important species, *Euphausia pacifica* and *Calanus pacificus*. Incubation results showed that these zooplankters consumed relatively more carbon of heterotrophic origin with decreasing PP, confirming trophic flexibility. In addition, the one location where *E. pacifica* was not an exclusive herbivore

(TP ~2.4) was where anomalously high mesozooplankton concentrations had significantly grazed the phytoplankton community down to ~25% of its initial concentration over the course of 5 days (Landry et al. 2009). This indicated an increase in trophic position in response to phytoplankton depletion resulting from mesozooplankton grazing pressure.

In Chapter 4, entitled "The 1998/1999 El Niño Southern Oscillation event and the isotopic content of amino acids in California Current zooplankton: effects on baseline ^{15}N and trophic structure", I used stable isotopes to investigate temporal shifts in trophic position for the same two species, *C. pacificus* and *E. pacifica*, before and after the El Niño/La Niña conditions of 1998/1999. This particular El Niño event had a marked effect on the pelagic ecosystem, including significant decrease in Chl *a* (Kahru and Mitchell 2000), decrease in *E. pacifica* abundance (Brinton and Townsend 2003), and bulk tissue ^{15}N enrichment of individual *C. pacificus* (Rau et al. 2003; Ohman et al. submitted).

I used Compound-Specific Isotope Analysis (CSIA) of Amino Acids (AAs) to deconvolve the isotopic enrichment that could arise due to changes in baseline ^{15}N versus trophic elongation. *C. pacificus* did not shift trophic positions between years, while *E. pacifica* fed at a higher trophic position during 1998. Additional evidence based on CSIA-AA results from 1997 and 2000, suggested that rather than shifting up the trophic web during 1998, the euphausiids experienced enhanced herbivory during 1999, shifting down in trophic position.

Overall, trophic flexibility (based on stable isotopes), was found to be species-specific among these primarily herbivorous zooplankters, which could have important implications for community composition responses to climate perturbations.

References

Ainley, D. G., and R. J. Boekelheide. 1990. Seabirds of the Farallon Islands: Ecology dynamics and structure of an upwelling system community. Stanford University Press: Stanford, California, USA. p 450.

Behrenfeld, M. J., R. T. O'Malley, D. A. Siegel, C. R. McClain, J. L. Sarmiento, G. C. Feldman, A. J. Milligan, P. G. Falkowski, R. M. Letelier, and E. S. Boss. 2006. Climate-driven trends in contemporary ocean productivity. Nature **444:** 752-755.

Bograd, S. J., and R. J. Lynn. 2003. Long-term variability in the Southern California Current System. Deep-Sea Res. II **50:** 2355-2370.

Brinton, E., and A. Townsend. 2003. Decadal variability in abundances of the dominant euphausiid species in southern sectors of the California Current. Deep-Sea Res. II **50:** 2449-2472.

Calbet, A. 2001. Mesozooplankton grazing effect on primary production: A global comparative analysis in marine ecosystems. Limnol. Oceanogr. **46:** 1824-1830.

Calbet, A., and M. R. Landry. 1999. Mesozooplankton influences on the microbial food web: Direct and indirect trophic interactions in the oligotrophic open ocean. Limnol. Oceanogr. **44:** 1370-1380.

Croll, D. A., B. Marinovic, S. Benson, F. P. Chavez, N. Black, R. Ternullo, and B. R. Tershy. 2005. From wind to whales: trophic links in a coastal upwelling system. Mar. Ecol. Prog. Ser. **289:** 117-130.

Cushing, D. H. 1989. A difference in structure between ecosystems in strongly stratified waters and in those that are only weakly stratified. J. Plankton Res. **11:** 1-13.

Dam, H. G., X. S. Zhang, M. Butler, and M. R. Roman. 1995. Mesozooplankton grazing and metabolism at the equator in the central Pacific: Implications for carbon and nitrogen fluxes. Deep-Sea Res. II **42:** 735-756.

Di Lorenzo, E., N. Schneider, K. M. Cobb, P. J. S. Franks, K. Chhak, A. J. Miller, J. C. McWilliams, S. J. Bograd, H. Arango, E. Cuchitser, T. M. Powell, and P. Riviere. 2008. North Pacific Gyre Oscillation links ocean climate and ecosystem change. Geophysical Research Letters **35:** L08607.

Dorman, J. G., T. M. Powell, W. J. Sydeman, and S. J. Bograd. 2011. Advection and starvation cause krill (Euphausia pacifica) decreases in 2005 Northern California coastal populations: Implications from a model study. Geophysical Research Letters **38:** L04605.

Emerson, C. W., and J. C. Roff. 1987. Implications of fecal pellet size and zooplankton behavior to estimates of pelagic-benthic carbon flux. Mar. Ecol. Prog. Ser. **35:** 251-257.

Fessenden, L., and T. J. Cowles. 1994. Copepod Predation on Phagotrophic Ciliates in Oregon Coastal Waters. Mar. Ecol. Prog. Ser. **107:** 103-111.

Field, J. C., R. C. Francis, and K. Aydin. 2006. Top-down modeling and bottom-up dynamics: Linking a fisheries-based ecosystem model with climate. Prog. Oceanogr. **68:** 238-270.

IPCC. 2007. Working group 1 Report. http//www.ipcc.ch/.

Kahru, M., and B. G. Mitchell. 2000. Influence of the 1997-98 El Nino on the surface chlorophyll in the California Current. Geophysical Research Letters **27:** 2937-2940.

Kim, H. J., and A. J. Miller. 2007. Did the thermocline deepen in the California current after the 1976/77 climate regime shift? J. Phys. Oceanogr. **37:** 1733-1739.

Landry, M. R., C. J. Lorenzen, and W. K. Peterson. 1994. Mesozooplankton grazing in the Southern California Bight .II. Grazing impact and particulate flux. Mar. Ecol. Prog. Ser. **115:** 73-85.

Landry, M. R., M. D. Ohman, R. Goericke, M. R. Stukel, and K. Tsyrklevich. 2009. Lagrangian studies of phytoplankton growth and grazing relationships in a coastal upwelling ecosystem off Southern California. Prog. Oceanogr. **83:** 208-216.

Lavaniegos, B. E., and M. D. Ohman. 2003. Long-term changes in pelagic tunicates of the California Current. Deep-Sea Res. II **50:** 2473-2498.

Lavaniegos, B. E., and M. D. Ohman. 2007. Coherence of long-term variations of zooplankton in two sectors of the California Current System. Prog. Oceanogr. **75:** 42-69.

Legendre, L., and F. Rassoulzadegan. 1995. Plankton and nutrient dynamics in marine waters. Ophelia **41:** 153-172.

Longhurst, A. R., A. W. Bedo, W. G. Harrison, E. J. H. Head, and D. D. Sameoto. 1990. Vertical flux of respiratory carbon by oceanic diel migrant biota. Deep-Sea Res. I **37:** 685-694.

Mackas, D. L., and G. Beaugrand. 2010. Comparisons of zooplankton time series. J. Mar. Syst. **79:** 286-304.

Mantua, N. J., and S. R. Hare. 2002. The Pacific decadal oscillation. J. Oceanogr. **58:** 35-44.

Martin, E. S., X. Irigoien, R. P. Harris, A. Lopez-Urrutia, M. V. Zubkov, and J. L. Heywood. 2006. Variation in the transfer of energy in marine plankton along a productivity gradient in the Atlantic Ocean. Limnol. Oceanogr. **51:** 2084-2091.

Ohman, M. D., and J. A. Runge. 1994. Sustained fecundity when phytoplankton resources are in short supply - omnivory by *Calanus finmarchicus* in the Gulf of St-Lawrence. Limnol. Oceanogr. **39:** 21-36.

Ohman, M. D., G. Rau, and P. Hull. in press. Multi-decadal variations in stable N isotopes of California Current zooplankton. Deep-Sea Res. I

Overland, J. E., J. Alheit, A. Bakun, J. W. Hurrell, D. L. Mackas, and A. J. Miller. 2010. Climate controls on marine ecosystems and fish populations. J. Mar. Syst. **79:** 305-315.

Perry, R. I., H. P. Batchelder, D. L. Mackas, S. Chiba, E. Durbin, W. Greve, and H. M. Verheye. 2004. Identifying global synchronies in marine zooplankton populations: issues and opportunities. ICES J. Mar. Sci. **61:** 445-456.

Rau, G. H., M. D. Ohman, and A. Pierrot-Bults. 2003. Linking nitrogen dynamics to climate variability off central California: a 51 year record based on $^{15}N/^{14}N$ in CalCOFI zooplankton. Deep-Sea Res. II **50:** 2431-2447.

Rebstock, G. A., and Y. S. Kang. 2003. A comparison of three marine ecosystems surrounding the Korean peninsula: Responses to climate change. Prog. Oceanogr. **59:** 357-379.

Richardson, A. J. 2008. In hot water: zooplankton and climate change. ICES J. Mar. Sci. **65:** 279-295.

Roemmich, D., and J. McGowan. 1995a. Climatic Warming and the Decline of Zooplankton in the California Current. Science **267:** 1324-1326.

Roemmich, D., and J. McGowan. 1995b. Climatic Warming and the Decline of Zooplankton in the California Current (Vol 267, Pg 1324, 1995). Science **268:** 352-353.

Roman, M. R., H. G. Dam, R. Le Borgne, and X. Zhang. 2002. Latitudinal comparisons of equatorial Pacific zooplankton. Deep-Sea Res.II **49:** 2695-2711.

Sarmiento, J. L., R. Slater, R. Barber, L. Bopp, S. C. Doney, A. C. Hirst, J. Kleypas, R. Matear, U. Mikolajewicz, P. Monfray, V. Soldatov, S. A. Spall, and R. Stouffer. 2004. Response of ocean ecosystems to climate warming. Glob. Biogeochem. Cycle **18:** 35.

Schwing, F. B., R. Mendelssohn, S. J. Bograd, J. E. Overland, M. Y. Wang, and S. Ito. 2010. Climate change, teleconnection patterns, and regional processes forcing marine populations in the Pacific. J. Mar. Syst. **79:** 245-257.

Sheridan, C. C., and M. R. Landry. 2004. A 9-year increasing trend in mesozooplankton biomass at the Hawaii Ocean Time-Series Station ALOHA. ICES J. Mar. Sci. **61:** 457-463.

Stoecker, D. K., and J. M. Capuzzo. 1990. Predation on Protozoa: its importance to zooplankton. J. Plankton Res. **12:** 891-908.

Straile, D. 1997. Gross growth efficiencies of protozoan and metazoan zooplankton and their dependence on food concentration, predator-prey weight ratio, and taxonomic group. Limnol. Oceanogr. **42:** 1375-1385.

Stromberg, K. H. P., T. J. Smyth, J. I. Allen, S. Pitois, and T. D. O'Brien. 2009. Estimation of global zooplankton biomass from satellite ocean colour. J. Mar. Syst. **78:** 18-27.

Stukel, M. R., M. R. Landry, C. R. Benitez-Nelson, and R. Goericke. 2011. Trophic cycling and carbon export relationships in the California Current Ecosystem. Limnol. Oceanogr. **56:** 1866-1878.

Taylor, A. H., J. I. Allen, and P. A. Clark. 2002. Extraction of a weak climatic signal by an ecosystem. Nature **416:** 629-632.

CHAPTER 1

Broad scale patterns in mesozooplankton biomass and grazing in the eastern equatorial Pacific

By Moira Décima, Michael R. Landry and Ryan R. Rykaczewski

Abstract

We investigated biomass distributions and grazing rates of mesozooplankton in the eastern equatorial Pacific between 110°-140°W and 4°S-4°N during cruises in December 2004 (EB04) and September 2005 (EB05). Median (± SE) euphotic zone estimates of zooplankton biomass, collected with a 200-μm mesh net, varied from 2.27 ± 0.24 g dry weight m^{-2} during EB04 to 3.13 ± 0.22 g dry weight m^{-2} for EB05 (however, when stations from overlapping regions were compared, no significant differences were found between years). Trends in gut fluorescence estimates of mesozooplankton grazing followed biomass, with significantly higher median rate estimates during EB05 (3.39 ± 0.32 mg pigment m^{-2} d^{-1}) than during EB04 (2.31 ± 0.34 mg pigment m^{-2} d^{-1}). Spatial gradients in mesozooplankton biomass and grazing on meridional transects sampled at 110°W in 2004 and 140°W in 2005 could be interpreted as either *in situ* growth/grazing responses or downstream advective flows relative to spatial patterns in phytoplankton. The present zooplankton biomass estimates for the equatorial Pacific are 80-90 % higher than those from similar measurements made by the US Joint Global Ocean Flux Studies EqPac Program in 1992. Our grazing rates

similarly exceed EqPac estimates by a factor of 2 or 3, in absolute terms and as percent of phytoplankton biomass consumed daily (11% - EB04; 14% - EB05). Although the equatorial region has not been regularly sampled between EqPac and the present study, both the magnitude and the direction of the observed changes are consistent with the documented decadal increase in mesozooplankton biomass in the adjacent North Pacific Subtropical Gyre based on monthly sampling at Stn. ALOHA, as well as an increase in the strength of the trade winds. These results may be indicative of a general shift up in productivity or community size structure and role of mesozooplankton in the open-ocean tropical/subtropical Pacific, and they provide important time points for validating the performance of ecosystem models of the region.

Introduction

Animals comprising the mesozooplankton size fraction (0.2-20 mm) of ocean biota perform a number of essential functions in pelagic ecosystems. They can be important and often seasonally dominant grazers, especially in more productive regions (Escribano et al. 2007; Richardson 2008; Takahashi et al. 2008). They are the major carbon and energy transfer link between production processes in the microbial food web and higher trophic levels of fish, marine mammals and seabirds (Ainley and Boekelheide 1990; Croll et al. 2005). They also contribute significantly to export fluxes of carbon and nutrients from the euphotic zone via the passive settling of their large fecal pellets (Emerson and Roff 1987; Landry et al. 1994) and the active transport of materials to depth during diel vertical migrations (Longhurst et al. 1990; Al-Mutairi and Landry 2001). The absolute and relative importance of each of these functions depend critically on the biomass, size structure and composition of mesozooplankton, which vary among and within ocean ecosystems in response to changing seasonal as well as climatic conditions.

Mesozooplankton biomass and composition fluctuate with seasonal and spatial variations in primary production in all systems to varying degrees (Miller 2004), and El Niño Southern Oscillation (ENSO) cycles are another well characterized source of variability on the interannual scale throughout the Pacific Ocean (White et al. 1995; Peterson et al. 2006). Lower frequency changes have also been noted in the north Pacific, with notable examples from decadal time-series studies in the productive boundary currents. For instance, mesozooplankton biomass and copepod concentrations in the Yellow and Japan/East Sea have increased since the early 1990's (Rebstock and Kang 2003), and an increasing trend in

zooplankton biovolume has been noted recently for the CalCOFI sampling region in the California Current (Fig. 2 in Lavaniegos and Ohman 2007). In addition, a decadal increase in open-ocean standing stock of mesozooplankton has been documented from monthly time-series sampling at Station ALOHA in the oligotrophic subtropical north Pacific (Sheridan and Landry 2004).

The present study was conducted as part of a broader investigation of processes that control phytoplankton production in the eastern equatorial Pacific, a region characterized by high nutrient-low chlorophyll (HNLC) conditions (Minas et al. 1986). Research was conducted on two cruises in December 2004 and September 2005 in the area bounded by 4°N-4°S, 110-140°W. Our goals were to quantify the current states of mesozooplankton biomass, community size structure, diel variability associated with vertical migration and gut pigment indices of grazing. We aimed first to assess spatial patterns among the measured mesozooplankton parameters and their relationships to variability in the physical environment and the lower trophic levels encountered during these cruises. Our sampling also provided a basis of comparison to the results of the previous intensive study of the equatorial region at 140°W by the US Joint Global Ocean Flux Study (US JGOFS) EqPac program in 1992 (Dam et al. 1995; Roman et al. 1995; White et al. 1995; Zhang et al. 1995). From this comparison, our data provide the first evidence of a potential decadal increase of mesozooplankton biomass in the eastern equatorial Pacific that roughly parallels changes observed in the subtropical north Pacific. The results have important implications for understanding the physical mechanisms that potentially link production processes in these adjacent open-ocean ecosystems and for modeling the ecological and biogeochemical responses of the equatorial system to varying physical forcing and climate change.

Materials and methods

Our study was conducted during two cruises aboard the *R/V Roger Revelle*. We sampled stations in zonal and meridional transects on both cruises. For EB04, we first sampled at 110°W from 4°N to 4°S at 1° spacing, followed by an east-west transect along the equator from 110° to 140°W. For EB05, the initial sampling was done from 4°N to 2.5°S at 140°W, followed by an west-east transect at 0.5°N from 140° to 123.5°W (Fig. 1).

Mesozooplankton net collections

Mesozooplankton collection and size fractionation were carried out similarly to Landry et al. (2001). Sampling was conducted at each station twice daily, typically at 1000-1100 to capture daytime populations and at 2200-2300 to include nocturnal migrants. We used a standard 1-m^2 ring net with 202-μm Nitex mesh, towed obliquely for 20 min at a ship speed of 1-2 kts (roughly 2-4 kmh^{-1}). A General Oceanics flowmeter was attached across the net mouth to record volume filtered, and a Vyper Suunto dive computer was fastened to the net frame to record tow depth and duration. A total of 59 samples were taken on the two cruises. Mean (± SE) tow depth and volume sampled of both cruises combined, assuming 100% net efficiency, were 144 ± 3.6 m and 311 ± 7.5 m^3, respectively. The sampled depth included the full depth of the euphotic zone to 0.1% surface irradiance, which ranged from 96 to 131 m in EB04 and 94 to 130 m during EB05 (Taylor et al. 2011).

Once on deck, the net was washed down with seawater and the contents of the cod end placed in a bucket with carbonated water to prevent gut evacuation (Kleppel and Pieper 1984). The collected sample was then subsampled with a Folsom splitter, and half of the sample was preserved with 4% buffered formalin solution. Separate splits (each of typically $1/8^{th}$ of the sample) were used for biomass and gut-fluorescence determinations, with the

latter done first to minimize pigment degradation. Each of these subsample splits was wet sieved into five size classes of 0.2-0.5, 0.5-1, 1-2, 2-5 and >5 mm.

Biomass estimates

Each size-fractioned sample for biomass was concentrated onto a pre-weighed 0.2-mm Nitex screen, rinsed with either ammonium formate (EB04) or Milli-Q water (EB05) to remove interstitial sea salt, placed in Petri dishes and frozen at -80°C for later analysis on shore. The frozen samples were thawed and dried in an oven at 60°C for at least 24 h. Dried samples were weighed to 0.01 mg at room temperature on an analytical microbalance (Denver Instrument). After subtracting the initial weight of the Nitex screen, the dry weight (DW) of each size fraction was obtained by the appropriate multiplication factors for previous sub-sampling, and total mesozooplankton DW was estimated from the combined biomass values of all size fractions. Areal biomass estimates (i.e., mg DW m^{-2}) were computed from total net sample estimates by multiplying by the factor, D/vol, which reflects the water depth (D, m) and volume filtered (vol, m^3). Areal mean biomass is reported only when paired daytime and nighttime-collected samples were taken at the same station (13 stations for EB04; 14 stations for EB05). These day-night paired samples were also used to compute migrant biomass by subtracting the daytime from the nighttime measurements.

Gut pigment and grazing estimates

Each size-fractioned sample for gut pigment analysis was concentrated onto a 47-mm GF/F filter and immediately frozen in the dark at -80°C for later processing on shipboard (EB05) or in the lab (EB04). The GF/F filters were subsampled for the three smallest size classes, by placing the frozen filters centered under a plastic template and sectioning into 8 pie-shaped fractions with a thin knife blade. Analysis was carried out in duplicate. The

replicate 1/8th samples were ground in 90% acetone using a tissue homogenizer to extract pigments, and the homogenate was centrifuged to remove particulates. For the 2-5 mm size class typically the whole sample was processed, although if very dense we took 1/4th of the sample. The >5mm size class was always processed in its entirety. Concentrations of chlorophyll *a* (Chl *a*) and phaeopigments (Phaeo) were then measured using a Turner TD-700 (EB04) or 10AU fluorometer (EB05) (Strickland and Parsons 1972). For each size-fraction analyzed, we computed the depth-integrated concentration of gut pigment (Chl *a*, Phaeo) in the euphotic zone as:

$$GPC = \frac{pig * D}{vol * f} \quad (1)$$

where *GPC* is gut pigment content (mg m^{-2}), *pig* is the measured pigment value (mg), *f* is fraction of sample analyzed, *D* is depth of tow (m) and *vol* is the volume of water filtered (m^3). We did not correct our phaeopigment estimates by a factor of 1.51 (the Chl *a*: Phaeo weight ratio), as is often done in grazing assessments using the gut-fluorescence method. Conover et al. (1986) showed that such a correction was redundant because standard fluorometric equations used to obtain phaeopigment estimates already compute these values in terms of chlorophyll weight equivalents.

For each size fraction and for the total mesozooplankton assemblage, grazing rates (G, mg pigment m^{-2} d^{-1}) were estimated as

$$G = GPC * K \quad (2)$$

where *K* (h^{-1}) is the gut evacuation rate constant. To avoid biases introduced by the potential contamination of gut pigment contents with net-concentrated living phytoplankton, we used only the *GPC* measurements of Phaeo for the grazing calculation. The effect of only taking

Phaeo into account varied with size class and tow, but at times Chl *a* equaled Phaeo estimates. The rate estimates are thus conservative. We further assumed that the fraction of Phaeo degradation to non-fluorescent products during digestion was inherently accounted for in experimental determinations of gut evacuation rate (Durbin and Campbell 2007), and thus made no additional correction for this loss. For *K*, we used the rate constant of 2.1 h^{-1} derived from shipboard gut evacuation experiments at 140°W during the JGOFS EqPac program (Zhang et al. 1995). A similar experimental estimate of 2.3 h^{-1} was also found for the mesozooplankton community sampled between 4°S, 105°W and 7°S, 110°W during IronEx II (Rollwagen Bollens and Landry 2000). In order to compute biomass-specific rates of phytoplankton grazing by the whole mesozooplankton community and for individual size classes, we calculated $G*B^{-1}$ (where *B* is biomass expressed as mg DW m^{-2}). We also computed daily removal rates of phytoplankton due to mesozooplankton grazing as $G*Chl_z^{-1}$. Phytoplankton standing stocks were estimated by Chl_z^{-1}, which is the depth-integrated concentration of Chl *a* in the euphotic zone (mg Chl *a* m^{-2}). Lastly, day-night differences in grazing rates were computed analogously to migrant biomass for each station at which we had paired day-night net tows.

Spectral slopes

We investigated the patterns in biomass and grazing size spectra by fitting a linear-least square line to the following formula:

$$\log\left(\frac{Bx}{\Delta x}\right) = m * \left[\log(x)\right] + b \qquad (3)$$

where *Bx* is the DW (or grazing rate) of the sample for each size class, Δx is the size of the interval for each size class (0.303, 0.495, 1, 3, and 5 mm in this case), and *m* and *b*

correspond to the parameters of the linear best fit line, the slope and the *y*-intercept, respectively (see Rykaczewski and Checkley 2008). Only nighttime estimates were considered for these analyses, since they best represent the total community present under a square meter of sea surface. Typically, the linear regression was determined by five data points (corresponding to the five mesh sizes). However, when estimates in the largest size fraction were zero, as happened occasionally, the regression was adjusted to fit fewer points. R^2 values were investigated to ensure a good fit to the model. R^2 values averaged 0.87 for both biomass and grazing slopes during EB04 (biomass: range 0.69-0.97; grazing: 0.73-0.93). For EB05, mean R^2 values were 0.86 and 0.87 for biomass and grazing slopes, respectively (biomass: range 0.67-0.95; grazing: 0.75-0.96). The spectral slopes were always negative, with the steepness of the regression slope indicating the degree of size dominance (i.e. higher negative values indicate stronger dominance of small size classes).

Results

To better elucidate relationships between the mesozooplankton community and the physical and biological characteristics of the waters they inhabit, we report our results in subsections. The first briefly summarizes the hydrography and nutrient profiles of the region during our sampling. The next two subsections report mesozooplankton biomass and grazing estimates along meridional and zonal transects, which line up roughly orthogonal to and with the dominant flows of equatorial currents, respectively. The fourth and final subsection compares regional mean estimates between cruises.

Hydrography, nutrients and phytoplankton community patterns

Detailed descriptions of the physical environment can be found in Kaupp et al. (2011), Krause et al. (2011), Selph et al. (2011), and Strutton et al. (2011). The dominant flow at the equator, the eastward flowing equatorial undercurrent, was in meridional transects at both 110°W and 140°W, with a core velocity of ~110 cm sec^{-1} at the base of the euphotic zone, decreasing with latitude and disappearing at ~2°S and 2°N. Euphotic zone depths, defined as the depth of penetration of 0.1% surface irradiance, ranged from 120-131 m along 110°W and from 95 to 130 m along 140°W (Taylor et al. 2011), with shallowest depths in the equatorial region deepening towards the poles. All zooplankton sampling therefore extended over the depth range of the euphotic zone, defined as the depth of 0.1% penetration of surface irradiance. Surface concentrations of Nitrate + Nitrite were typically high (5-7 μM) throughout the region with lower values of 2-4 μM in two areas around the equator (120°W –EB04; 132.5°W – EB05) and < 2 μM poleward of 2°N, 110°W (EB04). Dissolved iron concentrations were undetectable in the upper 100 m at 110°W between 1°S and 1°N, and increased poleward. The phytoplankton community was also not symmetrically distributed around the equator, with autotrophic microplankton and diatoms showing distinct peaks on the northern end of the transect, 1-2 degrees from the equator (for details see Taylor et al. 2011). The meridional transect during EB05, at 140°W, was characterized by doming isopycnals and peaks in nitrate and dissolved iron concentrations at 1°S, which marked this station as the area of active equatorial upwelling (Selph et al. 2011). The highest biomass levels of all phytoplankton groups were present at this station (Taylor et al. 2011).

Zonal transects during both cruises showed a general W-E shoaling of the equatorial undercurrent, with the depth of 100 cm sec^{-1} current velocities shoaling from ~110 m at

140°W to ~ 90 m at 110°W (see Selph et al. 2011). In addition, we also encountered elevated meridional flows indicating Tropical Instability Waves (TIW's) along the zonal transects (Strutton et al. 2011). The alternating northward and southward flows of the TIW's, were associated with peaks of different microplankton community groups (Taylor et al. 2011). A TIW sampled during EB05 caused a shoaling of isopycnals at ~125°W, coinciding with peaks in nitrate and chlorophyll but not in autotrophic biomass (Selph et al. 2011; Taylor et al. 2011). Nitrate concentrations were elevated on the western side of the transect, with eastward shoaling evident on the equatorial transect on EB04, but relatively constant along the 0.5°N shorter transect on EB05. Dissolved iron varied opposite to nitrate, with a marked decreasing trend from west to east on EB04, and a less pronounced yet similar trend on EB05 (Kaupp et al. 2011; Selph et al. 2011). Regional microplankton community patterns followed these spatial gradients in nutrient distributions, with noticeably higher chlorophyll, auto- and heterotrophic microplankton biomass on the western side of the study region (Taylor et al. 2011).

Latitudinal trends

Mesozooplankton biomass, migrant biomass and size structure displayed asymmetric patterns with respect to the equator that differed for the 140°W and 110°W transects (Fig. 2). For EB04, a distinct local minimum in day-night averaged biomass was present at the equator (Fig. 2a). In addition, the estimates significantly increased from south to north at 110°W *(p*<0.05), peaking at the northernmost station at 4°N. This trend was also roughly reflected in higher slopes of the biomass size spectra at 3-4°N as compared to the southern stations (Fig. 2b). For EB05, higher biomass estimates were measured south of the equator at 140°W, and spectral slopes were more symmetrically distributed, with very similar values from 0.5°S to

4°N, and a small maximum coinciding with peaks in average biomass and migrant biomass at 1°S (Fig. 2).

Size structure at 110°W showed greater relative abundance of smaller animals in the equatorial upwelling center and increasing abundance of larger animals 1 or 2 degrees to the north and south (Fig. 2b). Mean biomass was slightly higher at 1°N and 2°S than at the equator, but the biomass difference across the region was due to the higher density of large migrant zooplankton on either side of the equatorial minimum (Fig. 2c). At 140°W, a modest local low in mean zooplankton biomass at 0.5°N coincided with a minimum biomass of migrants. This however was not reflected as a change in size spectral slope.

Mesozooplankton community grazing estimates for the two cruises showed similar latitudinal patterns, with local minima in the vicinity of the equator and downstream peaks to the north and south (Fig. 3a). The magnitude of the grazing impact (as measured with pigment techniques) was higher however along 140°W than for the 110°W transect. Absolute values of spectral slopes were also higher at 140°W (Fig. 3b), suggesting that the higher rate of chlorophyll removal was due, in part, to the greater filtering efficiency of larger organisms. Spectral slopes for grazing were higher at the northern end of the EB04 transect and lowest in the south (Fig. 3b), and they did not exactly follow the pattern for biomass spectra. Grazing size spectra were similar and generally highest from 1°S to 1°N, except for 4°N. Thus, despite latitudinally variable biomass spectra, grazing rates were similarly distributed by size class along these latitudes on the 110ºW transect. However, spectral patterns 3 degrees to the north and south of the equator were remarkably similar for biomass and grazing estimates. Day-night differences in grazing also looked similar to migrant biomass estimates (not shown), including the distinct local minimum at the equator.

During EB05, the 140°W community grazing estimates and size-spectra (Fig. 3) were roughly symmetrical with respect to the equator. This suggests similar processes to the north and south, in contrast to the asymmetrical pattern for EB04. Grazing patterns were similar between 0.5°S - 0.5°N, both in terms of daily Chl *a* removal as well as size distribution of the herbivorous community. The peaks at 1°S - 1°N are consistent with an assemblage varying along the mean flow patterns, orthogonal to the equator. These can be inferred to be caused by the high biomass of large suspension feeders, as indicated by the co-occurring peaks in biomass (Fig. 2a) and spectral slopes of the grazing community (Fig. 3b).

Longitudinal trends

Mesozooplankton biomass was higher on the western end of the equatorial transect (Fig. 4a) during EB04, but the biomass increase was modest, and the trend was not significant. Nighttime estimates of community grazing were, however, significantly higher (p<0.05) towards the west on the equatorial transect (Fig. 5b). The migrant estimates showed no clear pattern (Fig. 4c), but the sample size was small due to few day tows along this transect. A notable peak was encountered at 125°W, however, coinciding with shoaling isopycnals and peaks in diatom and prymnesiophyte abundance (Taylor et al. 2011). Spectral slopes of biomass did not show a clear zonal trend (Fig. 4b), but modest peaks centered roughly around 115°, 125° and 132°W, coinciding with areas of uplifted isopycnals and peaks in either diatoms (i.e. at 125°W) or phytoplankton biomass at 115° and 132°W (Selph et al. 2011; Taylor et al. 2011). Variability in grazing size-spectra increased towards the west (Fig. 5b), and the peaks and troughs roughly coincided with the biomass slopes, suggesting that fluctuations in the biomass spectra were largely attributable to herbivorous suspension feeders.

The TIW sampled at 125.7°W on EB05 resulted in a shoaling of the base of the mixed layer as well as meridional advection of cool and warm waters and peaks in surface nitrate and Chl *a* (Krause et al. 2011; Selph et al. 2011) . Zooplankton nighttime biomass was high in this area (Fig. 4a), although migrant biomass was lower at the TIW core than at adjacent stations (Fig. 4c). These peaks in migrant biomass at 123.5° and 130°W coincided with areas of anomalous meridional flow (NE flow at 130°W; SW flow at 123.5°W). Microscopical analyses at 123.5°W showed elevated concentrations of autotrophs, dinoflagellates, and heterotrophic protists (Taylor et al. 2011). This station was also strongly dominated by the smaller size classes, which were responsible for the highest grazing and the highest biomass estimates of the zonal transect during EB05 (Figs. 4b, 5b). The higher migrant biomass at 130°W was not coincident with elevated community biomass, but was one of the highest grazing stations along the transect. Diatom biomass had the highest surface values observed for the zonal transect at this station (Taylor et al. 2011), suggesting that zooplankton grazing was elevated in response to enhanced concentration of larger phytoplankton.

Cruise comparisons

Median mesozooplankton biomass (± SE) estimated from the day-night averaged tows differed significantly between cruises: 2.27 ± 0.24 g DW m^{-2} in EB04 vs 3.13 ± 0.22 g DW m^{-2} in EB05 (Wilcoxon rank test, $p<0.05$). Substantial cruise differences were also apparent in community size structure (Fig. 6a). During EB04, the community was skewed towards smaller size classes, with < 2-mm animals composing 80% of biomass. Absolute biomass estimates were significantly higher for the three largest size classes during EB05 (Fig. 6a), and values for > 2-mm animals were over double those for EB04. Accordingly,

migrant biomass was higher during EB05, though not significantly so. Migrant biomass estimates also increased monotonically with size class for EB05 (Fig. 6b), but showed no coherent trend with size class during EB04. In particular, the vertically migrating fraction of > 5-mm zooplankton was markedly higher during EB05.

Cruise differences in total mesozooplankton grazing were similar to biomass trends, with significantly higher median (± SE) estimates during EB05 (3.39 ± 0.32 mg pigment m^{-2} d^{-1}) than EB04 (2.31 ± 0.34 mg pigment m^{-2} d^{-1}) (Wilcoxon rank test, $p<0.05$). During EB04, community grazing was strongly dominated by the small size classes, whereas EB05 displayed similar grazing across all size classes except the largest (Fig. 7a). Grazing estimates were thus significantly higher for the three largest classes in EB05 relative to EB04 *(*$p<0.05$), and lower, but not significantly so, for the smallest size class.

In addition to the different magnitudes and size-distributions of biomass between cruises, different patterns of biomass-specific grazing contributed substantially to the higher estimates of grazing by larger zooplankton on EB05 (Fig. 7b). While specific grazing rates were comparable between cruises for < 1-mm animals, the rates dropped much more sharply with increasing size for EB04 compared to EB05. Specific grazing estimates for the > 5 mm class on EB05 showed the highest variability. Very high values (high grazing, low biomass) were coincident with the presence of salps and other gelatinous organisms noted at the time of size fractionation. Diel grazing did not differ significantly among size classes in either year (not shown, Kruskal-Wallis $p>0.05$). During EB04, specific grazing rates were highest at night for the two smallest size classes, implying a natural cycle of nighttime-enhanced grazing by the smaller grazers, independent of vertical migration (Fig. 8a). The larger size classes showed no specific diurnal pattern.

During EB05, specific grazing was inversely related to size (Fig. 7b), with a pattern similar to EB04; the smaller size classes exhibited greater mean specific grazing rates, although the variability in this estimate increased with size. Biomass and grazing patterns in EB05 differed from EB04 in the higher daytime versus nighttime rates for the two largest size classes (Fig 8b). We attribute this difference to the presence of salps, which dominated biomass and gut pigment estimates when they occurred in the daytime collections in 2005 but were averaged with the influx of migrants in nighttime samples. Thus, the high filtration:biomass of salps disproportionately enhanced specific grazing rates during the day compared to the night. In addition, the hit-or-miss nature of collecting salps in any net tow underlies the high variability in grazing rate estimates for the large size classes in 2005.

Total percent removal of phytoplankton standing stock by mesozooplankton grazers was higher in 2005 than 2004, although this difference was not significant. Median (± SE) daily estimates, measured as the percentage of the water column swept clear of chlorophyll per day, were 10.7 ± 1.0 % d^{-1} for EB04 and 14 ± 1.4 % d^{-1} for EB05.

In order to investigate temporal variability in the region, we used estimates from stations located between 1°S-1°N, and 140°-122.5°W (see the delimited box in Fig. 1). The zonal section spans the transect portions sampled in both years. Number of stations considered for EB04 were substantially decreased due to few day/night stations sampled along the equatorial transect (n=3 for EB04; n=10 for EB05). Median mesozooplankton biomass estimates from the day-night averaged tows were not significantly different between years: 2.3 g DW m^{-2} (SE ± 0.9) in EB04 vs 2.9 g DW m^{-2} (SE ± 0.8) in EB05 (Wilcoxon rank test, $p<0.05$). Cruise differences in total mesozooplankton grazing were similar to biomass trends with no significant statistical differences between median (± SE) estimates of EB04

(4.12 ± 0.57 mg pigment m^{-2} d^{-1}) and EB05 (3.43 ± 0.34 mg pigment m^{-2} d^{-1}) (Wilcoxon rank test, $p<0.05$). Community size-structure patterns from this subset of stations were similar to the overall cruise trends, with a community dominated by smaller organisms during EB04 and a more equally distributed size-structure during EB05 (not shown).

Discussion

Mesozooplankton variability in relation to lower trophic levels

Latitudinal patterns of plankton biomass in the equatorial Pacific are often interpreted as a maturation of community composition with distance and time from the upwelling divergence source. Thus, in the advective flow from the upwelling source, suspension-feeding mesozooplankton are expected to peak at latitudes intermediate between those of their phytoplankton prey and carnivorous predators in accordance with their different rates of population response to changing environmental conditions (White et al. 1995; Zhang et al. 1995; Roman et al. 2002; Le Borgne et al. 2003). During EB04, for example, the increase in mesozooplankton biomass north of the equator at 110°W coincided with decreasing nitrate and iron concentrations and the shoaling of isotherms and Chl *a* isopleths (Selph et al. 2011). Integrated pigments and phytoplankton biomass were highest at 2°N (Selph et al. 2011; Taylor et al. 2011), and strong diatom peaks were present at 1° and 2°N (Taylor et al. 2011), while areal estimates of mesozooplankton biomass and spectral slopes increased to the northern end of our transect (4°N), consistent with the notion of slower growth rate resulting in spatial lags of biomass peaks (Figs. 2a, b). For a cross-equatorial transect at 180°W, Le Borgne et al. (2003) likewise reported high mesozooplankton biomass coincident with low phytoplankton biomass, and also with high indices of nitrogen regeneration, concluding that

these characteristics were indicative of a mature system with strong regulation by heterotrophs. Latitudinal progressions as a result of community maturation and *in situ* responses to the phytoplankton community can be observed at 110°W on the northern portion of the transect. Very strong peaks in diatom abundance were observed at 1°- 2°N, and peaks in total autotrophic carbon were present at 2°N. Mesozooplankton migrant biomass at 110°W showed a maximum at 2°N (Fig. 2b), while total biomass continued to increase to the end of the transect, with a maximum at 4°N (Fig. 2a), where migrant biomass was virtually absent (Fig. 2b). In general, mesozooplankton distributions to the south of the equator were quite different from those to the north, reflecting distinct asymmetry with respect to temperature, nutrients and phytoplankton community structure (Selph et al. 2011).

During EB05, mesozooplankton peaks at 1°S were prominent in distributions of total and migrant biomass and size spectral slopes. Outcropping of isopycnals and high concentrations of nitrate and iron at this station mark it as the source of equatorial divergence during our transect, and it was also the location of the highest integrated estimates of Chl *a* and phytoplankton biomass (Selph et al. 2011; Taylor et al. 2011). Relative to expectation, therefore, this transect was anomalous in having the highest concentrations of nutrients, phytoplankton and mesozooplankton at the same location. Interpretations of latitudinal patterns on cross equatorial transects can be complicated by the passage of instability waves and other features that cause the physical structure to vary around long-term means (e.g. Roman et al. 1995; Le Borgne et al. 2003) and by temporally aliased sampling along the transect. The extent of general southward flow both north and south around the equator on the EB05 transect (Selph et al. 2011), suggests that it was sampled during a period of unusual complexity which may have compressed the more typical latitudinal separation of phyto- and

zooplankton maxima (e.g. White et al., 1995). The mesozooplankton biomass maximum at 1°S, for example, is largely attributable to a peak in large diel migrants rather than smaller surface-living forms (Fig. 2b, c). Thus, it is possible that the unusual circumstances encountered at this station represent a displacement of surface water and biota into an area of migrant accumulation in deeper water, rather than an *in situ* response to local surface conditions.

Zonal variability in mesozooplankton biomass and grazing during EB04 generally showed spatial coherence with the meridional flow structure. The alternating peaks and troughs in mesozooplankton grazing coincided with meridional meanderings of the equatorial current, similar to the pattern observed for biogenic silica production (Krause et al. 2011). In addition, the higher biomass and grazing on the western end of the equatorial transect were positively associated with the gradients in dissolved iron (Kaupp et al. 2011), Chl *a* concentration (Selph et al. 2011) and phytoplankton biomass (Taylor et al. 2011) showing an apparent response to larger phytoplankton. Biomass and grazing estimates, and especially migrant biomass, also increased in the vicinity of 125°W, a station of high surface concentrations of diatoms and fucoxanthin (Selph et al. 2011; Taylor et al. 2011). Nonetheless, the enhancement of lower trophic levels did not always result in increased zooplankton. Consistent with the strong association between mesozooplankton and larger phytoplankton, a substantial peak in phytoplankton biomass at 115°W during EB04 was due mainly to autotrophic picoplankton (Taylor et al. 2011), and was not consequently reflected in either mesozooplankton biomass or grazing (Figs. 3b, 4b).

The TIW during EB05 resulted in high zooplankton biomass at ~125°W coinciding with strong southward meridional flow. The source of newly upwelled waters was probably

at 127°W, indicated by isopycnal outcropping and high nitrate concentration (Selph et al. 2011; Strutton et al. 2011), and these became advected to the west and east. A community dominated by small mesozooplankton grazers developed over these ~ 2 degrees, resulting in the observed biomass peak. Stations sampled west of the core of the TIW had very high surface concentrations of diatoms (Taylor et al. 2011), coinciding with higher dominance of large mesozooplankters (Fig. 4b) as well as a grazing community skewed towards the larger size classes (Fig. 5b). These mesozooplankton community parameters suggest a more mature community in which individual growth and population responses had sufficient time to develop the difference in size dominance structure evident in Figures 3b and 4b. Northward meridional flow suggests that these waters correspond to the leading edge of the TIW (Strutton et al. 2011), and the spatial differences in community composition along this transect can be thought of as analogous to those of the time evolution of a community responding to an increase in surface water nutrient concentrations.

Although variations in physical forcing and advection along the equatorial transects complicate biological interpretations at individual stations, a number of significant relationships emerge between mesozooplankton and lower trophic levels in the composite data. Table 1 compares mesozooplankton parameters (day-night biomass and grazing, migrant biomass and grazing) and mixed layer integrated and peak values of different components of the microplankton community (autotroph, heterotroph and total community carbon). Linear regressions were computed for each of these comparisons, and R^2 values are reported when relationships were significant (Table 1). As illustrated for nighttime zooplankton collections in Fig. 9, the strongest relationships ($p<0.01$) are between mesozooplankton biomass and peak biomass estimates of autotrophic, heterotrophic and total

protistan prey (data from Taylor et al. 2011). Peak biomass of autotrophs (i.e., phytoplankton) accounts for 70% of the observed variability in nocturnal zooplankton biomass, and the regressions for daytime and migrant biomass, while weaker, are also significant. No relationships were found between mesozooplankton and diatoms, which represent a very small component (~5%) of the phytoplankton (not shown). Depth-integrated biomass of the microplankton assemblage also did not predict zooplankton biomass, presumably because deeper euphotic zones compensate for lower plankton concentrations in the depth integrations and/or because zooplankton can effectively locate and exploit the depth strata of highest concentration or nutritional value. A combination of both these effects is suggested by the relationship of the 30 m integrated autotrophic and total microplankton biomass with mesozooplankton nighttime biomass, which is statistically significant (in contrast to full euphotic zone integrated values) yet explains less variability than peak concentrations (Table 1). The fact that no relationship was found between microplankton peak concentrations or standing stocks and mesozooplankton grazing rates is consistent with similar conclusions from previous studies done at 0°, 140°W. Dam et al. (1995), for example, found no statistical correlation between community grazing rate and integrated chlorophyll, primary production or chlorophyll-specific primary productivity.

Only migrant biomass was positively and significantly correlated with some estimates of euphotic zone and mixed-layer integrated microplankton biomass, as well as peak water column concentrations (Table 1). In addition, only migrants showed significant grazing relationships to prey (peak biomass) concentrations. If zooplankton migrants act in such a way as to maximize foraging success while minimizing vulnerability to predators, the biomass correlation can be understood as a consequence of their ability to locate efficiently

and exploit concentrations of suitable prey during their nocturnal excursions into the euphotic zone. Additionally, we can infer that a significant portion of the migrants are suspension feeders, as indicated by the singular positive relationship between migrant grazing and peaks in the microplankton prey field (Table 1).

Inter-cruise comparisons

The significant differences are a consequence of the gradients in physical conditions, with higher concentrations of Fe, phytoplankton and mesozooplankton in the western area of the region (140°W) than the east. The lack of significant differences between mean cruise comparisons when considering only overlapping stations is consistent with similar integrated values of phytoplankton community parameters (Taylor et al. 2011). However, climatological conditions were slightly different among years, with mild ENSO conditions occurring during EB04 and normal climatological conditions during EB05 (Balch et al. 2011; Strutton et al. 2011). This would account for the different community biomass and grazing size structures, as well as the observed differences in specific rates. The significant increase in biomass of the >2 mm size class suggests the potential for a more efficient transfer to higher trophic levels. Higher migrant biomass in 4 of the 5 size classes during EB05 (Fig. 6b, 7b), all of which contribute to community grazing, also implies greater export from the euphotic zone via fecal pellet production and transport and respiration at daytime depth (Zhang and Dam 1997).

In addition, the greater presence of filter-feeding gelatinous grazers during EB05 is reflected in the high ratios of grazing:biomass (i.e. specific grazing) in the 2-5 and > 5 mm size classes (Fig. 7b). The expected consequences of this change in community composition include more efficient grazing on smaller phytoplankton that are typically less available to

crustacean grazers, and enhanced production of large fast-sinking fecal pellets and carbon export from the euphotic zone. Consistent with slightly more oligotrophic conditions during EB04, biomass and grazing rates were more skewed towards the smaller organisms on that cruise (Fig. 6a, Fig. 7a). White et al. (1995) found similar biomass differences between the two EqPac Survey cruises conducted in 1992. They speculated that the reduction in size of zooplankton during El Niño years would translate to a reduction of export via reduced abundance, size and sinking rate of fecal pellets, leading to a reduction in carbon export with increasing oligotrophy in the system. While the measurements to specifically address this question were not taken in either of these studies, the size-structured biomass and grazing estimates of EB04 compared to EB05 are consistent with this prediction. In addition, comparing the spectral slopes of biomass (-2 to -1; Fig. 2b) and grazing (-3 and -2; Fig. 3b) along the meridional transect during EB04 indicates that herbivorous animals were disproportionately small relative to the total zooplankton assemblage. This difference could also be due to the half degree latitude offset of these two transects, allowing for the growth of the herbivorous community as waters are advected from the equator. However, if we consider the variation in size spectra for the meridional transects, the change across half a degree is usually less than a 0.5 difference in slope. This difference was also observed in the zonal transect along 110°W (Fig. 4b, Fig. 5b), but was not evident at 140°W and could therefore be reflective of different conditions in these two areas.

Because the number of day tows in the region of overlapping stations for the two cruises was very low for EB04, we use the nighttime estimates for quantitative comparisons of the microplankton community. Within this area, nighttime estimates of mesozooplankton biomass were 30% higher during EB05 relative to EB04 (3.9 ± 0.5 vs 3.0 ± 1.2 g C m^{-2},

respectively; p=0.016). Standing stocks of autotrophs (0.87 ± 0.13 vs 0.64 ± 0.016 g C m^{-2} ; p=0.00025) and total protists (1.34 ± 0.19 vs 0.93 ± 0.02 g C m^{-2}; p=0.00025) for the upper 30 m (microscopy data from Taylor et al. 2011) were also significantly elevated, although in slightly higher proportional quantities, 36 and 52%, respectively. Total depth-integrated values of protistan biomass for the full euphotic zone were not different between cruises. These results suggest that changes in upper mixed layer concentrations of phytoplankton and microzooplankton biomass more or less translated to proportional changes in mesozooplankton nighttime standing stocks. Such a relationship is absent when comparing euphotic zone integrated values, consistent with previous studies in the region (e.g. Le Borgne et al. 2003).

Comparison with other equatorial studies

We can compare our mesozooplankton biomass to previous estimates from the US JGOFS EqPac Program in 1992 (Roman a; Roman b; Roman c; Roman d), with modest adjustments to account for slightly different methods. The JGOFS estimates, for example, considered only organisms up to 2 mm in size and were integrated to 200 m. We thus computed our estimates for the same size range and considered our shallower sampling depth to give conservative estimates of the upper 200 m standing stocks. We also converted our dry weights to carbon biomass equivalents using % C:DW factors determined for the different size fractions in the subtropical North Pacific at Station ALOHA (Landry et al. 2001): 36, 35 and 38% for the 0.2-0.5, 0.5-1 and 1-2 mm size classes respectively. From EqPac, we used pooled data from samples collected between 1°N and 1°S on two spring cruises (El Niño conditions) and two fall cruises (normal upwelling), yielding median (± SE) biomass estimates of 27.5 ± 1.9 (n = 18) and 35.4 ± 4

(n = 14) mmol C m^{-2}, respectively. In comparison, our median cruise estimates for the 1°S-1°N, 140°-122°W box were 59 ± 9.5 (EB04; n = 8) and 71.5 ± 4 mmol C m^{-2} (EB05; n = 9). The number of tows considered during our study are about half those of EqPac, hence the greater SE. Considering the lower range of the median estimates from EB04 and EB05 (49.5 and 67.5 mmol C m^{-2}, respectively), mesozooplankton nighttime biomass was 80–90% higher than during the EqPac Program.

The difference between EqPac and present mean biomass estimates is intriguing in the context of other trends noted in north Pacific ecosystems over the same decade. For instance, zooplankton biomass increases have been noted in the Yellow and Japan/East Sea beginning in the early 1990's (Rebstock and Kang 2003). In collections of the CalCOFI program in the southern California Current, zooplankton biovolume has increased over the latter part of the decade from 1996-2006 (Fig. 2 in Lavaniegos and Ohman 2007). Moreover, monthly sampling in the North Pacific Subtropical Gyre (NPSG, Stn. ALOHA) beginning in 1994 has also shown a significant decadal increase in zooplankton standing stock (Sheridan and Landry 2004).

Nighttime biomass estimates for EqPac and the present study are plotted with respect to comparable NPSG data in Figure 10. Consistent with the relative rates of productivity in these adjacent open-ocean ecosystems and their different phytoplankton community size structures (Landry 2002), mesozooplankton standing stocks are on the order of double those found in the NPSG. That would be the conclusion from comparing results from both systems in the early 1990s, although EqPac predated the start of sampling at Stn. ALOHA by about a year. It would also be the conclusion from contemporaneous sampling of both systems in 2004 and 2005. Several scenarios can be

advanced to explain the relationships depicted in Fig. 10: 1) EqPac sampling may have underestimated mesozooplankton biomass because of the 1992 El Niño or other sampling artifacts. We doubt that this was the case because the study also included cruises during normal upwelling conditions. Nonetheless, if true, then the biogeochemical and ecological modeling of this region, which is based heavily on EqPac results, could be systematically underrepresenting the standing stock and roles of mesozooplankton. 2) Differences in sampling between these two studies could account for the observed trend. EqPac used a 0.25 m^2 MOCNESS net, while we used a 1 m ring net. One could speculate that our net caused higher plankter avoidance due to the existence of a bridle or less retention due to the coarser mesh used in our study (202 um) relative to that of EqPac (64 um). Conversely, our net may have fished more efficiently due to the reduced drag and bow wave associated with the use of a coarser mesh. The net effect of these methodological differences is therefore difficult to quantify. 3) Lastly, there have been proportional decadal increases in mesozooplankton standing stocks in the equatorial region and the NPSG, though not necessarily following the same timelines.

Although HNLC equatorial and subtropical systems are physically distinct and limited by different growth substrates (Fe vs N, P), they share some characteristics, such as dominance by small phytoplankton that grow at rapid, yet not maximal, physiological rates (Landry et al. 1997), and could be responsive to common physical mechanisms that make those substrates more available. Corno et al. (2007), for example, reported a 50% increase in primary production in the NPSG, at Stn. ALOHA, associated with decreased water column stability after the ENSO and PDO reversal event in 1997-1998. Increases in eukaryotic phytoplankton biomass and changes in community structure in the NPSG

during 1999-2004 have also been linked to climate variations leading to weaker upper ocean stratification and increased mixing (Bidigare et al. 2009). Wind forcing of nutrient fluxes to the euphotic zone was hypothesized to be influenced by large-scale physical interaction of the ENSO and PDO signals, with weaker trade winds when the signals were out of phase (i.e. prior to 1997-1998) and strengthening when their phases coincided (Corno et al. 2007). Using data from TAO buoys, Feely et al. (2006) documented an increase in trade wind strength in the equatorial region following the spring of 1998. Stronger trade winds in the equatorial region would drive increased upwelling circulation, and likely enhance the rate of supply of Fe to the euphotic zone. We hypothesize therefore that subtle, yet significant, increases in trade wind forcing and nutrient delivery could underlie parallel increases in system productivity and/or community size structure in the NPGS and equatorial Pacific between the early 1990s and present time. Such effects, if they are small, may be difficult to document in the instantaneous production rates done by different investigators, with different methods and in somewhat different locations and years. However, they appear to be reflected in the accumulated biomass of zooplankton, which integrates production and food-web transfer efficiencies on the scale of weeks to months.

Compared to EqPac, we also found much higher rate estimates for mesozooplankton grazing in equatorial waters. Our overall cruise averages (4.1 and 3.4 mg Chl *a* m^{-2} d^{-1} for EB04 and EB05, respectively) were over double the estimates of Zhang et al. (1995) for the equatorial latitudes. The highest value reported for JGOFS Survey cruises was 1.6 mg Chl *a* m^{-2}, while average values around the equator were closer to 1 mg Chl *a* m^{-2}. Our mean estimates of % Chl *a* grazed d^{-1} were more than three times those of EqPac (3 and 2.2 %

compared to 11 and 14% Chl *a*). Even maximum rates for the JGOFS cruises - 7.7 and 3.5% Chl *a* d^{-1} for Survey 1 and 2 (Zhang et al., 1995) and 5 and 9% Chl *a* for Time-series 1 and 2 (Dam et al. 1995)- were substantially lower than our cruise averages. These grazing differences are at least partly explained by the higher biomass levels on our cruises. However, methodological differences may also contribute to the disproportionately low estimates of grazing from EqPac, compared to the <2-fold biomass difference between EqPac and present cruises. In the numbers reported above we are including the two size classes not sampled during EqPac. However, the smallest three size classes (0.2-2 mm, sampled during both studies) are responsible for over 80% of the grazing (see Fig. 7a). The exclusion of the largest size classes does not significantly affect these overall trends in community grazing estimates. Gut pigment measurements on EqPac were based on crustacean zooplankton hand-picked from the samples. This could lead to pigment degradation in the picking process. However, we considered only uncorrected phaeopigment concentrations in our estimates, which would tend to make them more conservative than EqPac grazing estimates that were based on the sum of Chl *a* and 1.5 * Phaeo. The EqPac approach however excluded gelatinous zooplankton (salps and appendicularians). Since gelatinous suspension feeders exert a substantially higher grazing impact per unit of biomass than crustacean herbivores (Alldredge and Madin 1982), this is one area where the low grazing rate estimates from EqPac approach could have substantially underestimated community grazing.

Conclusions

In summary, our investigation of mesozooplankton biomass and grazing in the eastern equatorial Pacific has shown spatial patterns and interannual differences which reflect

variations in ENSO state, north-south and east-west trophic gradients and TIW effects. On the whole, however, and even when observed differences are statistically significant, the magnitudes of the variability are relatively modest given the broad sampling coverage. We can, as a consequence, characterize the mean levels of zooplankton standing stocks and grazing rates as being significantly elevated relative to those reported from EqPac studies of the region in 1992. These results are important as they suggest a possible decadal change in productivity or trophic structure in the HNLC equatorial Pacific, which has led to higher standing stocks of mesozooplankton. The magnitude of the change, approximately double, is in proportion to the documented zooplankton increase in the adjacent open-ocean ecosystem, the NPSG, and the changes in both systems may be linked to increased strength of the trade winds over this time period. Because of methodological differences and the lack of accurate time-series data, we cannot unequivocally point to this as the underlying mechanism for the observed change. Regardless, however, our data suggest that biogeochemical and ecosystem models of the equatorial Pacific tuned to EqPac data may substantially underestimate the current roles and impacts of mesozooplankton in the system. Our results therefore provide an important time point for testing and validating the behaviors of the models to decadal changes and physical forcing, which is essential for developing skill in making climate change predictions.

Acknowledgements

We are very grateful to the captain and crew of the *R.V. Roger Revelle* for their invaluable dedication and assistance. We also thank Chief Scientist, David Nelson and all of our colleagues for their key contributions to a successful study. Special thanks go to Karen Selph, Michael Stukel and Andrew Taylor for help with shipboard sampling, laboratory analyses and data sharing. This project was supported by National Science Foundation Grants OCE 0322074 and 0324666.

Chapter 1, in full, has been published in Deep-Sea Research II: Topical Studies in Oceanography: Décima, M, Landry, M. R., Rykaczewski, R. R., 2011. " Broad scale patterns in mesozooplankton biomass and grazing in the eastern equatorial Pacific". Deep-Sea Res II **58**: 387-399. The dissertation author was the primary investigator and author of this paper.

Table 1.1 Statistical results of regressions between mesozooplankton and microplankton community parameters for all values from EB04 and EB05. Significant relationships are indicated by a p-value < 0.05. R^2 values are reported when significant. All significant regression lines are positive. Microplankton data is from Taylor et al. (2011)

Mesozooplankton Night Biomass		
Mix layer biomass (mg m^{-2})	**R²**	***p*-value**
Autotrophs	**0.3**	**<<0.01**
Heterotrophs	-	NS
Peak biomass (μgC L^{-1})		
Autotrophs	**0.7**	**<<0.01**
Heterotrophs	**0.6**	**<<0.01**
All	**0.6**	**<<0.01**

Mesozooplankton Night grazing		
Mix layer biomass (mg m^{-2})	**R²**	***p*-value**
Autotrophs	-	NS
Heterotrophs	-	NS
Peak biomass (μgC L^{-1})		
Autotrophs	-	NS
Heterotrophs	-	NS
All	-	NS

Mesozooplankton Day Biomass		
Mix layer biomass (mg m^{-2})	**R²**	***p*-value**
Autotrophs	-	NS
Heterotrophs	-	NS
All	-	NS
Peak biomass (μgC L^{-1})		
Autotrophs	**0.2**	**0.03**
Heterotrophs	**0.2**	**0.02**
All	-	NS

Mesozooplankton Day grazing		
Mix layer biomass (mg m^{-2})	**R²**	***p*-value**
Autotrophs	-	NS
Heterotrophs	-	NS
All	-	NS
Peak biomass (μgC L^{-1})		
Autotrophs	-	NS
Heterotrophs	-	NS
All	-	NS

Migrant biomass		
Integrated biomass (mg m^{-2})	**R²**	***p*-value**
Autotrophs	-	NS
Heterotrophs	**0.2**	**0.048**
All	**0.2**	**0.03**
Mix layer biomass (mg m^{-2})		
Autotrophs	**0.2**	**0.02**
Heterotrophs	-	NS
All	**0.2**	**0.04**
Peak biomass (μgC L^{-1})		
Autotrophs	**0.5**	**<0.01**
Heterotrophs	**0.2**	**0.047**
All	**0.2**	**0.02**

Migrant grazing		
Integ. biomass (mg m^{-2})	**R²**	***p*-value**
Autotrophs	-	NS
Heterotrophs	-	NS
All	-	NS
Mix layer biomass (mg m^{-2})		
Autotrophs	-	NS
Heterotrophs	-	NS
All	-	NS
Peak biomass (μgC L^{-1})		
Autotrophs	**0.4**	**<0.01**
Heterotrophs	**0.2**	**0.027**
All	**0.2**	**0.04**

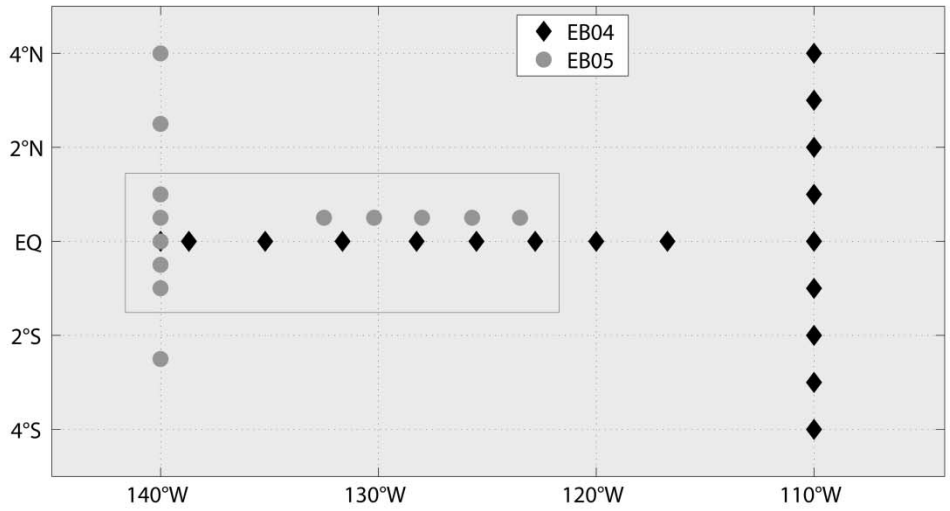

Figure 1.1. Station map. Meridional sampling during EB04 (♦) took place along 110°W, and along 140°W during EB05 (●). Zonal transects were conducted at the equator (EB04) and 0.5°N (EB05). The box marks the area sampled during both cruises, used for our seasonal comparison.

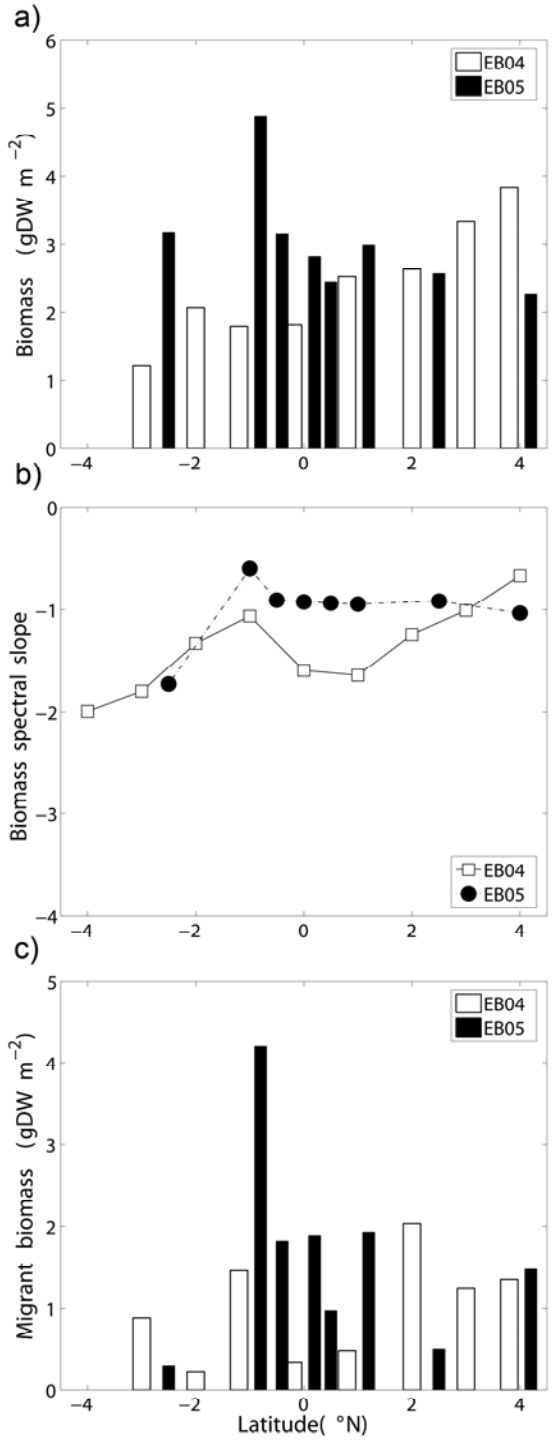

Figure 1.2. Latitudinal estimates of mesozooplankton biomass along 110°W during EB04 and along 140°W during EB05. a) Average day-night estimates; b) nighttime biomass spectral slopes; c) migrant biomass. Note that biomass estimates for 110°W only extend as far as 3°S, which was the last station with paired day-night tows.

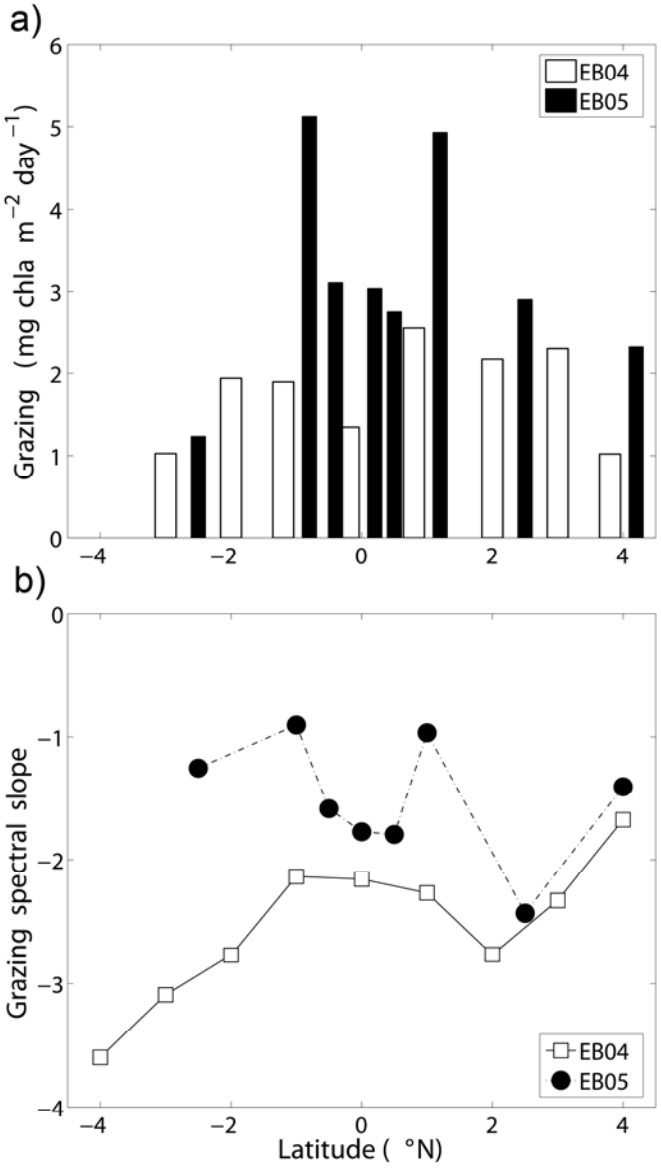

Figure 1.3. Latitudinal estimates of mesozooplankton grazing along 110°W during EB04 and along 140°W during EB05. a) Day-night averages; b) nighttime grazing spectral slopes.

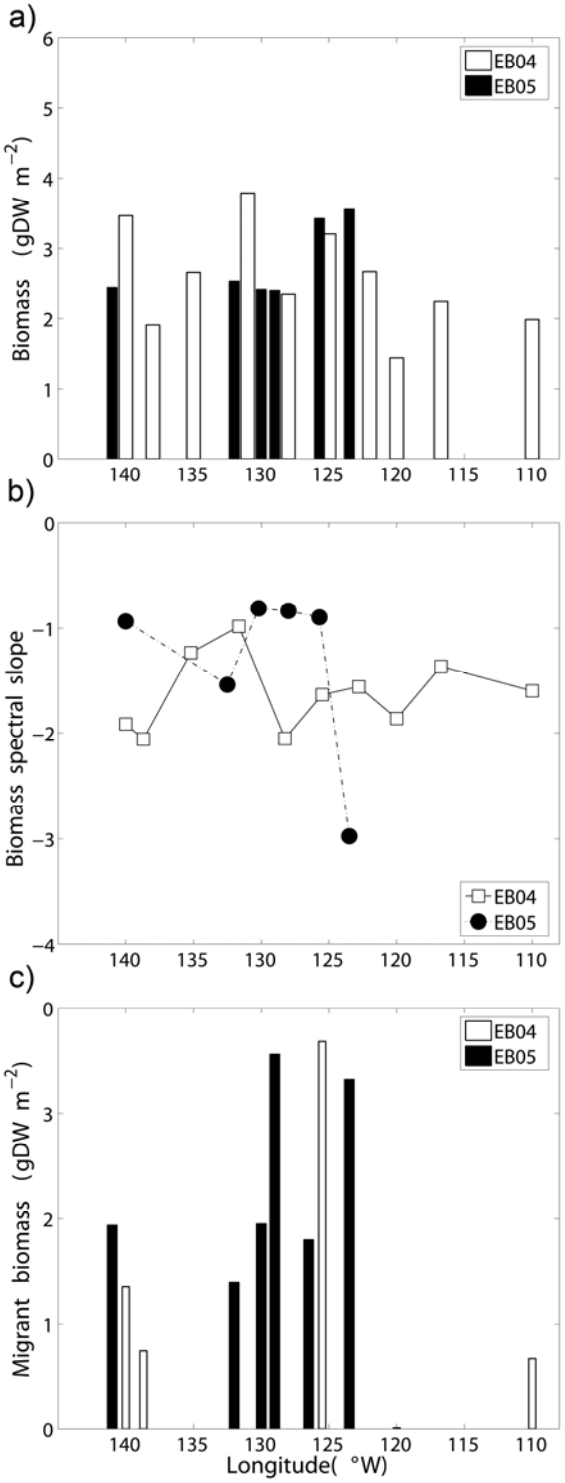

Figure 1.4. Zonal estimates of mesozooplankton biomass along the equator during EB04 and along 0.5°N during EB05. a) Average day-night estimates; b) nighttime biomass spectral slopes; c) migrant biomass.

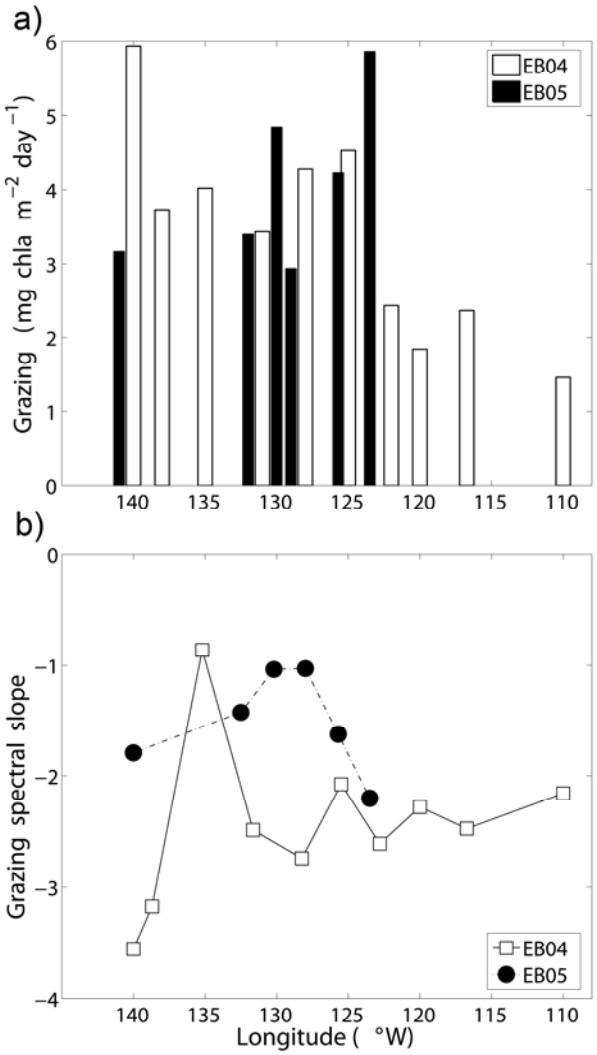

Figure 1.5. Zonal estimates of mesozooplankton grazing along the equator during EB04 and along 0.5°N during EB05. a) Day-night averages; b) nighttime grazing spectral slopes.

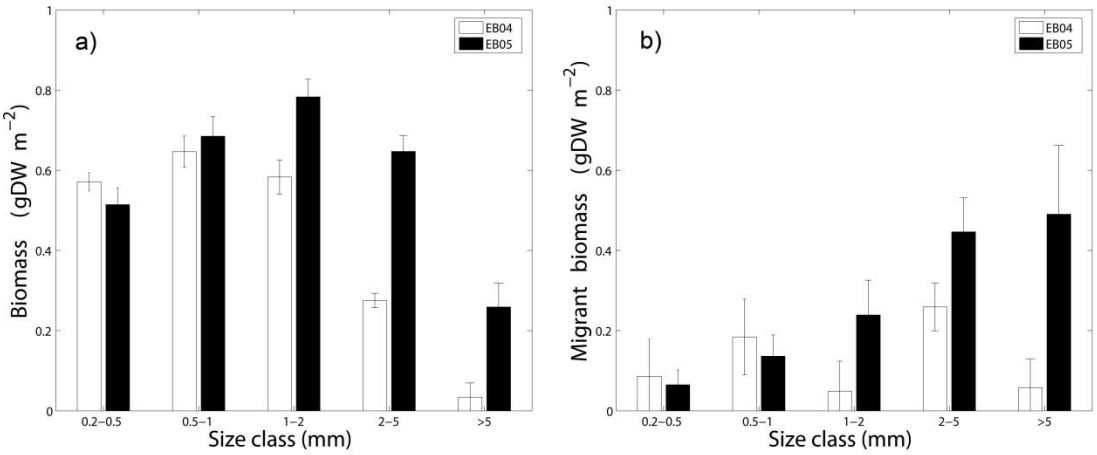

Figure 1.6. Median cruise average day-night biomass estimates of mesozooplankton by size class during EB04 and EB05 in the equatorial Pacific. a) Total community biomass; b) migrant biomass. Error bars are ± SE (n=12, EB04; n=14, EB05).

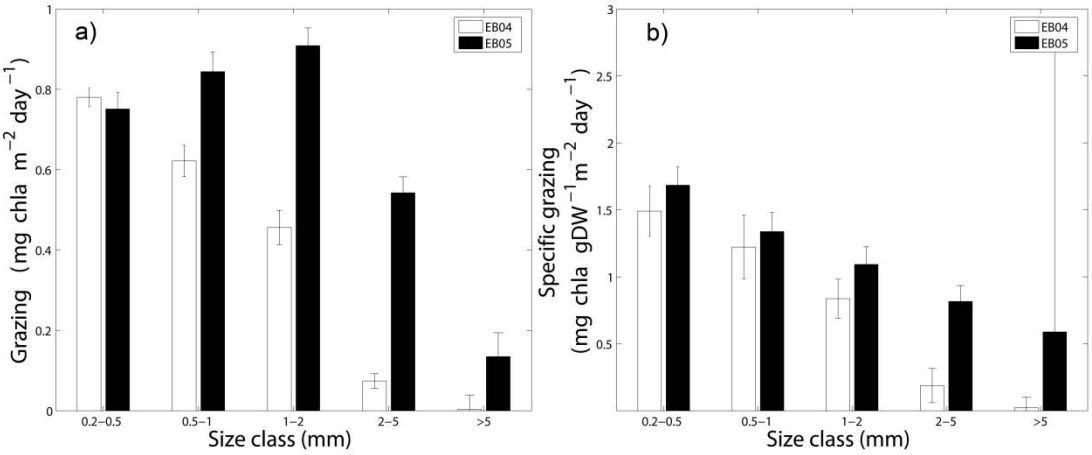

Figure 1.7. Median cruise grazing estimates of mesozooplankton by size class during EB04 and EB05 in the equatorial Pacific. a) Average day-night community grazing; b) biomass-specific grazing. Error bars are ± SE (n=12, EB04; n=14, EB05).

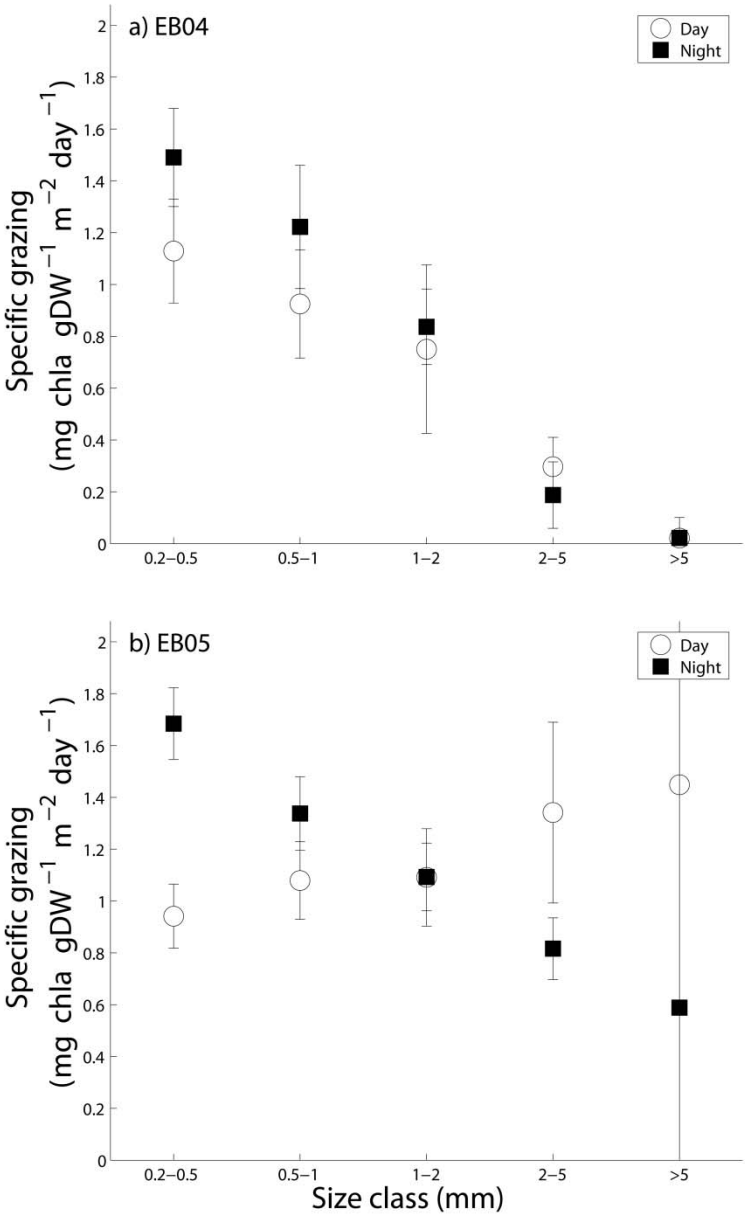

Figure 1.8. Day and night-time estimates of biomass-specific grazing rates during cruises EB04 (a) and EB05 (b). Error bars are ± SE (n=12, EB04; n=14, EB05).

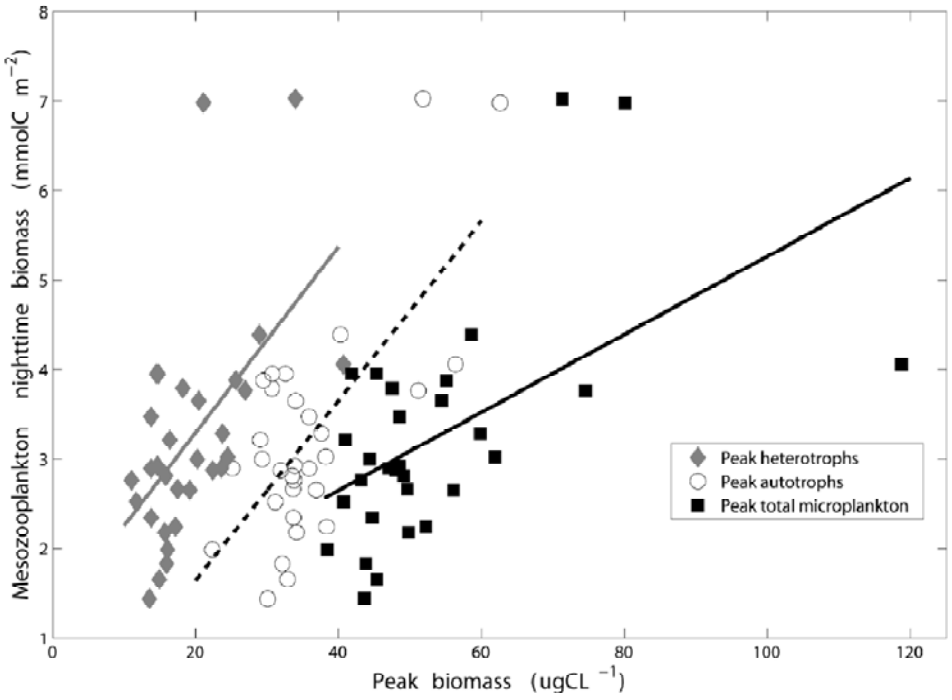

Figure 1.9. Relationship between nighttime biomass estimates of mesozooplankton and peak water-column concentrations of microplankton biomass for stations sampled on EB04 and EB05 cruises. *p*- and R^2 values are in Table 1.

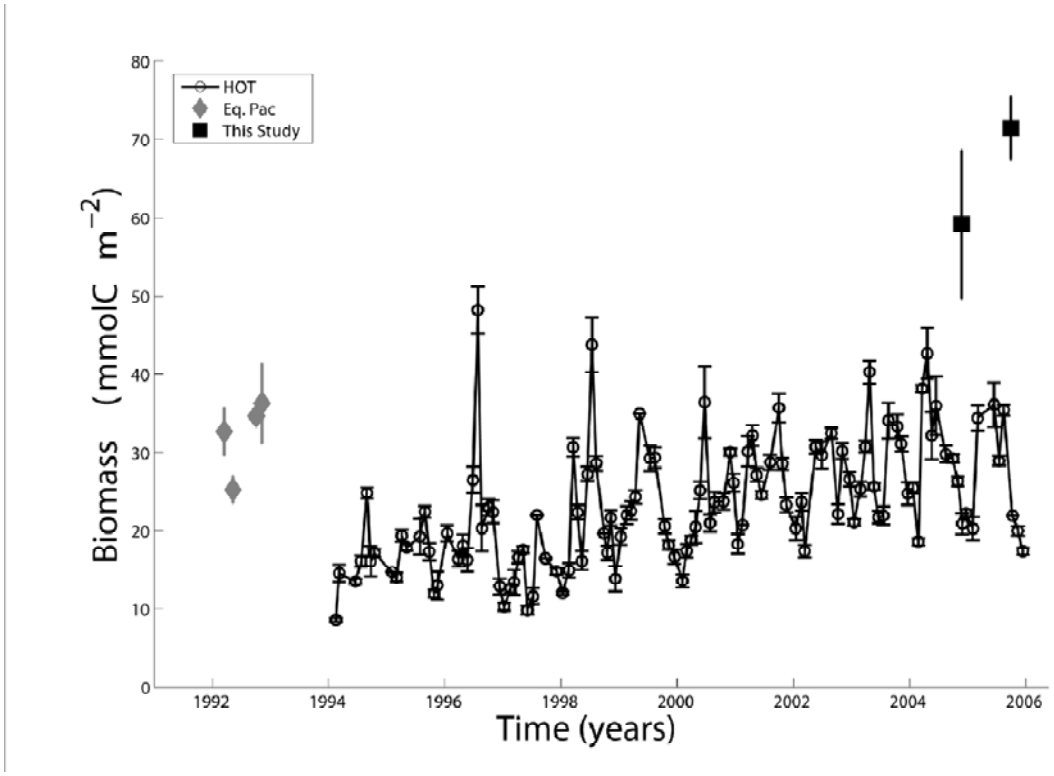

Figure 1.10. Temporal relationship between nighttime biomass estimates of mesozooplankton in the equatorial Pacific and the North Pacific Subtropical Gyre (NPSG). NPSG values are from time-series sampling at Stn. ALOHA; equatorial estimates are from US JGOFS EqPac program for 1992 and the present study for 2004 and 2005. The decadal increase for the NPSG extends the trend reported by Sheridan and Landry (2004).

References

Ainley, D. G., and R. J. Boekelheide. 1990. Seabirds of the Farallon Islands: Ecology dynamics and structure of an upwelling system community. Stanford University Press: Stanford, California, USA. p 450.

Al-Mutairi, H., and M. R. Landry. 2001. Active export of carbon and nitrogen at Station ALOHA by diel migrant zooplankton. Deep-Sea Res. II **48:** 2083-2103.

Alldredge, A. L., and L. P. Madin. 1982. Pelagic tunicates: unique herbivores in the marine plankton. Bioscience **32:** 655-663.

Balch, W. M., A. J. Poulton, D. T. Drapeau, B. C. Bowler, L. A. Windecker, and E. S. Booth. 2011. Zonal and meridional patterns of phytoplankton biomass and carbon fixation in the Equatorial Pacific Ocean, between 110°W and 140°W. Deep-Sea Res. II **58:** 400-416.

Bidigare, R. R., F. Chai, M. R. Landry, R. Lukas, C. C. S. Hannides, S. J. Christensen, D. M. Karl, L. Shi, and Y. Chao. 2009. Subtropical ocean ecosystem structure changes forced by North Pacific climate variations. J. of Plankton Res. **31:** 1131-1139.

Conover, R. J., R. Durvasula, S. Roy, and R. Wang. 1986. Probable loss of chlorophyll-derived pigments during passage through the gut of zooplankton, and some of the consequences. Limnol. Oceanogr. **31:** 878-887.

Corno, G., D. M. Karl, M. J. Church, R. M. Letelier, R. Lukas, R. R. Bidigare, and M. R. Abbott. 2007. Impact of climate forcing on ecosystem processes in the North Pacific Subtropical Gyre. Journal of Geophysical Research, Oceans **112:** doi: 10.1029/2006JC003730

Croll, D. A., B. Marinovic, S. Benson, F. P. Chavez, N. Black, R. Ternullo, and B. R. Tershy. 2005. From wind to whales: trophic links in a coastal upwelling system. Mar. Ecol. Prog. Ser. **289:** 117-130.

Dam, H. G., X. S. Zhang, M. Butler, and M. R. Roman. 1995. Mesozooplankton grazing and metabolism at the equator in the central Pacific: Implications for carbon and nitrogen fluxes. Deep-Sea Res. II **42:** 735-756.

Durbin, E. G., and R. G. Campbell. 2007. Reassessment of the gut pigment method for estimating *in situ* zooplankton ingestion. Mar. Ecol. Prog. Ser. **331:** 305-307.

Emerson, C. W., and J. C. Roff. 1987. Implications of fecal pellet size and zooplankton behavior to estimates of pelagic-benthic carbon flux. Mar. Ecol. Prog. Ser. **35:** 251-257.

Escribano, R., P. Hidalgo, H. Gonzalez, R. Giesecke, R. Riquelme-Buguenio, and K. Manriquez. 2007. Seasonal and inter-annual variation of mesozooplankton in the coastal upwelling zone off central-southern Chile. Prog. Oceanogr. **75:** 470-485.

Feely, R. A., T. Takahashi, R. H. Wanninkhof, M. J. McPhaden, C. E. Cosca, S. C. Sutherland, and M.-E. Carr. 2006. Decadal variability of the air-sea CO_2 fluxes in the equatorial Pacific Ocean. Journal of Geophysical Research, Oceans **111:** doi:10.1029/2005JC003129.

Kaupp, L. J., C. I. Measures, and K. E. Selph. 2011. The distribution of dissolved Fe and Al in the upper waters of the eastern Equatorial Pacific. Deep-Sea Res. II **58:** 296-310.

Kleppel, G. S., and R. E. Pieper. 1984. Phytoplankton pigments in the gut contents of planktonic copepods from coastal waters off southern California. Mar. Biol. **78:** 193-198.

Krause, J. W., D. M. Nelson, and M. A. Brzezinski. 2011. Biogenic silica production and diatoms' contribution to primary and new production in the eastern equatorial Pacific. Deep-Sea Res. II **58:** 434-448

Landry, M. R. 2002. Integrating classical and microbial food web concepts: Evolving views from the open-ocean tropical Pacific. Hydrobiologia **480:** 29-39.

Landry, M. R., H. Al-Mutairi, K. E. Selph, S. Christensen, and S. Nunnery. 2001. Seasonal patterns of mesozooplankton abundance and biomass at Station ALOHA. Deep-Sea Res. II **48:** 2037-2061.

Landry, M. R., R. T. Barber, R. R. Bidigare, F. Chai, K. H. Coale, H. G. Dam, M. R. Lewis, S. T. Lindley, J. J. McCarthy, M. R. Roman, D. K. Stoecker, P. G. Verity, and J. R. White. 1997. Iron and grazing constraints on primary production in the central equatorial Pacific: An EqPac synthesis. Limnol. Oceanogr. **42:** 405-418.

Landry, M. R., C. J. Lorenzen, and W. K. Peterson. 1994. Mesozooplankton grazing in the Southern California Bight .II. Grazing impact and particulate flux. Mar. Ecol. Prog. Ser. **115:** 73-85.

Lavaniegos, B. E., and M. D. Ohman. 2007. Coherence of long-term variations of zooplankton in two sectors of the California Current System. Prog. Oceanogr. **75:** 42-69.

Le Borgne, R., G. Champalbert, and R. Gaudy. 2003. Mesozooplankton biomass and composition in the equatorial Pacific along 180°. Journal of Geophysical Research, Oceans **108:** doi: 10.1029/2000JC000745

Longhurst, A. R., A. W. Bedo, W. G. Harrison, E. J. H. Head, and D. D. Sameoto. 1990. Vertical flux of respiratory carbon by oceanic diel migrant biota. Deep-Sea Res. I **37:** 685-694.

Miller, C. B. 2004. p. i-ix, 1-402. Biological oceanography. Blackwell Publishing; Malden, Oxford & Carlton.

Minas, H. J., M. Minas, and T. T. Packard. 1986. Productivity in upwelling areas deduced from hydrographic and chemical fields. Limnol. Oceanogr. **31:** 1182-1206.

Peterson, B., R. Emmett, R. Goericke, E. Venrick, A. Mantyla, S. J. Bograd, F. B. Schwing, S. Ralston, K. A. Forney, R. Hewitt, N. Lo, W. Watson, J. Barlow, M. Lowry, B. E. Lavaniegos, F. Chavez, W. J. Sydeman, D. Hyrenbach, R. W. Bradley, P. Warzybok, K. Hunter, S. Benson, M. Weise, and J. Harvey. 2006. The state of the California current, 2005-2006: Warm in the north, cool in the south. Calif. Coop. Ocean. Fish. Invest. Rep. **47:** 30-74.

Rebstock, G. A., and Y. S. Kang. 2003. A comparison of three marine ecosystems surrounding the Korean peninsula: Responses to climate change. Prog. Oceanogr. **59:** 357-379.

Richardson, A. J. 2008. In hot water: zooplankton and climate change. ICES J. Mar. Sci. **65:** 279-295.

Rollwagen Bollens, G. C., and M. R. Landry. 2000. Biological response to iron fertilization in the eastern equatorial Pacific (IronEx II). II. Mesozooplankton abundance, biomass, depth distribution and grazing. Mar. Ecol. Prog. Ser. **201:** 43-56.

Roman, M. a. "Biomass by organism size fraction and depth interval". United States JGOFS Data Server. Woods Hole Oceanographic Institution, USA: U.S. JGOFS Data Management Office, iPub: March 6, 1995.

Roman, M. b. "Biomass by organism size fraction and depth interval". United States JGOFS Data Server. Woods Hole Oceanographic Institution, USA: U.S. JGOFS Data Management Office, iPub: March 6, 1995.

Roman, M. c. "Biomass by organism size fraction and depth interval". United States JGOFS Data Server. Woods Hole Oceanographic Institution, USA: U.S. JGOFS Data Management Office, iPub: March 6, 1995. .

Roman, M. d. "Biomass by organism size fraction and depth interval". United States JGOFS Data Server. Woods Hole Oceanographic Institution, USA: U.S. JGOFS Data Management Office, iPub: March 6, 1995.

Roman, M. R., H. A. Adolf, M. R. Landry, L. P. Madin, D. K. Steinberg, and X. Zhang. 2002. Estimates of oceanic mesozooplankton production: a comparison using the Bermuda and Hawaii time-series data. Deep-Sea Res. II **49:** 175-192.

Roman, M. R., H. G. Dam, A. L. Gauzens, J. Urban-Rich, D. G. Foley, and T. D. Dickey. 1995. Zooplankton variability on the Equator at 140° W during the JGOFS EqPac Study. Deep-Sea Res. II **42:** 673-693.

Rykaczewski, R. R., and D. M. Checkley. 2008. Influence of ocean winds on the pelagic ecosystem in, upwelling regions. Proceedings of the National Academy of Sciences, United States of America **105:** 1965-1970.

Selph, K. E., M. R. Landry, A. G. Taylor, E.-J. Yang, C. I. Measures, J. J. Yang, M. R. Stukel, S. Christensen, and R. R. Bidigare. 2011. Spatially-resolved taxon-specific phytoplankton production and grazing dynamics in relation to iron distributions in the Equatorial Pacific between 110° and 140°W. Deep-Sea Res. II **58:** 358-377.

Sheridan, C. C., and M. R. Landry. 2004. A 9-year increasing trend in mesozooplankton biomass at the Hawaii Ocean Time-Series Station ALOHA. ICES J. Mar. Sci. **61:** 457-463.

Strickland, J. D. H., and T. R. Parsons. 1972. A Practical Handbook of Seawater Analysis.Bulletin 167 Fisheries Research Board of Canada p 310.

Strutton, P., A. Palacz, R. C. Dugdale, F. Chai, A. Marchi, A. E. Parker, V. Hogue, and F. Wilkerson. 2011. The impact of equatorial Pacific tropical instability waves on hydrography and nutrients: 2004-2005. Deep-Sea Res. II **58:** 284-295

Takahashi, K., A. Kuwata, H. Saito, and K. Ide. 2008. Grazing impact of the copepod community in the Oyashio region of the western subarctic Pacific Ocean. Prog. Oceanogr. **78:** 222-240.

Taylor, A., M. R. Landry, K. E. Selph, and E. J. Yang. 2011. Biomass, size structure and depth distributions of the microbial community in the eastern equatorial Pacific. Deep-Sea Res. II **58:** 342-357.

White, J. R., X. S. Zhang, L. A. Welling, M. R. Roman, and H. G. Dam. 1995. Latitudinal gradients in zooplankton biomass in the tropical Pacific at 140°W during the JGOFS EqPac study: Effects of El Niño. Deep-Sea Res. II **42:** 715-733.

Zhang, X., H. G. Dam, J. R. White, and M. R. Roman. 1995. Latitudinal variations in mesozooplankton grazing and metabolism in the central tropical Pacific during the US JGOFS EqPac Study. Deep-Sea Res. II **42:** 695-714.

Zhang, X. S., and H. G. Dam. 1997. Downward export of carbon by diel migrant mesozooplankton in the central equatorial Pacific. Deep-Sea Res. II **44:** 2191-2202.

CHAPTER 2

Body size-dependence of euphausiid spatial patchiness

By Moira Décima, Mark D. Ohman and Alex De Robertis

Abstract

We analyzed size-dependent variations in spatial patchiness of the eight numerically dominant euphausiid species in the California Current System (*Euphausia pacifica, Nematoscelis difficilis, Nyctiphanes simplex, Thysanoessa gregaria, Euphausia recurva, Euphausia gibboides, Thysanoessa spinifera, and Euphausia eximia*). Patchiness was measured by using a count-based statistic using euphausiid densities, and applied to 11 years of detailed size-specific enumerations from the California Cooperative Oceanic Fisheries Investigation program. We rejected the hypothesis of size-independent patchiness for 7 of the 8 species. The most common pattern observed was a 'U-shaped' curve, showing elevated patchiness in the smallest size classes, a rapid decrease in patchiness of intermediate-sized euphausiids, and a later increase in patchiness of adults following the onset of reproductive maturity. These size-dependent changes parallel ontogenetic changes in spatial dispersion observed for some marine fishes. The initial descending limb of the patchiness curve appears to be caused by turbulent diffusion, while the later ascending limb of the curve is consistent with the onset of predator-induced aggregation behavior. The patterns were surprisingly

consistent across years and different reproductive characteristics (egg-brooding vs. broadcast spawning euphausiids).

Introduction

The ecological and evolutionary importance of spatial pattern of marine organisms has long been recognized (Hutchinson 1953; Steele 1978; Levin 1992) and efforts to establish and understand spatial distributions are a central issue in marine ecology. Patchiness (its existence, causes, dynamics) has been investigated for numerous organisms ranging from phytoplankton (Kierstead and Slobodkin 1953; Wroblewski and O' Brien 1976) to fish (Hewitt 1981), and on different spatial scales (Weber et al. 1986; Steele and Henderson 1992; Levin et al. 1993). Factors leading to aggregation are varied, with physical and biological processes contributing differentially to species' distributions. Wroblewski and O'Brien (1976) found that the combination of both physical factors (nutrients, light, etc.) and grazing pressure ultimately determine the critical size as well as persistence of a phytoplankton patch. Weber et al. (1986) described the variance in the spatial spectra for temperature, phytoplankton and Antarctic krill. Physical processes were largely responsible for the red spectrum displayed by phytoplankton, but in order to explain the flatter spatial spectrum of krill, biological processes were invoked (e.g., swimming behavior and/or vertical migration).

Common marine planktivores, such as adult pelagic fish, have distributions that are extremely patchy, typically caused by their schooling behavior (Matsuura and Hewitt 1995). Schooling may help fishes avoid predators, increase efficiency of finding and exploiting prey patches, increase swimming efficiency, and ensure reproduction (Matsuura and Hewitt 1995; Parrish and Turchin 1997). Previous studies of variations of patchiness with body size of some pelagic fishes have reported a 'U-shaped' curve with ontogeny (Hewitt 1981; McGurk 1987; Matsuura and Hewitt 1995). In this pattern,

patchiness of eggs and young larvae is typically very high, reflecting the aggregation of the spawning adults, followed by a rapid decrease in patchiness of older larvae as a consequence of turbulent diffusion. Later in the life history, patchiness increases rapidly as fish develop better sensory capabilities and body musculature, leading to the onset of schooling behavior (Hewitt 1981; Matsuura and Hewitt 1995). Fish patchiness may also be related to fish spawning modes and/or habitats (McGurk 1987). The distributions of demersal vs. pelagic eggs are affected differently by turbulent diffusion. Demersal spawning species are not affected by diffusion until the larval stages emerge into the water column, in contrast to free-spawning pelagic species whose propagules experience turbulence from the moment of spawning. These differences are thought to contribute to the different magnitudes of the U-shaped pattern observed in anchovy and jack mackerel, which are pelagic spawners, in contrast to Pacific herring, a demersal spawner (Hart 1973). The processes creating aggregated distributions are therefore of both physical and biological origins. The relative contribution of the two, however, is highly variable among species as a consequence of the variability of species characteristics such as body size, swimming ability, spawning mode, and other life-history traits.

Euphausiids are relatively large crustacean members of the zooplankton or micronekton. Many species have been reported to form dense aggregations, and in general their distributions are known to be extremely patchy, especially as adults (Mauchline 1980). When mature, euphausiids bear five pairs of pleopods that confer excellent routine swimming ability, in addition to their rapid caridoid escape behavior made possible by a muscular abdomen (Mauchline 1980). Hence, as adults, euphausiids have the potential to exhibit behavioral control over their local distributions.

Here we investigate patchiness as a function of euphausiid body size. We were specifically motivated to determine whether the U-shaped pattern documented for marine fishes is applicable to euphausiid crustaceans. In addition to testing the null hypothesis of size-independent spatial patchiness of euphausiids, we sought to determine whether patchiness varies with reproductive characteristics (free-spawning vs. egg brooding) of different euphausiid species. For these analyses we utilize the extraordinary data from E. Brinton's career analyses of euphausiid population biology in the California Current System (Brinton and Townsend 2003).

Methods

Euphausiid collection

Euphausiids were sampled by the California Cooperative Oceanic Fisheries Investigations (CalCOFI) program. Time series of euphausiid abundance have been presented by Brinton and Townsend (2003). We restricted our analyses to the Southern California portion of the CalCOFI pattern (Fig. 1) since this was the region most consistently sampled over time. Only night time samples were considered as they more accurately represent the underlying abundances; many of the species considered here are known to either exhibit diel vertical migration, net avoidance, or both (Brinton 1967). Eleven years of data (1953-1959, 1969, 1978, 1984, and 1991) were used, from winter, spring, summer, and fall cruises in most years, except 1978 when we did not have data for the fall, and 1991 when only springtime data were available (Table 1). These eleven years were selected because enumerations were available by euphausiid species and size class (to the nearest mm) from 1 mm sized individuals to adults. The smallest size class

considered here (1 mm) corresponds to the calyptopis phase. The water column was sampled by a 1-m ring net from 140-0 m in 1953-1959, the same net from 210-0 m in 1969, and a 0.71-m diameter bongo net sampled from 210-0 m from 1978 onwards (Table 1); net mesh sizes were either 0.550 mm or 0.505 mm (details in Ohman and Smith 1995). Numbers of euphausiids per 1000 m^3 of water filtered were converted to numbers m^{-2} from:

$$\frac{\text{No.}}{\text{m}^2} = \left[\frac{\left(\frac{\text{No.}}{1000\ \text{m}^3} \right)}{1000} \right] \text{Max Depth} \qquad (1)$$

where Max Depth is the maximum fishing depth of the sampling net.

The species considered here have different distributional ranges both in the Northeast Pacific and within the Southern California CalCOFI grid. While the eight species we analyze are the numerically dominant euphausiids in this region, they are neither restricted to our sampling area, nor are they equally distributed within this portion of the grid. The following classification is from Brinton and Townsend (2003): Cold water; widespread, oceanic, young phases commonly coastal: *Euphausia pacifica*; Cold water, coastal; strong net avoider: *Thysanoessa spinifera*; Transition Zone-cool; animals widespread within thermocline, not vertical migrators: *Nematoscelis difficilis*, *Thysanoessa gregaria*; Transition Zone-warm; to west and south-west in survey sectors, vertical migrators: *Euphausia recurva* and *Euphausia gibboides*; and Sub-tropical, and marginally tropical: *Euphausia eximia*, oceanic and *Nyctiphanes simplex*, coastal.

The patchiness index

In order to quantify patchiness we used an index modified from Lloyd's original index (Lloyd 1967). Lloyd's index, P, was designed for use with counts and is defined as:

$$P = 1 + \left(\frac{(\sigma^2 - m)}{m^2} \right) \quad (2)$$

where m and σ^2 are the mean and variance of the sample count, respectively. Although many studies use numerical densities for this computation, Bez (2000) points out that the use of this index is only sensible when using counts. Meaning is lost when densities are used for calculating m and σ^2 due to the heterogeneity of units. More importantly, different patchiness values arise when using different density units. An example would be expressing numbers of individuals per m^2 vs. per 10 m^2 (Table 2, case A vs. B). Bez (2000) suggests the use of another index of aggregation (I_a) which is appropriate for densities. I_a is given by:

$$I_a = \frac{\sum_i z_i^2}{\left[s\left(\sum_i z_i \right)^2 \right]} \quad (3)$$

where z_i is the density of organisms in a given sample and s is the size of the sampling unit used in the survey (note also that I_a is normalized and thus independent of total abundance in the sample area). The index assumes that the whole range of the species in question has been sampled, thus the addition of zeroes has no effect on the patchiness

value (Table 2, case B vs. D). We use an index similar to Bez's I_a, modified for our sampling site and scheme, because we cannot assume that we have sampled the whole range for any of the species here considered (Brinton et al. 1999). Our modified index is given by:

$$I_{mod} = \left[\frac{\sum_i z_i^2}{s\left(\sum_i z_i\right)^2} \right] N \qquad \text{or} \qquad I_{mod} = I_a \bullet N \tag{4}$$

where N is the number of stations sampled. For simplicity, we set s to 1 to generate a relative index, as approximately 1 m^2 was sampled by each net. Because sampling was done following similar protocols, the area sampled was similar for all our comparisons. For a different value of s the index would simply be scaled in proportion to 1/s. Any bias arising as a consequence of our choice of s (Bez 2000) would be consistent across all size classes and species. Analogous to I_a, I_{mod} is robust to changing density units (Table 2, Case A vs. B). It does not assume zero densities in unsampled areas, and accurately expresses the same value of patchiness when two underlying distributions are the same yet one is more completely sampled (Table 2, Case B vs. C). The index is sensitive to zeros (Table 2, Case B vs. D), such that greater sampling resulting in zero density estimates count towards greater patchiness, unlike I_a which assumes equal patchiness in both cases. I_{mod} is a more appropriate measure of patchiness for our study.

As mentioned earlier, not all species have the same distribution within the grid and some species are known to experience changes in their north-south ranges as a

function of oceanographic conditions (Brodeur 1986). Range reductions and expansions could affect the number of stations with zero individuals, and thus artificially inflate the patchiness value. To account for this effect we reduced the number of stations considered to the area within a cruise where each species occurred. We restricted our northern limit to the northernmost line with one individual at any station, and the southern limit in the same way. The offshore limit was set by the westernmost station with one individual present. These considerations were applied to the range of every species for a given quarter (winter, spring, summer, and fall), which were the sampling blocks used in the computation of the patchiness index.

Patchiness values were calculated for the entire inhabited region and separately for the inshore and offshore domains (defined as in Fig. 1, Aksnes and Ohman 2009). We computed mean values as well as the coefficient of variation ($(\text{c.v.} = \frac{\sigma_h^2}{m_h})$, where the subscript h refers to a hydrological variable) for chlorophyll *a* and temperature values from 30 m depth of all stations in the grid, together with Secchi disk depths, for all cruises from 1984 to present. For the physical-chemical data we used c.v. instead of I_{mod} to express heterogeneity because hydrographic variables have continuous underlying distributions, and thus I_{mod} is not appropriate. The physical-chemical data originate from the CalCOFI database.

Statistical analysis

Analysis was carried out using Matlab 7.5. Mean patchiness values were computed by averaging the 40 patchiness estimates (from the eleven years considered)

for each species, along with respective parametric 95% confidence intervals. The Jonckheere-Terpstra test for ordinal data (Hollander and Wolfe 1973) was used to test the significance of the descending and ascending limbs of the patchiness-length curves. This statistic tests the null hypothesis of no sequence to the population medians against the alternative hypothesis that the population medians are ordered in a particular direction. For multiyear comparisons, as well as for the comparison before and after 1978, we used Kruskal-Wallis one-way analysis of variance.

Results

Patchiness vs. body size

The eight numerically dominant euphausiid species in this region have substantially different average abundances (Fig. 2, note log scale). Abundances are listed primarily in decreasing order in Fig. 2 and throughout the presentation of our results. A clear pattern of higher patchiness in the smallest size classes, followed by an abrupt decrease in patchiness and a subsequent increase in the largest size classes, was evident for the four most abundant species: *Euphausia pacifica*, *Nematoscelis difficilis*, *Nyctiphanes simplex*, and *Thysanoessa gregaria* (Fig. 3). A similar, but less pronounced pattern was suggested for the next four species (*Euphausia recurva*, *Euphausia gibboides*, *Thysanoessa spinifera*, and *Euphausia eximia*, Fig. 3).

In order to test the null hypothesis of size-independent patchiness, we evaluated the initial decrease and the subsequent increase in patchiness separately. For the descending limb of the curve we considered the first four size classes (Fig. 4a). A significant decrease in the patchiness index I_{mod}, as measured by the Jonckheere-Terpstra

test for ordered alternatives, was detected for 6 of 8 species ($p < 0.05$, Fig. 4a). The initial decline was not significant ($p > 0.05$) for either *E. gibboides* or *T. spinifera*. For the ascending limb of the curve we considered the length class at which maximum patchiness was attained, along with the preceding four size classes (Fig. 4b). For 6 of 8 species, we observed increasing patchiness with increasing body size of adults ($p < 0.01$, Fig. 4b). The observed increase was not significant ($p > 0.05$) for either *T. spinifera* or *E. eximia*.

Arrows on the abscissa on Fig. 3 indicate the body length at the first appearance of secondary sexual characteristics for each species, from Brinton et al. (1999). The increase in patchiness of larger body-sized individuals did not coincide with this size class, however there was usually an inflection point denoting an increase in mean patchiness 3-5 mm after the first onset of secondary sexual characteristics.

Temporal differences in patchiness

We investigated temporal variability in patchiness at three different scales. We first examined seasonal differences in aggregation for all species, and found no consistent seasonal differences in patchiness as a function of body-size for any of these species (not shown).

We also investigated patchiness differences among the years of our study (Fig. 5) specifically with reference to the strong El Niño-Southern Oscillation (ENSO) conditions of 1958-59. Neither 1958 nor 1959 stands out for either abnormally high or low patchiness. However, 1955 showed generally higher patchiness in at least some size classes for all species. The year 1955 was characterized by early and intense upwelling

(Brinton 1976). These differences, however, were not statistically significant for any of the euphausiid species ($p>0.05$).

Finally, we examined aggregation patterns before and after the cool-to-warm transition in the Northeast Pacific 1976-1977. For this purpose we compared patchiness for the years prior to the transition (1953-1959 plus 1969) vs. those afterwards (1978, 1984, and 1991). Results were significant for only some size classes of some species (range 0-4 size classes, $p<0.05$), although no consistent relationship was found in these differences among species (not shown).

Spatial differences in patchiness

We divided the study region into two subregions, designated inshore and offshore (Fig. 1), in order to assess whether euphausiid patchiness varied with spatial differences in heterogeneity of the physical-chemical environment. The inshore region was, on average, cooler with higher chlorophyll *a* concentrations and shallower Secchi disk depths than the offshore (Fig. 6a-c), as would be expected since much of this region is influenced by coastal upwelling in the vicinity of Point Conception. The coefficient of variation (c.v.) of Secchi disk depth and temperature was elevated inshore relative to offshore stations ($p<0.05$, Wilcoxon Signed Rank test, Fig. 6d-f), but there was no significant difference in c.v. of chlorophyll *a* ($p>0.05$). Calculation of euphausiid patchiness in the corresponding two spatial regions revealed that when the ascending limb and descending limbs of the curve were present, they were found in both inshore and offshore regions for each species (Fig. 7). When there was a significant difference ($p < 0.05$) between the two patchiness curves, the inshore portion of a species population

was always characterized by higher patchiness with respect to the offshore counterpart. The two smallest Transition-zone species, *T. gregaria* (cool) and *E. recurva* (warm) showed increasing departures between inshore and offshore patchiness curves with increasing size (Fig. 7).

Reproductive differences: free spawners vs. brooders

We investigated the hypothesis that patchiness-length curves differ between species displaying different reproductive modes. For this purpose we considered the two egg-brooding species (*Nematoscelis difficilis* and *Nyctiphanes simplex*) in relation to the remaining six species, all of which spawn their eggs freely into the water column. There was no consistent difference in patchiness pattern between the two reproductive modes (*see* Fig. 3). In Fig. 8 we more closely compare two free-spawning species (*E. pacifica* and *T. gregaria*) with two egg-brooding species (*N. difficilis* and *N. simplex*). These pairs of species are the most comparable in abundance and also in having one member that reaches a relatively large adult length (22 and 26 mm for *E. pacifica* and *N. difficilis*, respectively) and one of each that reaches a relatively small adult length (13 mm and 16 mm for *T. gregaria* and *N. simplex)*. All four species have well defined U-shaped patchiness-length curves (Fig. 8, $p<0.01$ from Fig. 4) and the overall magnitude of patchiness was similar.

Discussion

We reject the hypothesis of size-independent patchiness for 7 of 8 species of numerically dominant California Current euphausiids. Only *T. spinifera* showed neither

an initial decrease in patchiness for the smallest size classes nor a subsequent increase in patchiness for the largest size classes, or both. The most common pattern we detected was a U-shaped trend with body size, characterized by elevated patchiness in the smallest size classes, a decline to minimum values in intermediate size classes, with an increase for the largest size classes after the onset of reproductive maturity.

The mechanisms that lead to zooplankton patchiness can be broadly classified into those of physical (e.g., turbulence, shear, habitat heterogeneity) and those of biological (e.g., intraspecific and interspecific interactions) origins. Our interpretation of the mechanisms leading to the U-shaped pattern observed in the euphausiid patchiness-length curves in some respects parallels patterns described previously in changes of fish patchiness with ontogeny (Hewitt 1981). The descending limb of the patchiness curve is most consistent with the consequences of physical processes: turbulent diffusion would lead to dispersion of organisms and a substantial decrease in larval patchiness with body size. The smallest size classes considered here correspond to the calyptopis life history phase (eggs, nauplii, and metanauplii were not collected quantitatively by the net mesh used). Development time to reach the calyptopis stage is highly variable among species (especially with different reproductive strategies) and is temperature-dependent, but seems to be on the order of hours to 10 days (Gomez-Gutierrez 2002; Gomez-Gutierrez 2003). Calyptopes are able to both feed and swim, however their ability to determine their position in the water column actively or respond to conspecifics is greatly reduced, given their small size and undeveloped pleopods (Brinton et al. 1999). We infer that the very high initial patchiness of the smallest size classes is a result of the aggregation of spawning adults, with passive dispersion of weakly swimming larvae assumed to be the

dominant process leading to subsequent low I_{mod} values as the organisms develop and grow.

In contrast, the ascending limb of the patchiness curve is inconsistent with physical processes alone. If the only mechanisms affecting aggregation were physical processes such as advection and diffusion we would expect the patchiness curve to approach a generally low, uniform pattern at large body size, as the distribution of the larger and older animals becomes more evenly spread out over time. Instead, we see increasing patchiness in the larger size classes of all euphausiids. Furthermore, the onset of this pattern is related to interspecific differences in adult body size rather than a fixed absolute size for all species. The ascending limb of the patchiness-length curve is likely governed by biological processes. We can subdivide the likely biological processes into those where euphausiids respond to one another (e.g., reproductive aggregations, schooling for hydrodynamically efficient swimming) and those in which euphausiids respond to external stimuli (e.g., changes in the physical-chemical environment, prey resources, or the predator field).

Active aggregation into cohesive units has been extensively reported and studied for the Antarctic species *Euphausia superba* (Hamner et al. 1989; Watkins and Murray 1998). The distribution pattern of each life history stage of this species has also been argued to be a product of both physical and biological processes (Nicol 2006). Differential aggregation with size has also been reported for this species (Watkins et al. 1992; Johnson and Tarling 2008). These aggregations are hypothesized to confer antipredatory benefits and increase foraging efficiency (Hamner and Hamner 2000), optimize food capture and energy expenditure (Ritz 2000), and also to confer

reproductive benefits as reported for many species of euphausiids (discussed below). The California Current species have not been reported to form true schools (i.e., individuals with parallel orientation and constant nearest-neighbor spacing) in situ, and therefore we do not consider it likely that schooling benefits such as hydrodynamic efficiency are the ultimate factors leading to their aggregation. A few California species, however, are known to form visible aggregations that do not have the organized character of a school, a form of aggregation we call a 'swarm.'

Although the absolute scale of patchiness cannot be inferred from the index of patchiness we have used, the station spacing at which we have sampled must be kept in mind while interpreting our results. The shortest spacing between two CalCOFI stations occurs inshore and is on the order of 20 km (Fig. 1). In general, our sampling is on the order of 20 to 60 km (considering the spacing of stations both inshore and offshore). For the species for which swarming has been documented, daytime surface swarms occur occasionally (Brinton and Townsend 2003) and nighttime dense aggregations have also been reported (H. C. Shin pers. comm.). These types of swarms would contribute to our measure of patchiness. Therefore, although the aggregations our metric has detected are, in principle, at the mesoscale, our index would also be influenced by smaller scale processes.

Surface swarms of euphausiids for sexual purposes have been observed in different regions of the Northeast Pacific for a number of species analyzed here (Endo et al. 1985; Smith and Adams 1988; Gendron 1992). In our case, we noted that the onset of increased adult patchiness began not at the size of first sexual maturity, but a few size classes later. A better metric of the reproductive status of the population than initial onset

would be the length at which 50% of individuals have attained reproductive maturity, though we do not have pertinent data available. The consistent increase in patchiness at a size 3-5 mm beyond the initial onset of maturity suggests that reproductive benefits cannot be ruled out as an explanatory factor.

Diel vertical migration (DVM) behavior of adult euphausiids could potentially also affect the observed pattern. Segregation between larval and adult stages has been shown to occur due to the migration of adults in areas of intense upwelling characterized by sheared flows, via transport of larvae offshore and retention of adults onshore (Mackas et al. 1997). Depth and timing of DVM have also been shown to vary with adult size, with larger organisms descending deeper in the water column (Bollens et al. 1992) and spending proportionally less time at the surface at nighttime (De Robertis 2002). However, two non-migrating species, *N. difficilis* and *T. gregaria*, have very strong ascending limbs in their patchiness curves (Fig. 3). DVM therefore seems unlikely to be the principal mechanism underlying the pattern we observed.

Where patchiness is exclusively a vectorial response (Hutchinson 1953), i.e., a response to common external stimuli in the environment, a general expectation is that aggregations of organisms would be enhanced where the external stimuli are heterogeneous. We observed that the inshore region we analyzed was more heterogeneous than the offshore region (Fig. 6) with respect to temperature and water column transparency (which influences encounter distances with visually hunting predators). For some euphausiid taxa we detected elevated patchiness in the inshore region, suggesting that increased environmental heterogeneity does indeed contribute to the non-random distribution of the organisms. However, it is noteworthy that the

ascending limb of the size-dependent patchiness curve also occurred in the offshore region, where the external environment showed less heterogeneity. Hence, we conclude that there is a biological cause of patchiness in larger-sized euphausiids that persists independent of the external environment, but can be enhanced by it. This is consistent with modeling studies that have shown individuals in homogeneous environments displaying behavior that leads to patchy distributions (Deutschman et al. 1993). Random movement coupled with predator-prey interactions has also been shown to produce aggregated distributions in homogenous environments (Deutschman et al. 1993).

Euphausiid aggregations in the California Current have been associated with topographic breaks (Schoenherr 1991; Croll et al. 2005), along continental shelf breaks (Simard and Mackas 1989; Mackas et al. 1997), submarine canyons (Croll et al. 2005), and around the vicinity of the Channel Islands (Croll et al. 1998). In the present study, the region we have defined as 'inshore' comprises the Southern California Bight, which overlies a region of complex bathymetry with deep basins, seamounts, ridges, and submarine troughs (*see* Fig. 1). Such topographic features could influence euphausiid patchiness through alterations in flow, nutrient enrichment, or via seamount-associated predators (Genin et al. 1988; Genin et al. 1994). This inshore region also is a region of high abundance of planktivorous fishes and elevated mortality of the copepod *Calanus pacificus* (Ohman and Hsieh 2008).

If euphausiid predators are size selective, they can cause differential mortality that could lead to the patterns discussed here. Baleen whales foraging on euphausiid aggregations in Monterey Bay, California, have been shown to be strongly size selective (Croll et al. 2005). A comparison between size frequency distributions of euphausiids in

the water column and euphausiid remains in fecal matter from whales feeding in the same area revealed that blue whales preferentially selected larger body-sized euphausiids. Consumption by these and other baleen whales accounts for a significant fraction of plankton production in the California Current (Barlow et al. 2008). Many other organisms in the California Current that feed on euphausiids (including fishes, seabirds, squid, and others) may also show size-dependent rates of encounter and consumption of euphausiids. Size-dependent predation could lead to size-dependent patchiness through at least two specific mechanisms. Consumption by predators would lead to 'gaps' in distributions as a direct consequence of prey removal, and this pattern would increase with body size due to cumulative mortality. Alternatively, the enhanced predation risk to larger body-sized euphausiids (De Robertis 2002) would select for more highly developed aggregation responses in successively larger size classes.

Concerning interannual differences in patchiness, 1955 was a year of abnormally high upwelling with noticeable effect on the population biology of *E. pacifica* (Brinton 1976). In light of the pattern of somewhat higher patchiness inshore, as well as observations of associations between euphausiid aggregations and regions of high chlorophyll (Croll et al. 2005; Ressler et al. 2005), perhaps years with higher production are associated with greater spatial variability of production and/or predators, and higher euphausiid patchiness (Brodeur and Pearcy 1992). The ENSO included in our analysis (1958-59) did not strongly affect euphausiid spatial patchiness, but we cannot conclude that ENSO consistently has no effect on euphausiid patchiness from this one event alone. In addition, ENSO conditions can surely affect euphausiid species ranges, modifying their north-south limits in the California Current (Brodeur 1986).

The lack of a clear difference in the U-shaped pattern with spawning mode (egg brooding vs. broadcast spawning) may constitute a true departure of euphausiids from fishes. For euphausiids, patchiness of the smallest size classes was similar between free spawners and brooders, and neither the magnitude of decrease in the subsequent size classes nor adult patchiness had any relationship to spawning mode. In contrast, differences in fish patchiness-age curves have been hypothesized to be linked to differences in the habitat into which eggs are spawned, specifically demersal vs. pelagic spawning (McGurk 1987), or to the inherent differences arising from these two spawning modes. For pelagic fishes, the patchy distribution of eggs and young larvae is introduced by the highly aggregated reproductive behavior of the adults, where fertilization and spawning occurs almost simultaneously. Alternatively, demersal eggs are laid on a substrate and must incubate over some period of time (Matsuura and Hewitt 1995); their distribution would not necessarily follow adult aggregation as closely as for pelagic fishes. In a similar way, brooding euphausiids carry egg sacs with developing embryos and larval hatching occurs hours to days after reproductive aggregations take place. However, the smallest size class we consider corresponds to calyptopis I, which is two or three stages removed from the egg stage (for brooders and free-spawners, respectively). A difference in patchiness arising from spawning mode would probably be most pronounced in the earlier naupliar and metanaupliar stages. Turbulent diffusion may have eliminated any difference in patchiness, if present, by the time organisms have developed into the smallest size classes considered here. Complete sampling of the youngest developmental stages would be needed to address this question.

In conclusion, we have established a U-shaped pattern of patchiness as a function of body length in California Current euphausiids. The descending limb of the euphausiid curve is consistent with turbulent diffusion acting to diminish the local patches of eggs and the youngest larval stages generated by spawning adults. The ascending limb of the patchiness curve is consistent with predator-induced aggregation, via mechanisms such as differential mortality and predator avoidance behavior. Spatial differences in habitat heterogeneity may secondarily modify the patchiness of euphausiids.

Acknowledgments

We thank Edward Brinton for generating, over the course of a career, the superb dataset that we were privileged to analyze, Annie Townsend for her contributions to sample enumerations and database construction, and Roger Hewitt and an additional referee for constructive comments. The sustained efforts of the California Cooperative Oceanic Fisheries Investigation program made this study possible. This is a contribution from the California Current Ecosystem Long Term Ecological Research site, supported by the National Science Foundation, and from the Pelagic Invertebrates Collection of the Scripps Institution of Oceanography.

Chapter 2, in full, has been published in Limnology and Oceanography: Décima, M, Ohman, M. D., DeRobertis, A. "Body size dependence of euphausiid spatial patchiness". Limnol. Oceanogr. **55**: 777-788. The dissertation author was the primary investigator and author of this paper.

Table 2.1. Years and seasons included in this study. Sampling protocol indicated for each year.

Year	Season	Net used	Depth sampled	Mesh size
1953	winter, spring, summer, fall	1-m ring net	140 m	0.550 mm
1954	winter, spring, summer, fall	1-m ring net	140 m	0.550 mm
1955	winter, spring, summer, fall	1-m ring net	140 m	0.550 mm
1956	winter, spring, summer, fall	1-m ring net	140 m	0.550 mm
1957	winter, spring, summer, fall	1-m ring net	140 m	0.550 mm
1958	winter, spring, summer, fall	Year	140 m	0.550 mm
1959	winter, spring, summer, fall	1-m ring net	140 m	0.550 mm
1969	winter, spring, summer, fall	1-m ring net	210 m	0.505 mm
1978	winter, spring, summer	0.71-m bongo net	210 m	0.505 mm
1984	winter, spring, summer, fall	0.71-m bongo net	210 m	0.505 mm
1991	spring	0.71-m bongo net	210 m	0.505 mm

Table 2.2. Comparison of three patchiness indices: Lloyd's index of patchiness (P, Lloyd 1967), Bez' index (I_a, Bez 2000), and our modified version of Bez' index (I_{mod}). Cases A through D refer to different assumptions about the distributions of organisms (*see* Methods).

Case	Density of organisms	P (Lloyd's)	I_a	I_{mod}
A	8,2	1.52	0.68	1.36
B	80,20	1.7	0.68	1.36
C	80,20,80,20	1.7	0.34	1.36
D	80,20,0,0	3.84	0.68	2.72

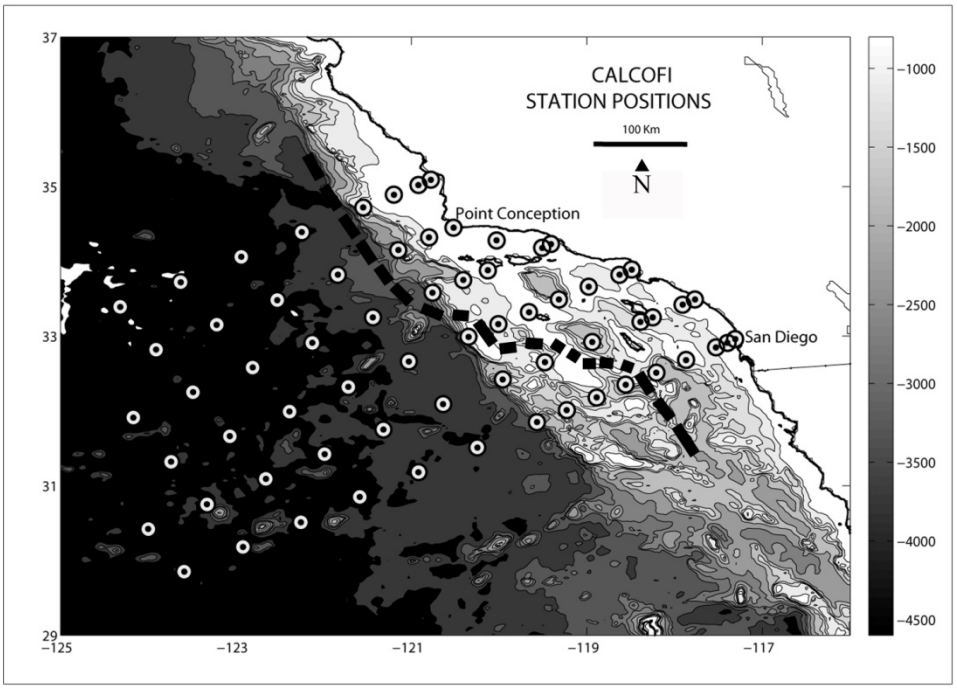

Figure 2.1. Sampling stations considered in our analysis, from the southern portion of the CalCOFI grid. Dashed line marks the separation between the 'inshore' and 'offshore' region. Grey shading indicates bottom topography (depth, in m).

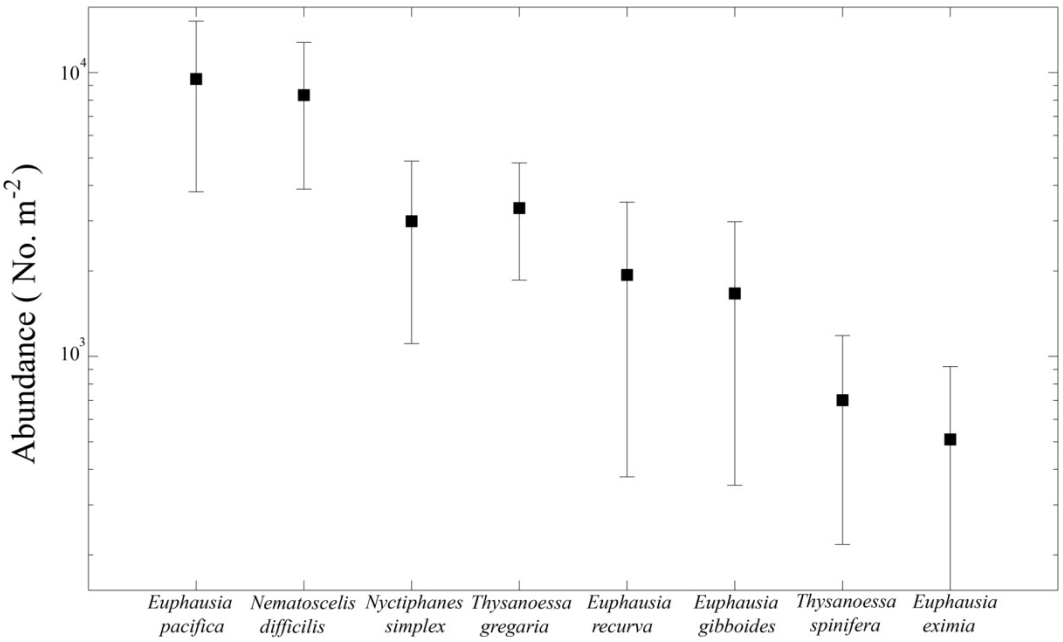

Figure 2.2. Average abundances for the eight numerically dominant species in the California Current System. Mean ± 95% C.I. for all cruises included in this analysis (note log scale). (*E.p.*: *Euphausia. pacifica*; *N.d.*: *Nematoscelis difficilis*; *N.s.*: *Nyctiphanes simplex*; *T. g.: Thysanoessa gregaria*; *E.r.*: *Euphausia recurva*; *E.g.*: *Euphausia gibboides*; *T.s.*: *Thysanoessa spinifera*; *E.e*: *Euphausia eximia*)

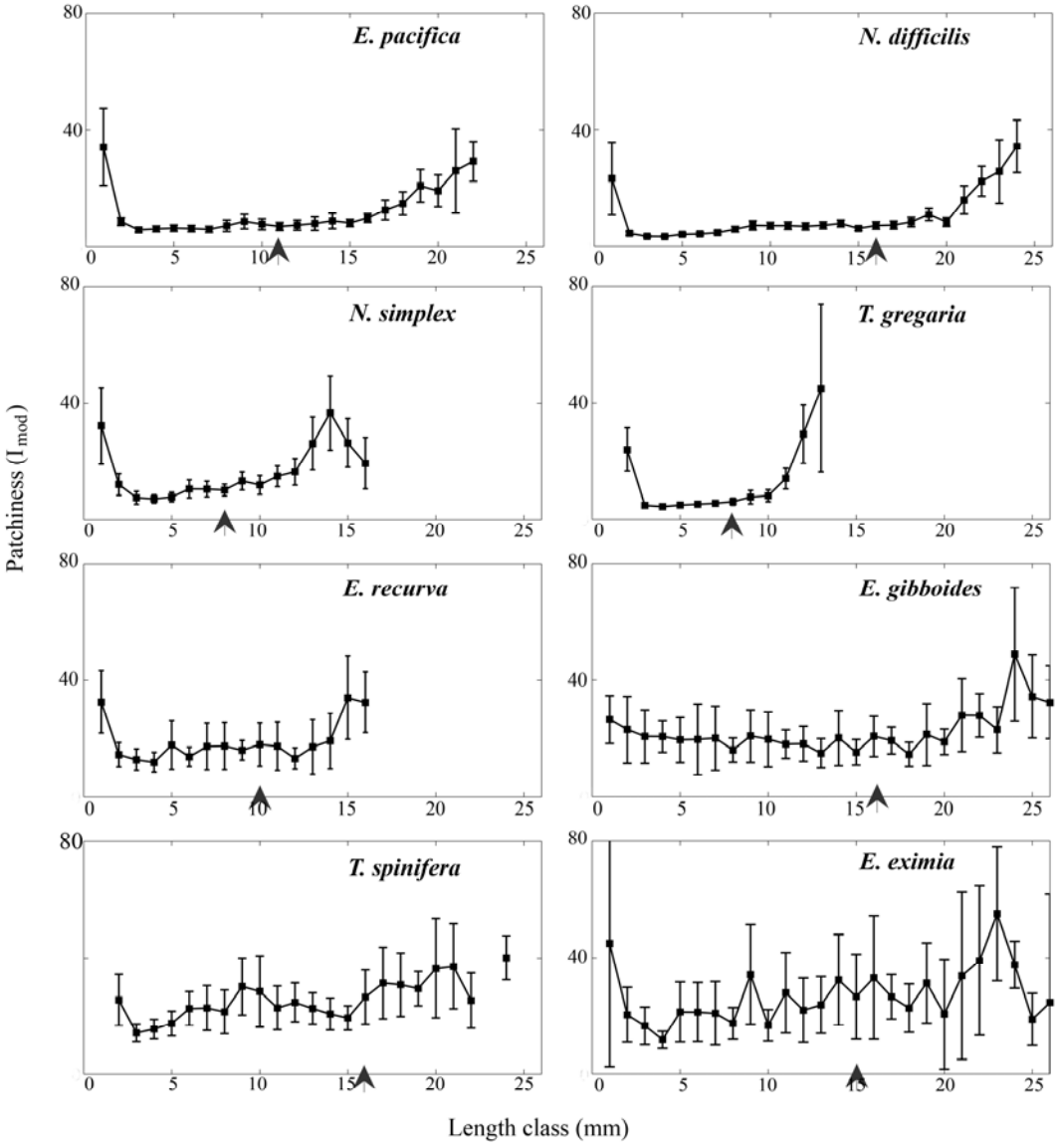

Figure 2.3. Patchiness (I_{mod}) as a function of euphausiid length (mean ± 95% C.I.). Arrows indicate length at onset of sexual maturity.

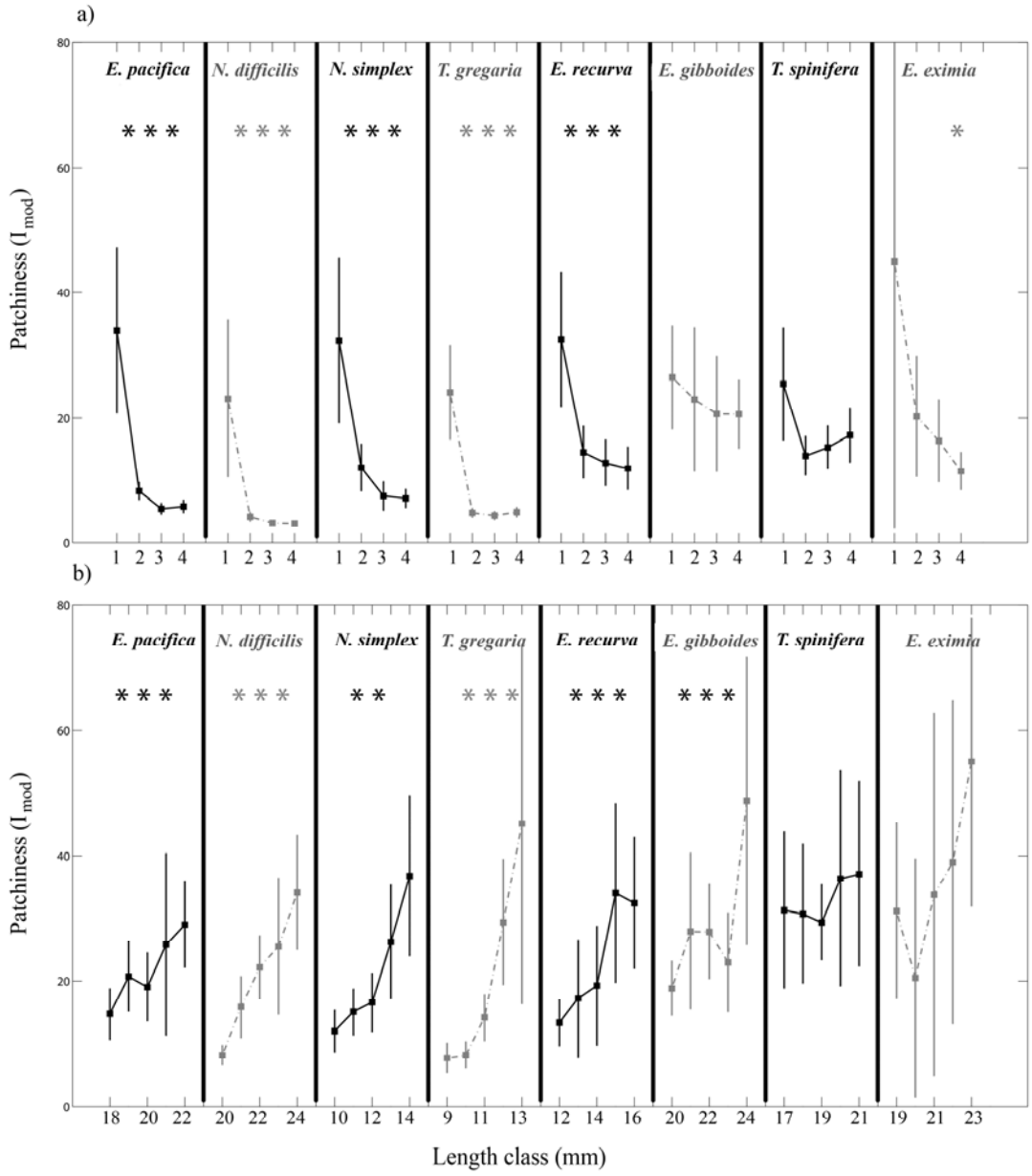

Figure 2.4. (a) Initial descending limb and (b) final ascending limb of euphausiid patchiness vs. total length. Statistical significance of Jonckheere-Terpstra test: $p < 0.001$ = ***; $p < 0.01$ = **; $p \leq 0.05$ = *.

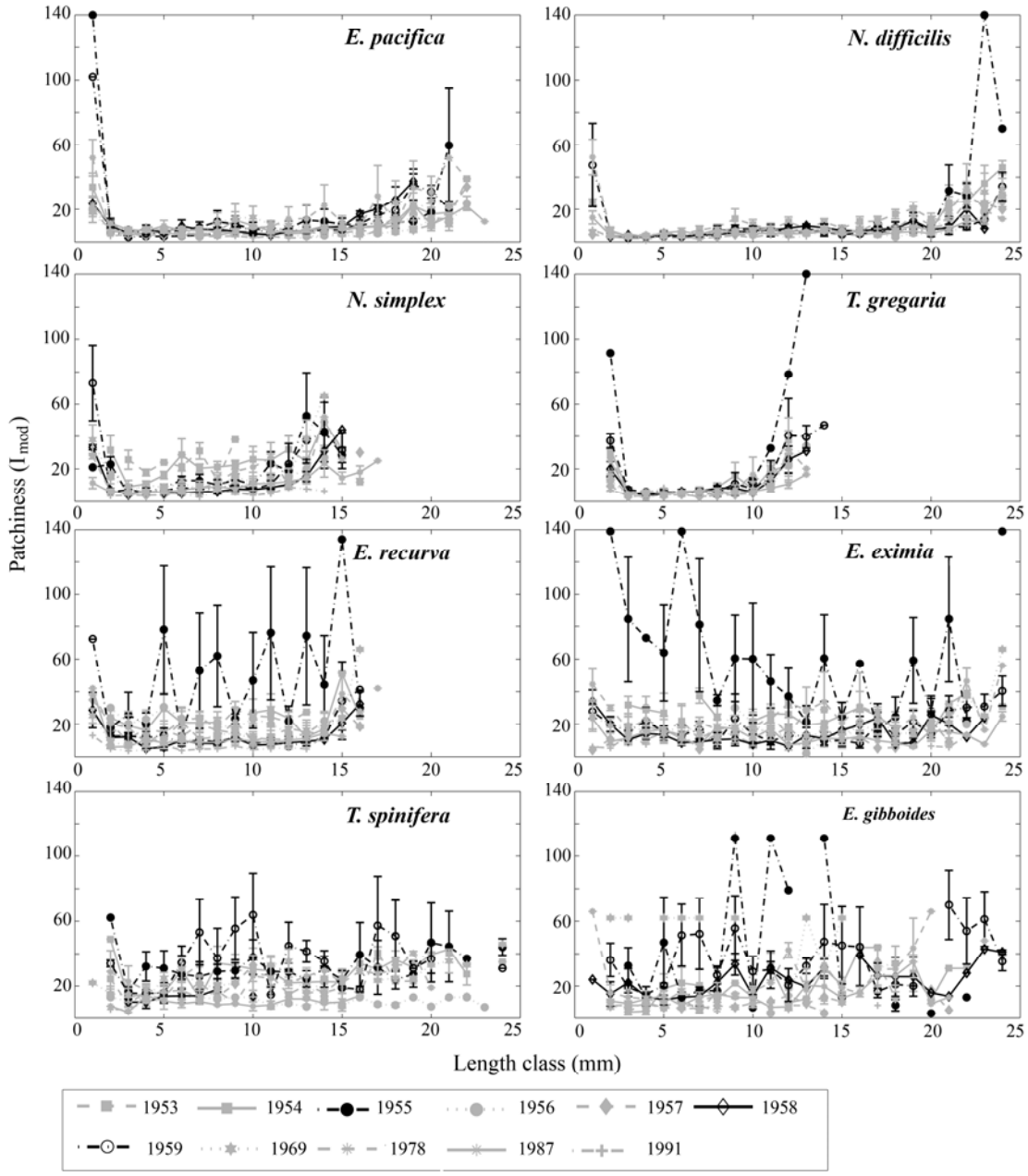

Figure 2.5. Interannual variations in patchiness vs. euphausiid total length.

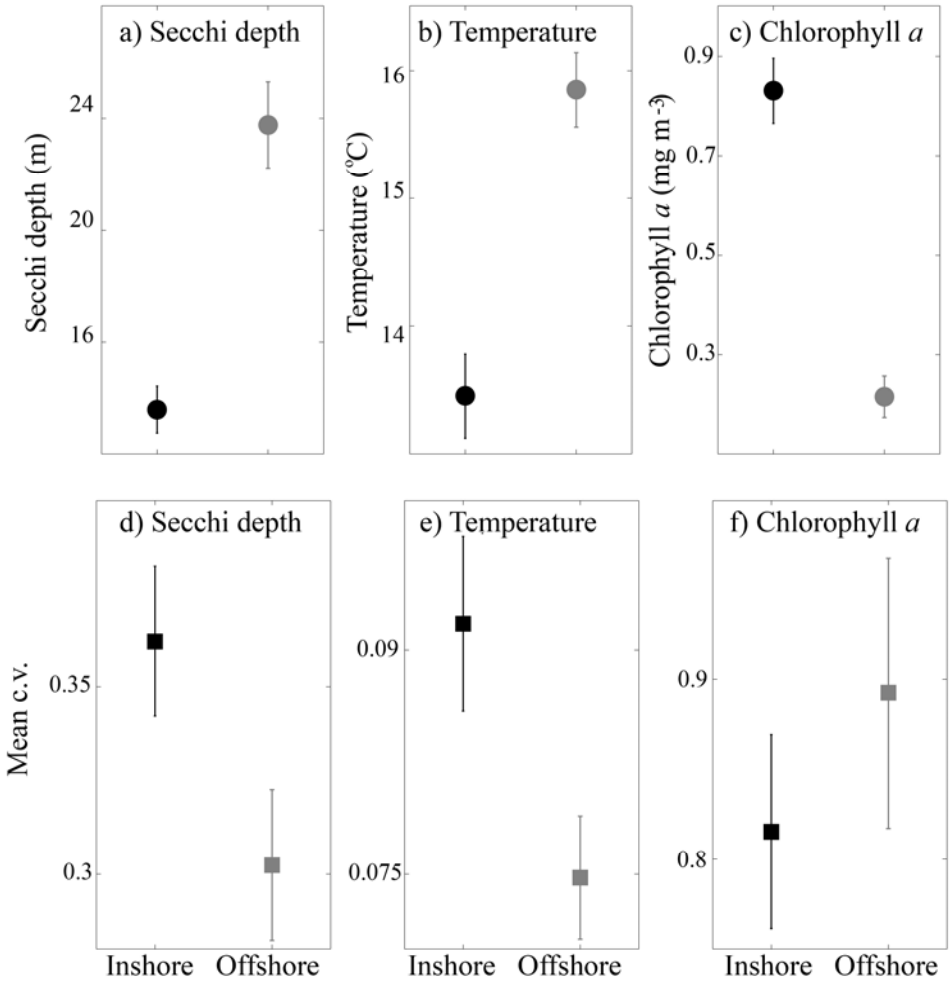

Figure 2.6. Upper panels: contrast between the inshore (black) and offshore (grey) regions in (a) Secchi disk depth, (b) temperature, and (c) chlorophyll *a*, the latter two measured at 30 m depth (mean ± 95 C.I.). Lower panels: contrast between the coefficient of variation (c.v.) in the inshore vs. offshore region (mean c.v. ± 95 C.I.) of (d) Secchi disk depth, (e) temperature, and (f) chlorophyll *a*.

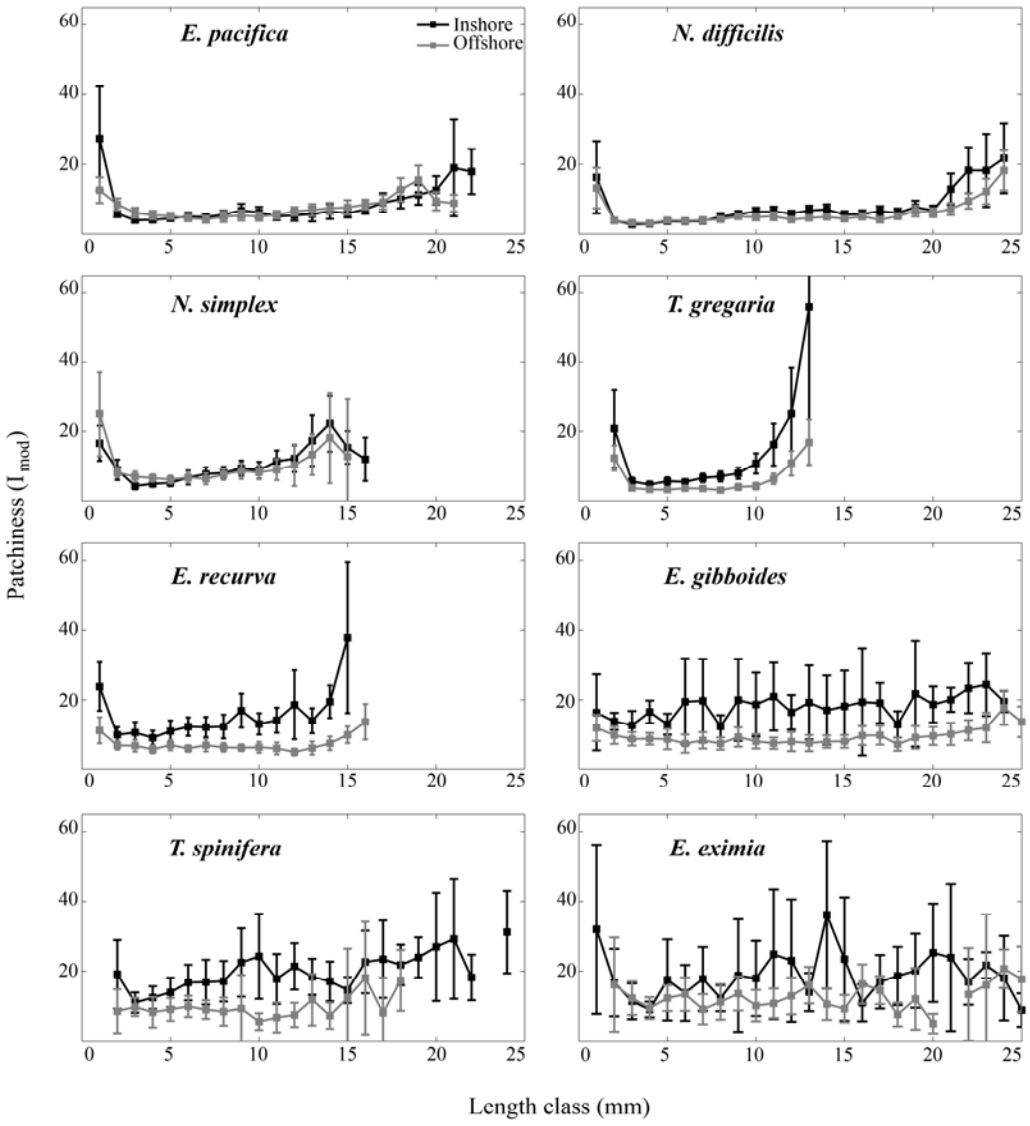

Figure 2.7. Contrast between the inshore (black) and offshore (grey) regions in patchiness (I_{mod}) vs. total length for the eight euphausiid species (mean ± 95 C.I.).

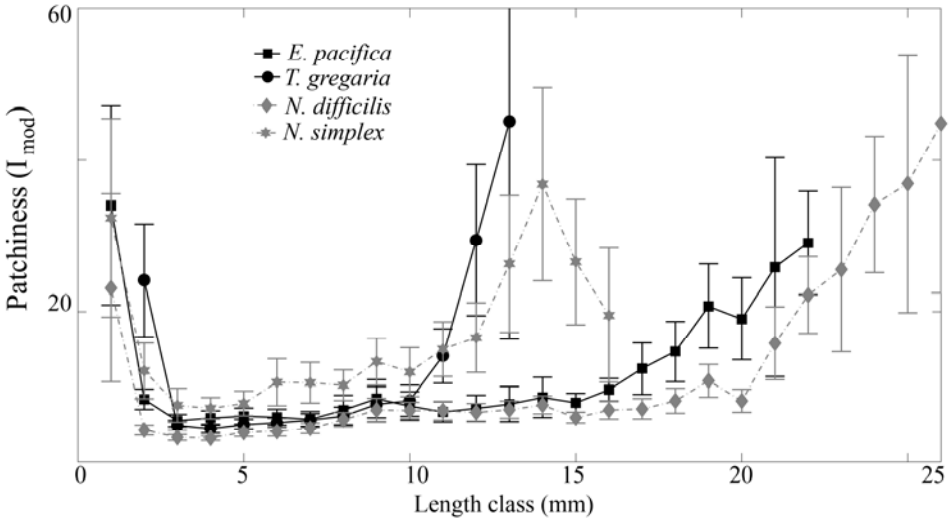

Figure 2.8. Patchiness ($I_{mod,}$ mean ± 95 C.I.) vs. total length for euphausiid species displaying two reproductive modes: broadcast spawners (black; *E. pacifica* and *T. gregaria*), and egg brooders (grey; *N. difficilis* and *N. simplex*)

References

Aksnes, D. L., and M. D. Ohman. 2009. Multi-decadal shoaling of the euphotic zone in the southern sector of the California Current System. Limnol. Oceanogr. **54:** 1272-1281.

Barlow, J., M. Kahru, and B. G. Mitchell. 2008. Cetacean biomass, prey consumption, and primary production requirements in the California Current ecosystem. Mar. Ecol. Prog. Ser. **371:** 285-295.

Bez, N. 2000. On the use of Lloyd's index of patchiness. Fisheries Oceanography **9:** 372-376.

Bollens, S. M., B. W. Frost, and T. S. Lin. 1992. Recruitment, growth, and diel vertical migration of *Euphausia pacifica* in a temperate fjord. Mar. Biol. **114:** 219-228.

Brinton, E. 1967. Vertical migration and avoidance capability of euphausiids in the California current. Limnol. Oceanogr. **12:** 451-483.

Brinton, E. 1976. Population biology of *Euphausia pacifica* off southern California. Fish. Bull. **74:** 733-762.

Brinton, E., M. D. Ohman, A. W. Townsend, M. D. Knight, and A. L. Bridgeman. 1999. Euphausiids of the world ccean (World Biodiversity Database CD-ROM Series). Expert Centre for Taxonomic Identifications (ETI), University of Amsterdam.

Brinton, E., and A. Townsend. 2003. Decadal variability in abundances of the dominant euphausiid species in southern sectors of the California Current. Deep-Sea Res. II **50:** 2449-2472.

Brodeur, R. D. 1986. Northward displacement of the euphausiid *Nyctiphanes simplex* Hansen to Oregon and Washington waters following the El Nino event of 1982-83. J. Crustac. Biol. **6:** 686-692.

Brodeur, R. D., and W. G. Pearcy. 1992. Effects of environmental variability on trophic interactions and food web structure in a pelagic upwelling ecosystem. Mar. Ecol. Prog. Ser. **84:** 101-119.

Croll, D. A., B. Marinovic, S. Benson, F. P. Chavez, N. Black, R. Ternullo, and B. R. Tershy. 2005. From wind to whales: trophic links in a coastal upwelling system. Mar. Ecol. Prog. Ser. **289:** 117-130.

Croll, D. A., B. R. Tershy, R. P. Hewitt, D. A. Demer, P. C. Fiedler, S. E. Smith, W. Armstrong, J. M. Popp, T. Kiekhefer, V. R. Lopez, J. Urban, and D. Gendron. 1998. An integrated approach to the foraging ecology of marine birds and mammals. Deep-Sea Res. II **45:** 1353-1371.

De Robertis, A. 2002. Size-dependent visual predation risk and the timing of vertical migration: An optimization model. Limnol. Oceanogr. **47:** 925-933.

Deutschman, D. H., G. A. Bradshaw, W. M. Childress, K. L. Daly, D. Grünbaum, M. Pascual, N. H. Schumaker, and W. Jianguo. 1993. Mechanisms of patch formation, p. 1-307. *In* S. A. Levin, T. M. Powell and J. H. Steele [eds.], Patch Dynamics. Lecture Notes in Biomathematics. Springer-Verlag.

Endo, Y., Y. Hanamura, and A. Taniguchi. 1985. *In situ* observations on the surface swarm of *Euphausia pacifica* in Sendai Bay Japan in early spring with special eeference to their biological characteristics. Mer (Tokyo) **23:** 135-140.

Gendron, D. 1992. Population structure of daytime surface swarms of *Nyctiphanes simplex* (Crustacea, Euphausiacea) in the Gulf of California, Mexico. Mar. Ecol. Prog. Ser. **87:** 1-6.

Genin, A., C. Greene, L. Haury, P. Wiebe, G. Gal, S. Kaartvedt, E. Meir, C. Fey, and J. Dawson. 1994. Zooplankton patch dynamics: daily gap formation over abrupt topography. Deep-Sea Res. I **41:** 941-951.

Genin, A., L. Haury, and P. Greenblatt. 1988. Interactions of migrating zooplankton with shallow topography: predation by rockfishes and intensification of patchiness. Deep-Sea Res. I **35:** 151-175.

Gomez-Gutierrez, J. 2002. Hatching mechanism and delayed hatching of the eggs of three broadcast spawning euphausiid species under laboratory conditions. J. of Plankton Res. **24:** 1265-1276.

Gomez-Gutierrez, J. 2003. Hatching mechanism and accelerated hatching of the eggs of a sac-spawning euphausiid *Nematoscelis difficilis*. J. of Plankton Res. **25:** 1397-1411.

Hamner, W. M., and P. P. Hamner. 2000. Behavior of Antarctic krill (*Euphausia superba*): schooling, foraging, and antipredatory behavior. Can. J. Fish. Aquat. Sci. **57:** 192-202.

Hamner, W. M., P. P. Hamner, B. S. Obst, and J. H. Carleton. 1989. Field observations on the ontogeny of schooling of *Euphausia superba* furciliae and its relationship to ice in Antarctic waters. Limnol. Oceanogr. **34:** 451-456.

Hart, J. L. 1973. Pacific fishes of Canada. Bulletin Fish. Res. Bd Canada **180:** 1-740.

Hewitt, R. 1981. Value of pattern in the distribution of young fish. Rapports et Proces-Verbaux des Reunions Conseil International pour l'Exploration de la Mer **178:** 229-236.

Hollander, M., and D. A. Wolfe. 1973. Nonparametric statistical methods. Wiley p 503.

Hutchinson, G. E. 1953. The concept of pattern in ecology. Proc Acad Nat Sci Philadelphia **105:** 1-12.

Johnson, M. L., and G. A. Tarling. 2008. Influence of individual state on swimming capacity and behaviour of Antarctic krill *Euphausia superba*. Mar. Ecol. Prog. Ser. **366:** 99-110.

Kierstead, H., and L. B. Slobodkin. 1953. The size of water masses containing plankton blooms. J. Mar. Res. **12:** 141-147.

Levin, S. A. 1992. The problem of pattern and scale in ecology. Ecology **73:** 1943-1967.

Levin, S. A., T. M. Powell, and J. H. Steele. 1993. Patch dynamics. Lecture Notes in Biomathematics **96:** 1-307.

Lloyd, M. 1967. Mean crowding. J. Anim. Ecol. **36:** 1-30.

Mackas, D. L., R. Kieser, M. Saunders, D. R. Yelland, R. M. Brown, and D. F. Moore. 1997. Aggregation of euphausiids and Pacific hake (*Merluccius productus*) along the outer continental shelf off Vancouver Island. Can. J. Fish. Aquat. Sci. **54:** 2080-2096.

Matsuura, Y., and R. Hewitt. 1995. Changes in the spatial patchiness of Pacific mackerel *Scomber japonicus*, larvae with increasing age and size. U S National Marine Fisheries Service Fishery Bulletin **93:** 172-178.

Mauchline, J. 1980. The biology of mysids and euphausiids. Advances in Marine Biology **18:** 1-681.

McGurk, M. D. 1987. The spatial patchiness of Pacific herring larvae. Environmental Biology of Fishes **20:** 81-89.

Nicol, S. 2006. Krill, currents, and sea ice: *Euphausia superba* and its changing environment. Bioscience **56:** 111-120.

Ohman, M. D., and C. H. Hsieh. 2008. Spatial differences in mortality of *Calanus pacificus* within the California Current System. J. of Plankton Res. **30:** 359-366.

Ohman, M. D., and P. E. Smith. 1995. A comparison of zooplankton sampling methods in the CalCOFI time series. Calif. Coop. Ocean. Fish. Invest. Rep. **36:** 153-158.

Parrish, J. K., and P. Turchin. 1997. Individual decisions, traffic rules, and emergent pattern in schooling fish, p. 126-142. *In* J. K. Parrish and W. H. Hamner [eds.], Animal groups in three dimensions. Cambridge University Press.

Ressler, P. H., R. D. Brodeur, W. T. Peterson, S. D. Pierce, P. Mitchell Vance, A. Røstad, and J. A. Barth. 2005. The spatial distribution of euphausiid aggregations in the Northern California Current during August 2000. Deep-Sea Res. II **52:** 89-108.

Ritz, D. A. 2000. Is social aggregation in aquatic crustaceans a strategy to conserve energy? Can. J. Fish. Aquat. Sci. **57:** 59-67.

Schoenherr, J. R. 1991. Blue whales feeding on high concentrations of euphausiids around Monterey submarine canyon. Can. J. Zool.-Rev. Can. Zool. **69:** 583-594.

Simard, Y., and D. L. Mackas. 1989. Mesoscale aggregations of euphausiid sound scattering layers on the continental shelf of Vancouver Island. Can. J. Fish. Aquat. Sci. **46:** 1238-1249.

Smith, S. E., and P. B. Adams. 1988. Daytime surface swarms of *Thysanoessa spinifera* (Euphausiacea) in the Gulf of the Farallones, California. Bull. Mar. Sci. **42:** 76-84.

Steele, J. H. 1978. Some comments on plankton patches, p. 1-20. *In* J. H. Steele [ed.], Spatial Pattern in plankton communities. Plenum Press.

Steele, J. H., and E. W. Henderson. 1992. A simple model for plankton patchiness. J. of Plankton R. **14:** 1397-1403.

Watkins, J. L., F. Buchholz, J. Priddle, D. J. Morris, and C. Ricketts. 1992. Variation in reproductive status of Antarctic krill swarms; evidence for a size-related sorting mechanism? Mar. Ecol. Prog. Ser. **82:** 163-174.

Watkins, J. L., and A. W. A. Murray. 1998. Layers of Antarctic krill, *Euphausia superba*: are they just long krill swarms? Mar. Biol. **131:** 237-247.

Weber, L. H., S. Z. Elsayed, and I. Hampton. 1986. The variance spectra of phytoplankton, krill and water temperature in the Antarctic ocean south of Africa. Deep-Sea Res.t I **33:** 1327-1343.

Wroblewski, J. S., and J. J. O' Brien. 1976. Spatial model of phytoplankton patchiness. Mar. Biol. **35:** 161-175.

CHAPTER 3

Zooplankton Trophic Variability in the California Current Ecosystem

By Moira Décima, Michael R. Landry and Mark D. Ohman

Abstract

The relationship between mesozooplankton biomass, grazing and trophic structure is of paramount importance for modeling carbon flow through the marine pelagic ecosystem. To elucidate patterns in these processes we conducted experimental studies near Point Conception, California, during 2006 and 2007. The high spatial variability present in the California Current Ecosystem (CCE) allowed for the investigation of mechanisms determining mesozooplankton biomass, grazing and trophic relationships across a significant gradient in primary productivity

In addition, we tested whether mesozooplankton energetic requirements can be fulfilled by consumption of the microplanktonic community, and to what extent exploitation of the heterotrophic component was necessary for growth and survival. Mesozooplankton community grazing estimates on phytoplankton were assessed using the gut pigment method while microzooplankton secondary production was estimated from dilution experiments and an estimated GGE of 0.3 [Straile, 1997]. Incubation experiments were carried out using two dominant zooplankton species, *Calanus pacificus* and *Euphausia pacifica*, to assess dietary shifts in response to changing phytoplankton

primary productivity. Results show high variability in biomass with primary production, likely due to advection, biological aggregation and mismatches in mesozooplankton and phytoplankton growth rates. Grazing as a function of primary production evinced a somewhat constant transfer of energy from phytoplankton to mesozooplankton, although a higher relative consumption nearshore is suggested. Incubation results show specific zooplankters consuming relatively more heterotrophic microplankton with decreasing primary production, indicating dietary shifts in response to environmental conditions. Autotrophic carbon is consumed in great excess of requirements for respiration, growth and defecation in the ~50 km closest to shore. Farther offshore, phytoplankton consumption is insufficient for basal requirements at two locations. Estimated consumption of microzooplankton is sufficient in all but one location to fulfill requirements for growth. We hypothesize that reserves built from excess consumption of phytoplankton nearshore, trophic structure shifts and advection are responsible for the existence of high mesozooplankton biomass in areas of reduced food supply.

Introduction

Plankton secondary production in the ocean is ultimately dependent on the magnitude of primary productivity, and the structure of the pelagic food web. While the maximum secondary production is limited by phytoplankton production, the way in which phytoplankton production is partitioned into growth and respiration of zooplankton is not. Existing relationships between system productivity and zooplankton grazing and growth are neither empirically strong nor mechanistically based, both desirable qualities for accurate predictions.

The percentage of primary production (PP) channeled through the larger zooplankton (>200 μm, hereafter referred to as the mesozooplankton) has traditionally been thought to be highest in productive areas where 'herbivorous' food web predominates, and lowest in oligotrophic areas dominated by microbial processes (Legendre and Rassoulzadegan 1995). This is consistent with the notion that carbon losses to respiration increase with food chain length. The amount of PP available to mesozooplankton from microzooplankton decreases with each trophic link (about 30%, Straile 1997), ultimately limiting flow up the food chain when primary production is too small for direct consumption.

This view has been challenged in recent years. In a global comparative analysis, Calbet (2001) found that mesozooplankton grazing scaled with primary production with a slope of 0.64, i.e. significantly less than 1, implying a higher fraction of PP consumed by zooplankton in less productive waters. Martin et al. (2006) used patterns in population structure to infer transfer efficiency of PP to secondary production, and found it to be independent of ecosystem productivity. More recently, Strömberg et al. (2009)

concluded (from model simulations) that more energy is transferred to zooplankton when PP is low.

The Southern sector of the California Current Ecosystem (CCE) is an upwelling-influenced ecosystem that sustains relatively high phytoplankton productivity and zooplankton biomass (Roesler and Chelton 1987; Hayward and Venrick 1998). Considerable spatial variability is coincident with different water masses influencing the region. Nearshore regions fueled by coastal upwelling sustain higher concentrations of plankton, and offshore regions are characterized by general oligotrophic conditions (Hayward and Venrick 1998; Venrick 2002).

Significant temporal perturbations, albeit transient, are linked to El Nino Southern Oscillation (ENSO) events and lead to substantial decreases in sea surface chlorophyll and zooplankton biomass (Kahru and Mitchell 2000; Lavaniegos and Ohman 2007). Community changes are also evident for individual species. The abundances of *Calanus pacificus* (one of the dominant copepods) and *Euphausia pacifica* (the dominant euphausiid) both fluctuate with ENSO and other climatic conditions (Rebstock 2002; Brinton and Townsend 2003). Fluctuations in euphausiid biomass within the CCE have been linked to failed reproductive years of marine seabirds (Peterson et al. 2006), and a myriad of fish and whales are dependent on zooplankton for survival.

Here we examined patterns in community zooplankton grazing, biomass and daily carbon requirements to elucidate mechanisms that can be useful in constructing biogeochemical models, for which secondary production and respiration are key components (del Giorgio and Duarte 2002; Hernandez-Leon and Ikeda 2005; Buitenhuis et al. 2006).

Trophic structure related to ecosystem spatial variability is explored by assessing nutritional status of mesozooplankton throughout the spatial domain. Energetic requirements satisfied by autotrophic carbon consumption is quantified by use of the gut pigment method (Mackas and Bohrer 1976) and inferences on the consumption of microzooplankton are drawn from the calculated metabolic needs for the entire community. Additional insight comes from a closer look at the dietary choices and shifts of the two numerically dominant and representative omnivorous zooplankters, *E. pacifica* and *C. pacificus* relative to the available auto- and heterotrophic carbon.

Material and Methods

Sampling and microplankton community analyses

Sampling was carried out during two oceanographic cruises, as part of the Long Term Ecological Research (LTER) California Current Ecosystem (CCE) program. The first set of experimental studies (cruise P0605) was done onboard the R/V *Knorr* from 10 May to 5 June, 2006. Cruise P0704 was conducted 3 to 20 April 2007, onboard the R/V *Thomas G. Thompson*. Coordinated sampling and experimental studies called 'cycles' were conducted in the vicinity of Point Conception, California, in a location extending from 10 to 400 km offshore (Fig. 1). Sampling locations were selected to represent the range of spatial variability encountered in the California Current. Detailed methods are outlined in Landry et al. (2009). Briefly, locations were initially chosen using MODIS-Aqua and/or SeaWifs satellite maps of sea surface temperature and Chl *a*, combined with Moving Vessel Profiler (Ohman et al., unpublished) and Spray Ocean glider (Davis et al., 2008) site surverys. Conditions representing different end members of system variability

were chosen for the different experimental cycles. These consisted typically of 3-5 days during which we tracked a water parcel with a satellite-tracked drift array that was used both to follow the path of the upper mixed layer, and to attach bottles used for *in situ* incubations.

We characterized the microplankton community with water column profiles of Chl *a*, and samples for microscopical analysis. Rates of primary productivity (^{14}C method), phytoplankton growth and microzooplankton grazing (dilution method, Landry and Hassett 1982) were measured in bottles incubated at 8 depths spanning the euphotic zone (to ~0.4 % surface irradiance). Full water-column profiles of phytoplankton growth and microzooplankton grazing are available in Landry et al. (2009). For the purpose of this paper, we integrated these estimates from the surface to the depth of the euphotic zone to calculate microzooplankton secondary production $Mzoo_{prod}$ (mg C m^{-2} d^{-1}), as

$$Mzoo_{prod} = \frac{g}{\mu} * PP * GGE$$

where g is microzooplankton grazing, μ is phytoplankton growth (both estimated from dilution experiments), *PP* is primary production estimated from the ^{14}C method, and *GGE* is approximated as 0.3, after Straile (1997).

Mesozooplankton community estimates

Mesozooplankton biomass. Zooplankton net tows were taken twice daily, usually around 1100 and 2300. Samples were collected using a 0.71-m^2 Bongo frame fitted with 202-μm Nitex mesh net and equipped with a General Oceanics flow meter. Tows were conducted using standard CalCOFI procedures (http://www.calcofi.org/). Typically, 300

m of wire were paid out (wire out was adjusted accordingly at shallower locations), to a target depth of 210 m. The net was lowered to depth at 50 m min^{-1}, allowed to settle for 30 seconds, and retrieved at 20 m min^{-1}. Vessel speed was 1-2 knots, adjusted to keep the wire angle at 45° (±30), and the angle noted every 10 m to estimate actual depth of tow. Tow duration was ~ 22 min. Upon retrieval, the port side net was quickly rinsed, the cod end contents poured into a bucket, and the collected animals immediately anesthetized using club soda to minimize gut evacuation (Kleppel and Pieper 1984). The sample was split with a Folsom splitter, with 3/8 processed for gut pigments, 3/8 for biomass determinations and 1/4 frozen immediately in liquid nitrogen for later gut pigment determinations of individual species. Contents from the starboard side were preserved in 1.8% buffered formaldehyde for community analysis.

Size-fractionation was done by wet sieving the biomass subsample through 5 nested Nitex sieves (0.2, 0.5, 1, 2 and 5 mm mesh). Each subsample was concentrated onto a pre-weighed 0.2-mm Nitex screen and rinsed with isotonic ammonium formate to remove interstitial sea salt, placed in Petri dishes and frozen at -80 °C for later analysis on shore. Frozen samples were thawed and dried in an oven at 60 °C for at least 24 h. Dried samples were weighed to 0.01 mg at room temperature on an analytical microbalance (Denver Instrument). After subtracting the initial weight of the Nitex screen, the dry weight (DW) of each size fraction was obtained by the appropriate multiplication factors for previous sub-sampling, and total mesozooplankton DW was estimated from the combined biomass values of all size fractions. Zooplankton biomass concentrations were computed using volume-filtered estimates from the flow meters. During many deployments, we encountered conditions of high winds, and flow meters were observed

to spin considerably during net deployment and retrieval. A linear regression between wind speed and volume filtered showed a strong relationship for both cruises, and the volume filtered of each tow was adjusted taking this wind factor into consideration. Each cruise was analyzed separately, and corrections resulted on average in a decrease of 20% (SD ± 7.5%) volume filtered for P0605, and 19% (SD ± 5%) for P0704. Daily areal estimates (g m^{-2}) were computed by multiplying zooplankton biomass concentrations by the depth of each tow, and averaging day and night tows.

Mesozooplankton grazing. Size-fractionation of mesozooplankton was done to quantify grazing by the gut pigment method (Mackas and Bohrer 1976). Typically 3/8 of the original sample was wet sieved through 5 nested Nitex sieves (0.2, 0.5, 1, 2 and 5 mm mesh). Samples were thoroughly washed with filtered seawater to minimize contamination of phytoplankton debris and detritus. Each size class was then collected on a 0.2-mm Nitex filter, and frozen in liquid N_2 for later analysis.

Samples for gut fluorescence were analyzed in the laboratory. Typically, 1/8 replicate splits of the 0.2-0.5 and 0.5-1 mm size fractions, replicate 1/4 splits of the 1-2 mm fraction, 1/4 of the 2-5 mm and the entire >5 mm sample were analyzed. The fractions for analysis were carefully examined under a stereomicroscope to remove phytoplankton debris and micronekton. They were then placed in test tubes with 90% acetone and sonicated four times for 5 s with an ultrasonic tissue homogenizer. Samples were kept on ice prior to and during sonication, stored for 1-3 h at -20 °C for pigment extraction, and finally centrifuged for 10 min at 1600 g. Analysis of the supernatant was carried out using a calibrated Turner Designs model 10 fluorometer. Chlorophyll and its fluorescent degradation products (phaeopigments) were measured before and after

acidification (Lorenzen 1967). We did not multiply the phaeopigments by the molar ratio of chl:phaeo because the equations compute phaeopigment values in terms of chlorophyll weight equivalents (Conover et al. 1986). In addition, we made no attempt to correct for pigment degradation in the gut, since Durbin and Campbell (2007) showed that this degradation is inherently accounted for in the ingestion calculation. Gut pigment turnover rate (K, min^{-1}) was estimated from Dam and Peterson (1988), using the temperature-dependent equation:

$$K = 0.0124\, e^{0.07675\, T}$$

where T (°C) is the temperature at the chlorophyll maximum, the depth at which zooplankton are assumed to be feeding on high prey concentrations. Daily rates were calculated as the average of the day and night estimates, weighted by the proportion of day light available by time of year. Chl *a* consumption rates were converted to carbon consumption by calculating the proportion of the Chl *a* standing stock consumed, and multiplying by the depth integrated carbon standing stock estimated from microscopy (Taylor et al., unpublished). The C:Chl resulting from this method varied among cycles, ranging 30-45 for the nearshore cycles, and 70-95 for the offshore cycles. These values are consistent with literature values for this area (Eppley 1968).

Daily carbon requirements. We estimated the carbon requirements of the mesozooplankton community using the equations of Ikeda (1985). We followed a similar procedure as to Al-Mutairi & Landry (2001), using DW estimates to calculate respiration rates (RO) as:

$$Ln\, RO = -0.251 + 0.789 * Ln(DW) + 0.49 * T$$

where *DW* (g m^{-2}) is the average dry weight of a zooplankter in a given size fraction, and *T* (°C) is the temperature at the chlorophyll maximum. Carbon equivalents (RC, μg C $organism^{-1}$ h^{-1}) were calculated from the following equation:

$$RC = RO * RQ * 12/22.4$$

where RQ is the respiratory quotient (molar ratio of carbon produced to oxygen utilized), 12 is the molecular weight of carbon and 22.4 is the molar volume of an ideal gas at standard temperature and pressure. An RQ value of 0.8 was used, implying a largely protein based diet (Omori and Ikeda 1984). Abundance in each size class is linearly related to the respective DW. We used published coefficients from Landry et al. (2001) to estimate the mean number of organisms per size class. We then divided each DW by the estimated abundance (Landry et al. 2001) to obtain average DW for each zooplankter in the size class. These dry weights were used to compute daily respiratory carbon requirements for the average zooplankter in each size class and multiplied by the estimated abundance to obtain an estimate per size fraction. We estimated total daily carbon requirements by assuming equal partitioning into respiration, growth and defecation, therefore multiplying the respiratory requirements by 3. The fraction of carbon requirements consumed was calculated as

$$C_{consumed}/(C_{respiration} * 3)$$

here $C_{consumed}$ is the amount of carbon obtained from phytoplankton or from phyto- and microzooplankton, and $C_{respiration}$ is calculated from the approach described.

Calanus pacificus *and* ***Euphausia pacifica*** *grazing estimates*

Feeding incubations. During cruise P0704, we incubated adult *C. pacificus* and *E. pacifica* once per cycle. Table 1 shows the zooplankton sampling and experiments that were carried out during each cruise. Incubations at the offshore cycle (Cycle 2) were only done with *C. pacificus* because we did not find adult *E. pacifica* in enough numbers, consistent with its distribution patterns (Brinton 1960).

Sea water collection. Natural sea water for mesozooplankton experiments was collected at 1800 h, using a CTD-rosette system with 24 ten- liter PVC Niskin bottles with Teflon coated springs. For all experiments we used water collected from the depth of the chlorophyll maximum, where zooplankton were assumed to concentrate and graze. Two-point dilution experiments (Landry and Hassett 1982; modified as in Landry et al. 2008) were carried out in parallel with bottle incubations to correct for trophic cascades due to microzooplankton grazing (see Nejstgaard et al. 2001). Typically 12 polyethylene jars (3.8 l) were filled directly from Niskin bottles using silicon tubing (always below the water level to avoid turbulence), and 3 bottles were filled with 0.1 μm filtered seawater to prepare diluted treatments. Containers with both whole and filtered seawater were stored for ca. 8 hours in the dark in a temperature controlled room (12 °C), until experimental set up. All jars, filters, and tubing were pre-cleaned in 10% HCl, rinsed three times in distilled (DI) water and subsequently rinsed three times with seawater.

Live animal collection. Adult *C. pacificus* and *E. pacifica* were collected during nighttime tows with Bongo frames fitted with 202-μm Nitex mesh. The nets were towed gently at 0.5 knots, obliquely from the depth of the chlorophyll maximum to the surface. Upon retrieval, the cod end contents were immediately diluted in a bucket of sea water, and kept in a temperature controlled room (12°C) until sorted. Aliquots of cod end

contents were transferred to petri dishes, placed on ice packs and sorted using a stereomicroscope. Healthy copepods with intact antennules were used for experiments. With a Pasteur pipette we gently transferred 30 female *C. pacificus* (for each of three treatments) into 20 ml vials containing filtered seawater. The vials were stored at 12°C for no longer than 30 minutes until experimental set up. Adult *E. pacifica* were collected from the original cod end contents by gently scooping healthy swimming individuals with a kitchen ladle (previously washed in 10% HCl, DI water and seawater) and transferring them into jars (3.8 l) containing filtered seawater.

Experimental set up. Vials usually containing 30 female *C. pacificus* were gently poured into replicate jars (3.8 l) containing whole sea water, and topped off to avoid bubbles in jars. Three individual adult *E. pacifica* were transferred using a kitchen ladle into each replicate jar, and the jars were topped off with seawater. Three replicates were set up for each of the following treatments: *i*) *C. pacificus* grazing, *ii*) *E. pacifica* grazing, *iii*) ambient sea water, and *iv*) diluted field sea water. Ambient and diluted treatments were included to quantify phytoplankton growth during incubations, and microzooplankton grazing during the incubation to correct for mesozooplankton grazing rates (see Nejstgaard et al. 2001). Bottles were set on a slowly rotating grazing wheel (0.5 rpm) to keep particles in suspension, and experiments were run for 24 h in dim light. Samples were taken for chlorophyll and microscopical analysis upon experiment termination. For epifluorescence microscopy, 500 ml samples were collected and preserved with 260 µl of alkaline Lugol's solution, followed by 500 µl sodium thiosulfate and 10 ml 3.7% buffered formaldehyde (modified from Sherr and Sherr 1993). These samples were allowed to fix for a few hours, then stained with proflavin (0.33% w/v) in the final 30

minutes. Slides were prepared by first filtering the samples onto 8-µm pore Nuclepore black filters, overlain on 20-µm Millipore backing filters to allow a uniform cell distribution on the filter. When the volume remaining to be filtered was ~ 3ml slides were stained with 1 ml DAPI (50 mg ml^{-1}). Filters were mounted on glass slides with immersion oil and cover slips, and stored at -80°C until analysis.

Microscopical analysis of the microplankton community. Image analysis of prepared slides was done using a Zeiss Axiovert 200M inverted epifluorescence microscope. Digital images were captured using a Zeiss AxioCam HRc color CCD digital camera. A minimum of 20 images per slide was taken at 200X, each image consisting of three fluorescence channels: Chl *a* (red), FITC (green) and DAPI (blue). The separate channels were combined into one RGB image for digital analysis using Image Pro Plus (4.0) software. Live cells were visually identified by use of the DAPI channel, which stains the DNA within the cell nucleus. We counted at least 400 cells, which corresponded typically to 10 digitized fields per slide. Cells were outlined in the FITC channel, which shows the proflavin stained proteins within the cell volume. Diatoms were visually identified due to their characteristic shapes. Measurements from all three channels were exported to Excel spreadsheets for later analysis using Matlab 7.5 (R2007b). Matlab scripts were run to convert cell dimensions to biovolume (BV) approximating cell shape to that of a prolate sphere, assuming cell height to be the same as cell width (BV = *pi**LWH/6). Biovolume to carbon conversions were done using the following equations, for diatoms:

$$\log(C) = 0.76 \log(BV) - 0.29$$

from Strathmann (1967) and:

$$\log(C) = 0.94 \log(BV) - 0.60$$

for non-diatoms from Eppley et al. (1970). We distinguished autotrophs from heterotrophs similar to Stukel et al. (2011). Autotrophs were separated from heterotrophs by plotting histograms of log (red/green), corresponding to Chl *a* channel/FITC channel. We chose a cutoff based on the observed bimodal distributions of the Chl *a* channel/ FITC ratio, interpreting the population with a low ratio as heterotrophs, and the higher ratio as autotrophs. We use this ratio instead of just the red channel values because protistan cells display some background red autofluorescence, which can lead to misclassification as autotrophs for biomass-dense heterotrophs.

Clearance rates were calculated for three categories of cells: diatoms, other autotrophs and heterotrophs. Because mesozooplankters are known to be size selective (Frost 1972), we report clearance rates by size. Particles were divided into four categories according to major axis size: 8-13, 14-23, 24-43 and >43 μm. Size categories were chosen based on the smallest particles recovered on the filter, determined to be on the small side of the range of particles consumed by these organisms from previous studies in the literature (Frost 1972; Runge 1980; Nakagawa et al. 2001). We calculated clearance rates using equations from Frost (1972), applying the corrections from Nejstgaard et al. (2001) to account for increases in phytoplankton due to trophic cascades resulting from mesozooplankton consumption of microzooplankton. Errors for rates were calculated from replicate treatments. Ingestion was calculated from clearances rates multiplied by the initial concentrations of different categories of cell types (diatoms, other autotrophs and heterotrophs)

Biomass and gut pigment determination of *C. pacificus* and *E. pacifica*.

Biomass estimates. Formalin preserved samples from the P0704 mesozooplankton Bongo tows were sorted to quantify the abundance of the adult populations of *C. pacificus* and *E. pacifica*. For *C. pacificus* we took subsamples with a 10-ml Stempel pipette, equivalent to 1-5% of sample, depending on location. Female and CV stages were enumerated; 20 individuals of each group were randomly selected, imaged and prosome length was measured using Image J (1.44). For *E. pacifica*, samples were split with a Folsom splitter to 1/8 or 1/32 of the total. Ten adults were randomly selected, imaged and measured from the base of the eye to the tip of the telson (total length) using Image J. Length to carbon regressions were used to estimate average carbon per animal. For *C. pacificus* we used the regression from Lavaniegos & Ohman (2007): log C(μg) = -6.76 + 2.512 log(PL), where PL is prosome length in μm. For *E. pacifica*, we used the equation from Ross (1982): log μg C = -0.473 + 3.174 log(TL), where TL is total length in mm.

Gut pigments. In order to compare directly the grazing estimates for the two dominant species with the remaining community, we estimated grazing on autotrophs using the same methods as those for the mesozooplankton as a whole. Animals were sorted from the 1/4 frozen mesozooplankton subsample. Aliquots were thawed for 5 min in filtered seawater, and sorted using a stereomicroscope under dim light. Organisms were gently picked with tweezers, rinsed in DI water and extracted in 90% acetone. Samples were prepared in the same way as whole community analyses. Three replicate samples from one day and one night tow, containing 5 female or CV stage *C. pacificus* or three adult *E. pacifica*, were analyzed per experimental cycle. Processed samples were collected on the dates that we conducted grazing incubations.

All statistical analyses were done using Matlab 7. 5 (R2007b).

Results

Oceanographic conditions

Springtime is the season of highest productivity and system spatial variability in the Southern California region (Hayward and Venrick 1998). Fig. 1 depicts cruise-averaged MODIS-AQUA maps of sea surface chlorophyll during both cruises, as well as experimental cycle drifter tracks. Conditions during each cycle are described in Landry et al. (2009), and general conditions are summarized in Table 1. Five cycles were conducted during P0604 and four during P0704. During May 2006, Cycle 1 (0605-1) conditions were consistent with relatively recently upwelled waters: high Chl *a* and nitrate concentrations (Table 1), low temperature and high salinity (not shown), and waters rapidly advecting westward (offshore). Cycle 2 (0605-2) was located in the core of the California Current (CC), characterized by low salinity, low water-column integrated Chl *a* and a deep nitracline. Cycle 3 (0605-3) was located very close to shore, with high Chl *a*, but with downwelling waters flowing northward. Cycle 4 (0605-4) was initiated close to the spot where 0605-1 ended, with lower Chl *a* and nitrate concentrations and water still rapidly moving offshore. Cycle 5 (0605-5) was the only real oligotrophic cycle, conducted offshore beyond the extension of the CC (Fig. 1). Upper euphotic zone conditions similar were to Cycle 0605-2, but with a well-developed deep Chl *a* maximum.

During April 2007, Cycle 1 (0704-1) was in a nearshore, eutrophic location with relatively high nitrate and Chl *a* concentrations. Cycle 2 (0704-2) was characterized by low salinity, CC proper conditions, located in an anticyclonic eddy with a deep nitracline. Cycle 3 (0704-3) was initiated south of Pt. Conception, but the drifter quickly moved

southwest and had to be retrieved to avoid shallow waters, and thus lasted only one day. We include it here because it represents an end point of conditions, with very high Chl *a*, primary productivity, and mesozooplankton concentrations. Cycle 4 (0704-4) began downstream of Cycle 0704-1, but storm conditions in the area had produced a deeper mixed layer and higher nitrate conditions than 0704-1 (Table 1).

Plankton community

Primary production (PP) integrated through the depth of the euphotic zone decreased roughly exponentially with distance from shore (Fig. 2). The phytoplankton community is fairly dynamic in the nearshore region, increasing or decreasing concentrations in response to highly variable grazing pressure and nutrient dynamics in the area (Landry et al. 2009). Mesozooplankton community biomass followed a similar pattern, decreasing quite rapidly within 100 km from shore, but generally displaying less variability than PP. While scatter exists around the observed pattern of decreasing biomass with distance from shore, there is only one location where this clearly does not hold. This occurred during Cycle 0605-3, which was closest to shore (11 km, Table 1) yet had surprisingly low areal DW, with an average comparable to the CC proper cycles (Table 2). In addition, the community was dominated by smaller organisms (not shown). Cycle 0605-3 was carried out in relatively shallow waters, with zooplankton tows to depths only of 70-100 m. The lower zooplankton concentrations at this location likely reflect the shallower integration depth as well as the loss of deep habitat for large migratory forms, such as adult euphausiids, which tend to preferentially inhabit deeper water associated with shelf breaks and canyon edges (Brinton 1976). In addition,

because upwelled waters are advected offshore in the vicinity of Pt. Conception, the slower growth rates of crustacean zooplankton compared to phytoplankton can translate into a community peaking at a greater distance from shore. All of these factors likely contribute to the lower biomass and small animal dominance of the Cycle 3 site. At distances farther than 150 km offshore, in the California Current proper and oligotrophic offshore conditions, both PP and mesozooplankton DW did not change appreciably (Fig. 2).

The primary production - mesozooplankton relationship was further investigated by plotting mesozooplankton biomass as a function of PP (Fig. 3). Even when values were log-transformed homoscedasticity was not achieved (not shown), so we choose to interpret non-transformed values. Variability is greater with medium to high values of PP, and no correlation between the two is evident. Although both cruises were conducted during spring conditions, zooplankton biomass in the nearshore was higher during P0704. The reasons for this pattern are not obvious and can be hypothesized to be related to advective processes and/or possible differences in predator conditions (Landry et al. 2009) or the type of phytoplankton community, but they cannot be inferred from patterns in PP alone (Fig. 3).

Mesozooplankton daily ingestion

Consumption of phytoplankton increased with primary production (Fig. 4). A linear regression (model I) was imposed on the relationship between the log-transformed values, for comparison with other studies (although we also report the values for a model II regression below). While the model I regression assumes no error in the *x* variable, an

assumption clearly violated in this case, it was chosen as the acceptable statistical test for two reasons. First, Calbet & Prairie (2003) have argued that it is the method of choice when the goal is to find a predictive relationship between *y* (ingestion) and *x* (PP). In addition, it is statistically accurate when the error variance in *y* is much greater than the error variance in *x* (McArdle 2003), which Calbet & Prairie (2003) have indicated is the case between our two variables. The main reason we choose this method, however, was for comparison with the global dataset. While the number of ingestion observations within our study is limited (n = 31, compared to 238 from Calbet 2001), the range in PP among our different cycles (~ 1 order of magnitude), the different regimes in the CCE (sensu Hayward and Venrick 1998), and our sampling scheme can lead to a more mechanistic understanding of the underlying relationship driving the flow of PP through the mesozooplankton.

The slope of this relationship, when all values were pooled, was 1.04 (95% CI: 0.54 -1.48, r^2= 0.45). A group of estimates falls considerably away from the regression line, corresponding to Cycle 0704-1, when grazing was anomalously high, driven by a very high zooplankton biomass. In fact, grazing at this time accounted for 150% of the PP at that location (Table 2). We investigated differences in the % PP consumed during each cycle (Table 2). The only location where consumption was significantly different was during Cycle 0704-1 (one-way ANOVA, Tukey-Kramer, $p < 0.001$). When the 95% CI of the residuals of the linear regression are investigated, only two observations are outliers, corresponding to the latter two measurements taken 0704-1.

Cycle 0605-5 had noticeably lower values than the other cycles (Fig. 4), but the cycle average was not statistically different from the other locations. If we remove the

estimates from the anomalous cycle, 0704-1, the slope of the linear regression becomes steeper (1.15, 95% CI: 0.86-1.5), and the amount of variability explained by the regression increases to 73% ($p < 0.001$).

We also report the slope values using the model II regression. Given the error existent in both these measurements this test is more appropriate. A commonly used model II method is to calculate the geometric mean of the two model I slopes, achieved by dividing the model I slope by the absolute value of r, in this case 0.67 (Ricker 1975; Laws 2003). This slope is 1.04/0.67 = 1.55 (95% CI = 0.89 – 2.2). The model II slope estimate would suggest that the amount of PP transferred to mesozooplankton is in fact higher in more productive regions.

Mesozooplankton daily carbon requirements

In the very nearshore region off of Pt. Conception (>50 km), the mesozooplankton community is able to satisfy daily carbon requirements by exploitation of phytoplankton alone. In fact, our estimates suggest that the community consumed two to four times their daily carbon requirements (Fig. 5), based on the equations of Ikeda (1985). At distances greater than 50 km, phytoplankton consumption was insufficient to sustain requirements for growth, and at two locations (~100 and 370 km), insufficient to sustain even basal metabolic requirements. An almost monotonic decreasing trend in daily carbon requirements met was evident in the first ~100 km from shore (Fig. 5). If we assume that the entire microzooplankton production is cropped by the mesozooplankton community, the overall pattern is similar to when phytoplankton is assumed to be the sole dietary component. However, daily requirements can now be met everywhere except at

one location: about 100 km from shore, corresponding to cycle 0605-4. Adding microzooplankton production to community diet at this location allows the community to sustain basal respiratory requirements, but not growth or defecation (Fig. 5).

There are no obvious differences between cruises in the extent to which mesozooplankton satisfied metabolism and growth requirements. Both exhibit a monotonic (P0605) or near monotonic (P0704) decrease for the three cycles nearest to shore (when considering just phytoplankton), with little change at greater distances (Fig. 5).

*Dietary choices of two dominant system 'herbivores': **C. pacificus** and **E. pacifica***

The abundances of late developmental stages of *C. pacificus* (CV and adult females) and *E. pacifica* decreased with distance from shore during P0704 (Fig. 6a), analogous to the pattern displayed by mesozooplankton DW (Fig. 2). The carbon contribution of adult *E. pacifica* to community DW followed the same pattern, but the percentage contribution of both adult and CV stages of *C. pacificus* to total biomass remained essentially constant throughout the spatial domain (Fig. 6b).

We investigated the importance of phytoplankton as food items for both species in the same way as for the total community, using the gut pigment method. Fig. 7 depicts the fraction of daily carbon consumed from autotrophic sources for the entire community and these two species individually (estimates separated by stage of *C. pacificus*). Both species show a linear decrease in carbon requirements met by phytoplankton, consistent with the decreasing patterns of production and the general trend of the overall community. Consumption in excess of calculated requirements is evident for each stage

and species during the most nearshore Cycle 0704-3. While *E. pacifica* always consumed phytoplankton carbon in excess of growth requirements, both stages of *C. pacificus* only did so during the cycle 0704-3, which had the highest productivity measured in the region during the 2007 cruise.

In the offshore region, phytoplankton consumption by *C. pacificus* was ~1% of body carbon day $^{-1}$ (both CV and adults), about 10% of the carbon necessary to sustain respiration.

Feeding incubations

Clearances rates (*F*, volume swept clear) based on prey disappearance in experimental incubations were high and relatively similar among locations (Fig. 8a, b). Because clearance rates reflect ingestion rates normalized to prey abundance, comparison of clearance rates are a better indication of prey selection. Rates calculated by particle size generally showed a stronger and more consistent pattern than by cell type.

C. pacificus females showed a strong size-selective behavior, with large particles and diatoms cleared at much higher rates (Fig. 8a, 9a). During the offshore cycle, particles in the large size category were present at very low concentrations, which would explain their negligible yet highly variable clearance rates. *E. pacifica* showed no consistent pattern of size or type selectivity, typically consuming the most abundant particles in proportion to their abundances. The one exception was cycle 0704-4 when large particles (large pennate diatoms resembling *Pseudo-nitzschia sp.*) were the preferred prey (Fig. 8b, 9b). Particle selection for the different types of cells were consistent with a size-selective behavior, *C. pacificus* generally preferred diatoms (which

were usually the larger particles), while *E. pacifica* consumed all particles types in proportion to their abundances (not shown).

During P0704 the abundant large particles were diatoms, constituting most of the diet of both species (Fig. 10a, b). Ingestion was highest at locations with higher productivity. Ingestion rates calculated using F (ml h^{-1}) and ambient particle concentrations consistently underestimated ingestion when compared to rates obtained from the gut pigment method of freshly collected animals. *C. pacificus* consumed enough food to sustain basic respiration rates only during Cycle 0704-3, where primary production was highest (Fig. 10a). *E. pacifica* ingested enough to satisfy metabolic requirements at two locations (Fig. 9b). However, none of the experimental bottle incubations showed that either species was able to consume enough to sustain growth. This underestimate is not entirely a product of bottle effects since the measured clearance rates, were on the higher end of values reported in the literature for both species (Fig. 8 & 9). The discrepancy between the two methods is not surprising since microplankton concentrations obtained from Niskin bottles generally represent average water column condition, while small scale patchiness, e.g. in the form of 'thin layers' (McManus et al. 2003), has been argued to play an important role in zooplankton nutrition (Sevadjian et al. 2010). It has long been known that 'average' dilute concentrations are insufficient to sustain dietary requirements (Mullin and Brooks 1976).

Estimated trophic position, based on dietary input, generally varied inversely with productivity and ingestion for *C. pacificus* (Fig. 10a), achieving a maximum TP of ~2.8 when prey concentrations were low. *E. pacifica* increased consumption of non-

autotrophic organisms (up to 40%) during Cycle 1 (Fig. 10b), which had the lowest average PP of all the nearshore locations (Table 2).

Discussion

Mesozooplankton biomass, grazing and phytoplankton

Globally it was been argued that the main variables determining zooplankton respiration and grazing are temperature and biomass (Ikeda 1985; Huntley and Lopez 1992). It is therefore slightly surprising that despite the variability in the relationship between biomass and PP, a significant relationship was found with community grazing. The conclusions that we can draw from interpreting the slope of this relationship differ from those of Calbet's (2001) global analysis. At least within the variability observed in our system, the proportion of PP flowing through the mesozooplankton seems to be relatively constant (Fig. 4, Table 2).

In addition, tracking the time evolution of the phytoplankton community and process rates in each of the experimental cycles allows for important insights into the relationships among the two variables. During 0704-1 and 0704-4 PP decreased appreciably during the experimental cycle, apparently as a consequence of high mesozooplankton grazing in excess of PP, which reduced phytoplankton biomass (Landry et al. 2009). Particularly during 0704-1, PP decreased from 2400 mg C m^{-2} to 580 mg C m^{-2}, while grazing was consistently high and remained relatively constant throughout these four days. In highly variable regions, where the mesozooplankton has the potential to negatively impact PP or where PP might suddenly increase due to an injection of nutrients, variability around the regression will always lead to a flattening of

the slope. Conclusions drawn from the instantaneous relationship of these two variables must be made cautiously because the time scales of variability for phytoplankton and zooplankton are different.

The fact that the PP directly consumed by zooplankton in the furthest offshore Cycle was lower than other cycles (Table 2) is consistent with long-standing notions of lower direct PP transfer to mesozooplankton in oligotrophic ocean regions. The lack of statistical significance may be a product of the variability inherent in ingestion measurements. In our study region the proportion of PP that flows through mesozooplankton is regionally relatively constant, though somewhat higher in the more eutrophic areas.

Considering the different time scales involved in phyto- and mesozooplankton turnover rates (Cushing 1989), the considerable advection of water parcels in the nearshore (Fig. 1), and the variable effect of mesozooplankton on PP, the lack of a correlation between PP and mesozooplankton biomass is not too surprising (Fig. 3). Two cycles stand out as distinctly challenging the notion that PP directly drives mesozooplankton secondary production at all locations. For example, Cycle 0605-3 had low mesozooplankton biomass due to shallow depths and a location very close to shore (Fig. 1). This departure from expectation is most likely due to differences in the developmental time-scales of zooplankton and phytoplankton in a parcel of water that had likely been recently upwelled. Cycle 0704-1 was located within a circulating eddy feature (Fig. 1). Zooplankton could have been accumulating due to *in situ* growth, biological aggregation, or a combination of both. Advection, mesoscale features,

temporal mismatches in growth and ecosystem productivity are all important determinants of biomass in this region, in addition to phytoplankton primary production.

Daily carbon requirements and the role of shifting trophic positions

The marine pelagic ecosystem is generally viewed as a nutritionally dilute environment, where the average zooplankter has difficulty procuring the necessary dietary requirements to sustain sometimes even basal metabolic demands, and often carbon requirements necessary for growth (e.g. Mullin and Brooks 1976; Dam et al. 1993; Dam et al. 1995; Calbet et al. 2009). Our results suggest that zooplankton in our region do sometimes go hungry. At least at one location during our study (cycle P0605-4), we were hardly able to account for basic metabolic rates even after assuming consumption of the entire microzooplankton production (Fig. 5). Significant consumption of fecal pellets or detritus is unlikely at this location because the majority of phytoplankton production could be accounted for by micro- and mesozooplankton grazing (Landry et al. 2009), and measured export suggested that most fecal matter (estimated as 0.3 * [phytoplanton grazed + $Mzoo_{prod}$]) was exported out of the euphotic zone (Stukel et al. *in press*). Carnivory can also be invoked (Landry 1980; Bonnet et al. 2004), yet it is generally thought that carnivory increases with size within the mesozooplankton community. Carbon requirements were calculated individually for each size class and never during this cycle were they met for any fraction (not shown). Even if carnivory was an important foraging strategy at this time, a significant portion of the community was probably still experiencing food deprivation.

With the exception of two locations, however, the fact that sufficient carbon is consumed from phytoplankton to meet respiratory demands in the remaining areas of the region is in stark contrast to other studies conducted in ecosystems with varying degrees of productivity, (Dam et al. 1993; Dam et al. 1995; Calbet et al. 2009).

The inferred nutritional status of the community is spatially quite variable, such that we will divide the region into three areas for discussion. Two of these areas have been characterized as distinct regimes (*sensu* Hayward and Venrick 1998), with distinct patterns in Chl *a* temporal variability and nearsurface nutrient enrichment (Hayward and Venrick 1998). Venrick (2002) indicated two recurrent floral phytoplankton clusters associated with these regions. The first region includes the highly productive, nearshore area (extending to ~50 km offshore during the times of our study). The offshore region extends from ~150 km and beyond, and water masses in this region seem to have distinctly different origins from the nearshore region. Drifter tracks from Cycle 0605-2 are southward (the general direction of the CC) and followed an anticyclonic eddy during 0704-2 (Fig. 1). The third region encompasses the transition between the two. The general location of this transition area coincides with the location where upwelling ends and weak downwelling begins, estimated from wind speeds averaged over a period of 20 years (Rykaczewski and Checkley 2008). This region is also within a wide area between the two floristic regions, where phytoplankton varies according to meanders of the California Current (Venrick 2002).

In general, the >200-μm zooplankton in the CCE are able to consume carbon in substantial excess of their total daily requirements in the nearshore area, up to ~50 km from shore near Pt. Conception (Fig. 5). Phytoplankton consumption was enough to

satisfy, at times, up to four times the carbon requirements for respiration, growth and defecation. Consumption of microzooplankton was not necessary to sustain energetic needs in this area, yet might still be necessary to supplement nutritional requirements not met by phytoplankton. Incubations with *C. pacificus* showed that 20% of the copepod diet was heterotrophic in this nearshore area, with the exception of the most productive location (Fig. 10a), where diatoms comprised the majority of microplankton biomass (84% of the initial biomass in the incubation bottles). *E. pacifica* only consumed heterotrophs during one cycle when PP was significantly decreased (Fig. 10b) and microheterotrophs had increased in relative concentration (not shown). This cycle was conducted ~50 km from shore and is still within the area where carbon consumption from phytoplankton typically exceeds requirements for growth.

Exploitation of the heterotrophic community is the most likely explanation for zooplankters being able to thrive in the offshore oligotrophic waters. For the two cycles conducted in the California Current proper (0605-2 and 0704-2), only basal requirements were consistently satisfied by autotrophic prey. This amount of nutrition is unsuitable for the persistence of populations over long periods of time. While zooplankton carnivory probably also increases in importance in this region, we hypothesize that predation pressure on microzooplankton is largely supporting the community as a whole. Switching in zooplankters has been extensively reported to occur in response to decreased phytoplankton concentrations, in both laboratory and field studies (Landry 1981; Fessenden and Cowles 1994; Ohman and Runge, 1994; Calbet and Saiz 2005). The observation that largely herbivorous copepods and euphausiids did gradually shift to a more omnivorous diet (Fig. 10a, b) in response to decreasing PP, supports the notion

that the mesozooplankton in the CCE as a whole shift to a more omnivorous diet. The ability of microzooplankton production to meet in excess all mesozooplankton carbon requirements in most locations suggests an important role in fueling the metazoan secondary production (Fig. 5).

The transition area is characterized by relatively high mesozooplankton biomass (Fig. 2), a similar yet changing species composition evinced by a decrease in the relative carbon contribution of adult *E. pacifica* to the entire community (Fig 6a,b), and a community that seemingly experiences varying degrees of starvation (Fig. 5, 7). Our results lend themselves to the interpretation that a significant portion of the mesozooplankton community consumes carbon in excess in the nearshore area building a high zooplankton biomass that gets advected to the more nutritionally dilute waters further offshore. We hypothesize that the community in this area is effectively seeded by healthy, growing, satiated zooplankters from close to shore. This issue does beg the question: how long can they happily survive and grow from reserves accrued in the nearshore area? How much can survival be extended by exploitation of heterotrophic food sources?

Incubations using the two dominant CC zooplankton species show that they gradually adjust their diets to ambient conditions, with *C. pacificus* reaching a trophic position of ~2.8 in the oligotrophic offshore region. This change in diet seemed to be driven primarily by size selective behavior (Fig. 8&9), consistent with previous studies of feeding behavior in copepods (Frost 1972; Runge 1980).

Calculations using gut pigments and estimates of microzooplankton production show that at this location, even while taking trophic shifts into account, *C. pacificus*

seemingly cannot sustain growth and respiration and *E. pacifica* abundance is negligible. However, the assumption that mesozooplankton consume all microzooplankton production can be erroneous. At the regional scale it is clearly an overestimate since trophic steps within the microzooplankton result in losses due to respiration (Calbet and Landry 1999). Over the small spatial scales encountered here, mesozooplankton consumption of protozoans might be underestimated if advection and low grazing pressure (due to preference for phytoplankton) lead to offshore transport and accumulation of their biomass. Carnivory can also potentially contribute to energetic requirements, since many copepods have been observed to consume eggs and nauplii in conditions of decreased phytoplankton supply (Landry 1980; Landry 1981; Ohman and Hirche 2001; Bonnet et al. 2004). Carbon flux estimates for P0605 argue against coprophagy as an important feeding strategy, since most fecal matter was exported out of the euphotic zone versus recycled and consumed within it (Stukel et al. *in press*).

These results point to a mesozooplankton community that is able to sustain a high biomass throughout an extensive spatial range, drawing on reserves originating from excess food nearshore and a gradual trophic shift to enhanced omnivory with distance from shore. Consumption of microzooplankton is energetically required by mesozooplankters throughout most of the region, even in areas relatively nearshore, with an increasing role in less productive regions.

Acknowledgements

This chapter would not have been possible without the cooperative efforts of the many different researchers, students, technicians, and volunteers on the P0605 and P0704 cruises of the California Current Ecosystem (CCE) Long-Term Ecological Research (LTER) program. I am particularly indebted to my co-workers in the Landry Lab (M. Landry, M. Stukel, A. Taylor and, D. Wick) for providing microzooplankton grazing and microscopy results, the Ohman Lab (M. Ohman, R. Rykaczewski, J. Powell, K. Tsyrklevich, D. Taniguchi) for mesozooplankton biomass and grazing results, the Goericke Lab (R. Goericke, S. Dovel, M. Roadman) for 14C-PP and chlorophyll. I am also grateful to the captains and crews of the R.V. *Knorr* and the R.V. *Thomas Thompson*.

Chapter 3, in full, is currently in preparation for submission: Décima, M.R., Landry, M. R., Ohman, M.D., "Zooplankton Trophic Variability in the California Current Ecosystem". The dissertation author was the primary investigator and author on this paper.

Table 3.1. Summary of conditions, and zooplankton studies during experimental cycles on CCE-LTER cruises P0605 and P0705. Distance from shore corresponds to beginning and end of each drifter cyle, integrated Chl *a* and surface nitrate are cycle averages (mean ± SD).

	Array dates (2006)	**Distance from shore (km)**	**Integrated Chl *a* (mg m^{-2})**	**Surface nitrate (μM)**	**Zooplankton experimental studies**
Cycle 1	11-15 May	29 - 49	185 ± 41	7.8 ± 3.6	Biomass & GF
Cycle 2	17-21 May	166 - 162	26 ± 0.9	0.08 ± 0.03	Biomass & GF
Cycle 3	22-25 May	11 - 12	110 ± 25	1.2 ± 0.8	Biomass & GF
Cycle 4	26-31 May	77 - 117	40 ± 8	0.9 ± 0.07	Biomass & GF
Cycle 5	1-5 June	353 - 392	26 ± 6	0.12 ± 0.04	Biomass & GF
	Array dates (2007)				
Cycle 1	4-8 April	39 - 44	62 ± 17	5.9 ± 1.7	Biomass & GF, incubations
Cycle 2	9-13 April	255 - 287	29 ± 2.3	0.05 ± 0.04	Biomass & GF, incubations
Cycle 3	14 April	24	31	10.5 ± 0.3	Biomass & GF, incubations
Cycle 4	15-20 April	62- 60	37 ± 10	7.6 ± 2.5	Biomass & GF, incubations

Table 3.2. Summary of euphotic zone integrated rates of primary production (PP, mg C m^{-2} d^{-1}), mesozooplankton dry weight (g DW m^{-2}) and % PP consumed by the entire community. Estimates are cycle averages (mean ± SD).

	PP (mg C m^{-2} d^{-1})	**Mesozooplankton DW (g m^{-2})**	**% PP consumed**
Cycle 1	4183 ± 1803	4.5 ± 1.7	19 ± 19
Cycle 2	562 ± 12	1.2 ± 0.3	20 ± 12
Cycle 3	4382 ± 364	1.6 ± 0.7	22 ± 5
Cycle 4	1352 ± 98.4	3.1 ± 0.8	14 ± 5
Cycle 5	483 ± 162	0.8 ± 0.1	4.6 ± 1.4
Cycle 1	1232 ± 831	8.4 ± 2.5	156 ± 66
Cycle 2	587 ± 79	1.4 ± 0.2	21 ± 7.7
Cycle 3	7060	10.6	18
Cycle 4	2314 ± 929	5.9 ± 0.7	13 ± 8

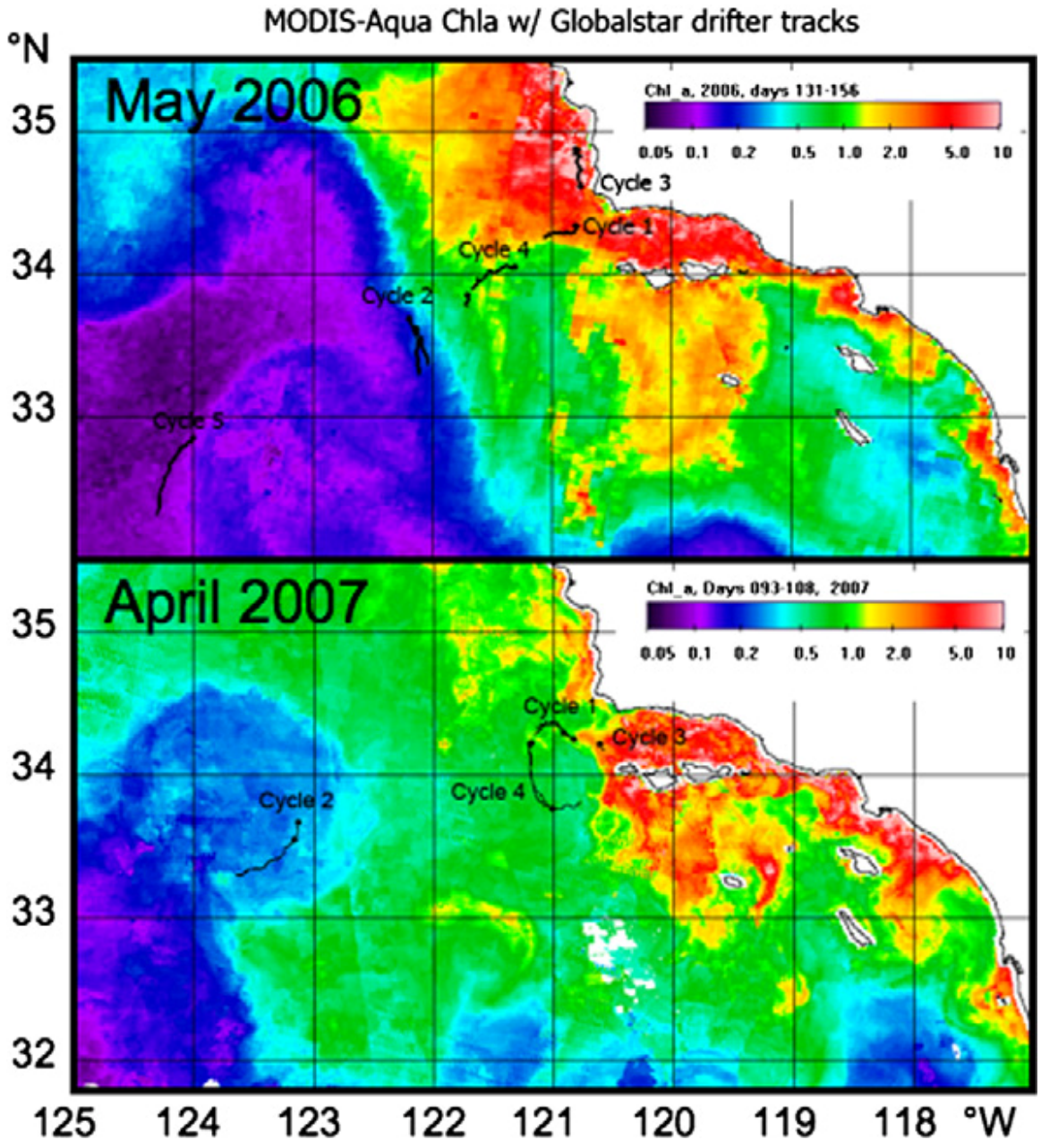

Figure 3.1. Cruise-averaged MODIS-Aqua maps of surface Chl *a* with overlain drifter tracks of experimental cycles conducted during two experimental cruises. Top box is cruise P0605 conducted during May 2006, bottom box shows conditions encountered during April 2007 (P0704). Figure from Landry et al. (2009).

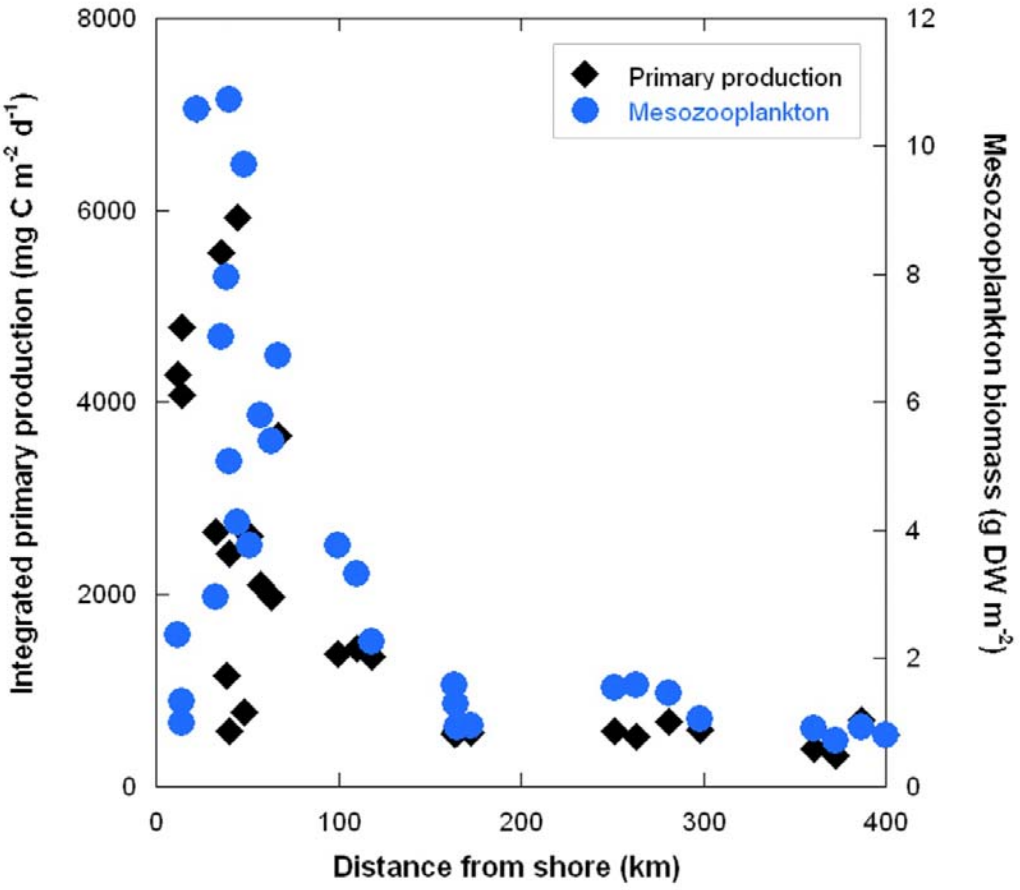

Figure 3.2. Euphotic zone estimates of integrated primary production (mg C m^{-2} d^{-1}) and mesozooplankton biomass (g DW m^{-2}) from P0605 and P0704 as a function of distance from shore. Note different scales on each *y*- axis.

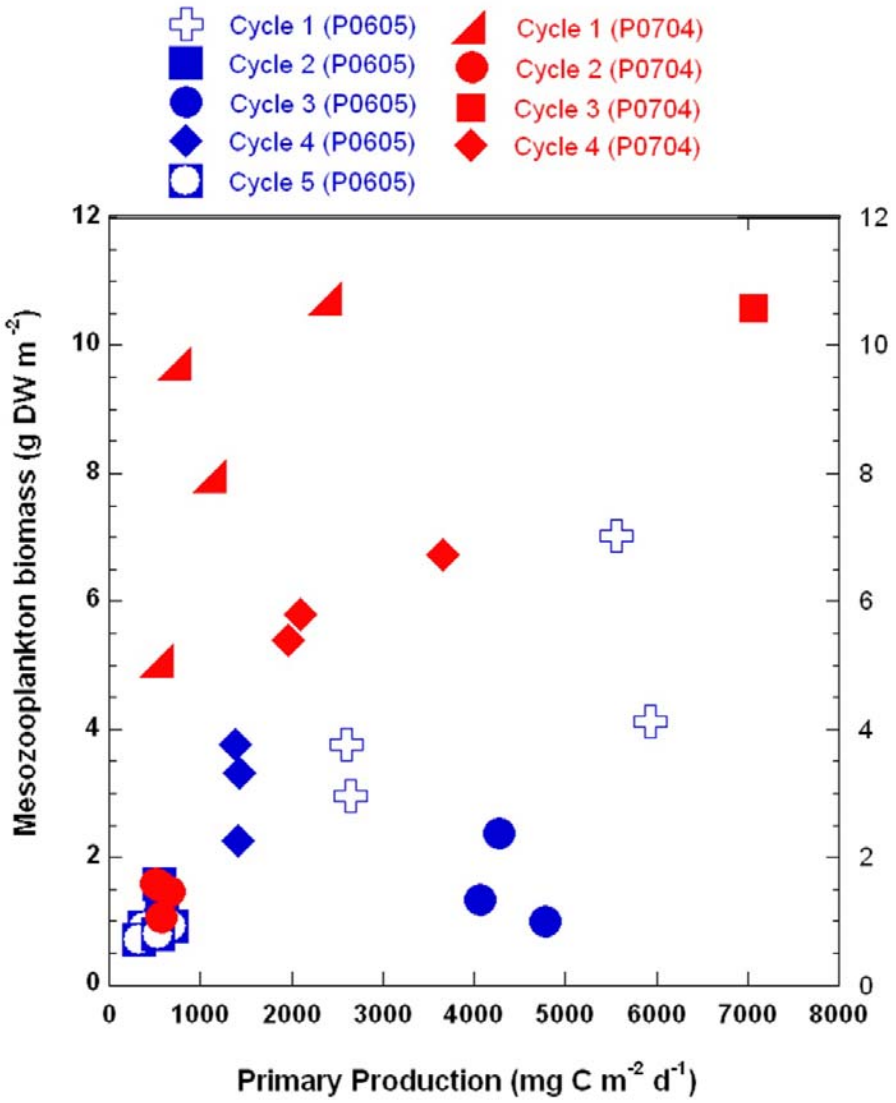

Figure 3.3. Scatter plot of areal estimates of mesozooplankton biomass (g DW m^{-2}) against phytoplankton primary production (mg C m^{-2} d^{-1}). Color coding is by cruise, and each experimental cycle is denoted with a different symbol (see legend).

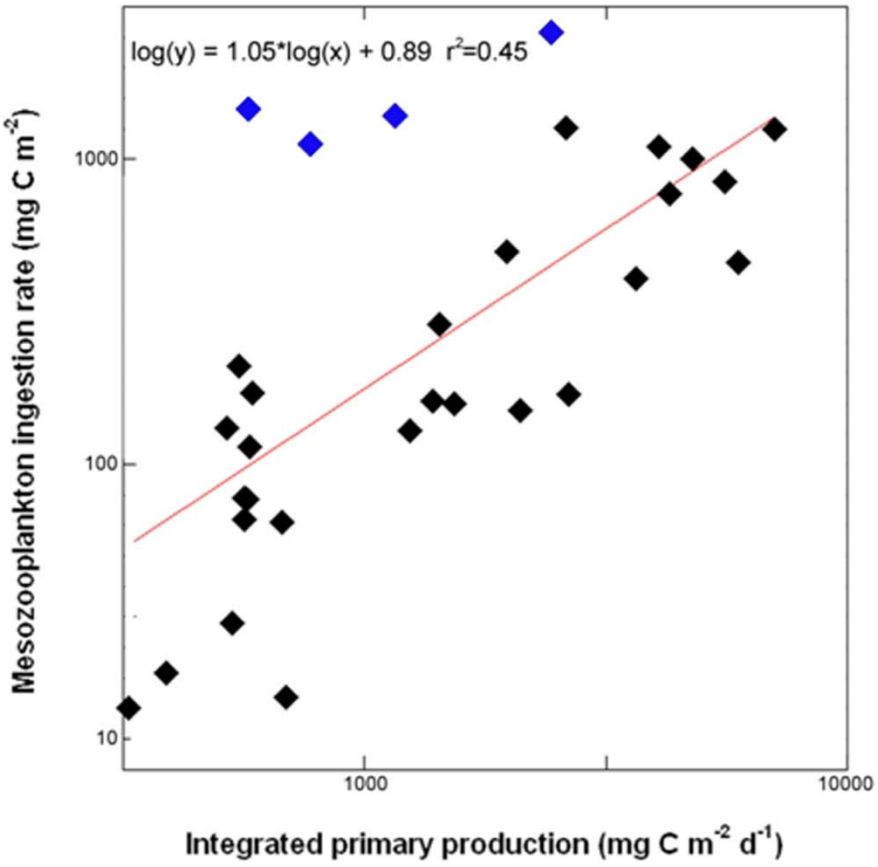

Figure 3.4. Model I regression of mesozooplankton ingestion as a function of phytoplankton primary production. Equation parameters (95% CI): intercept = -0.86 (-2.4, -0.51); slope = 1.04 (0.6-1.5), r^2 = 0.45, error variance = 0.22, p < 0.0001. Regression parameters without the high grazing of 0704-1 (diamods in blue) are: intercept = -1.38 (-2.3,-0.46); slope = 1.15 (0.87, 1.4); r^2 = 0.73, error variance = 0.09, p << 0.0001.

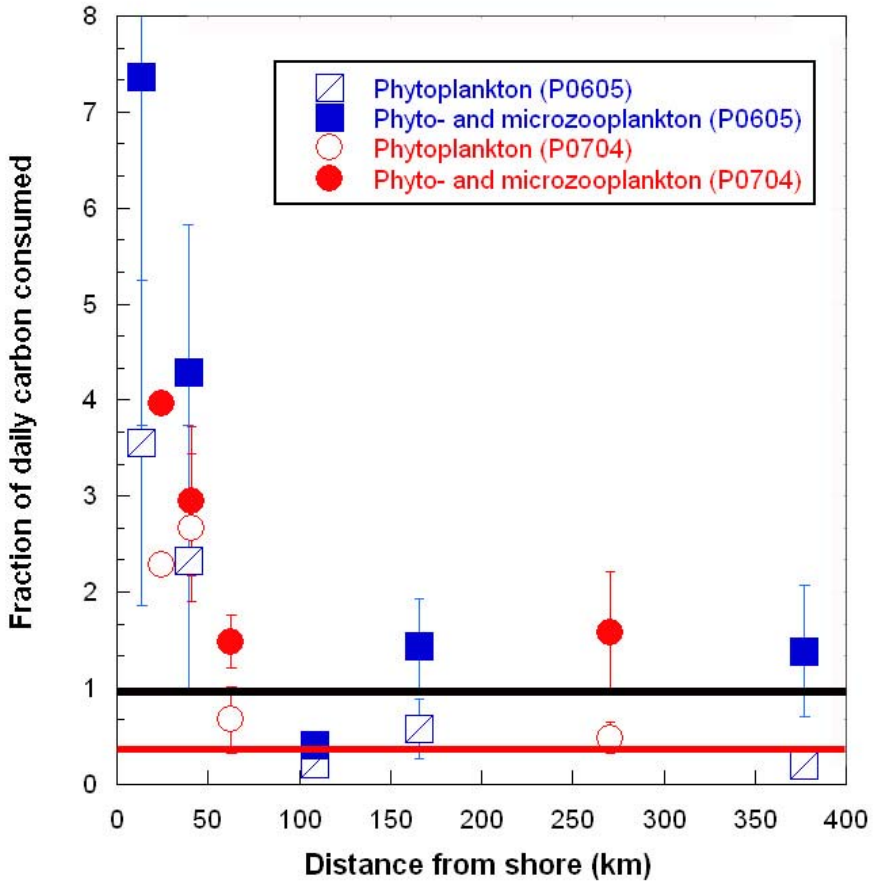

Figure 3.5. Fraction of daily carbon requirement consumed by the CCE mesozooplankton community, calculated as $C_{consumed}/(C_{respired}*3)$, for both cruises, with distance from shore. Legend indicates separate markers for calculations including phytoplankton consumption alone, and calculations assuming consumption of all microzooplankton production. Daily estimates were averaged for each experimental cycle (mean ± SD). Estimates below the black line correspond to instances when mesozooplankton consumption rates were insufficient to fulfill total carbon requirements. Estimates below the red line indicate times when respiratory requirements were not met.

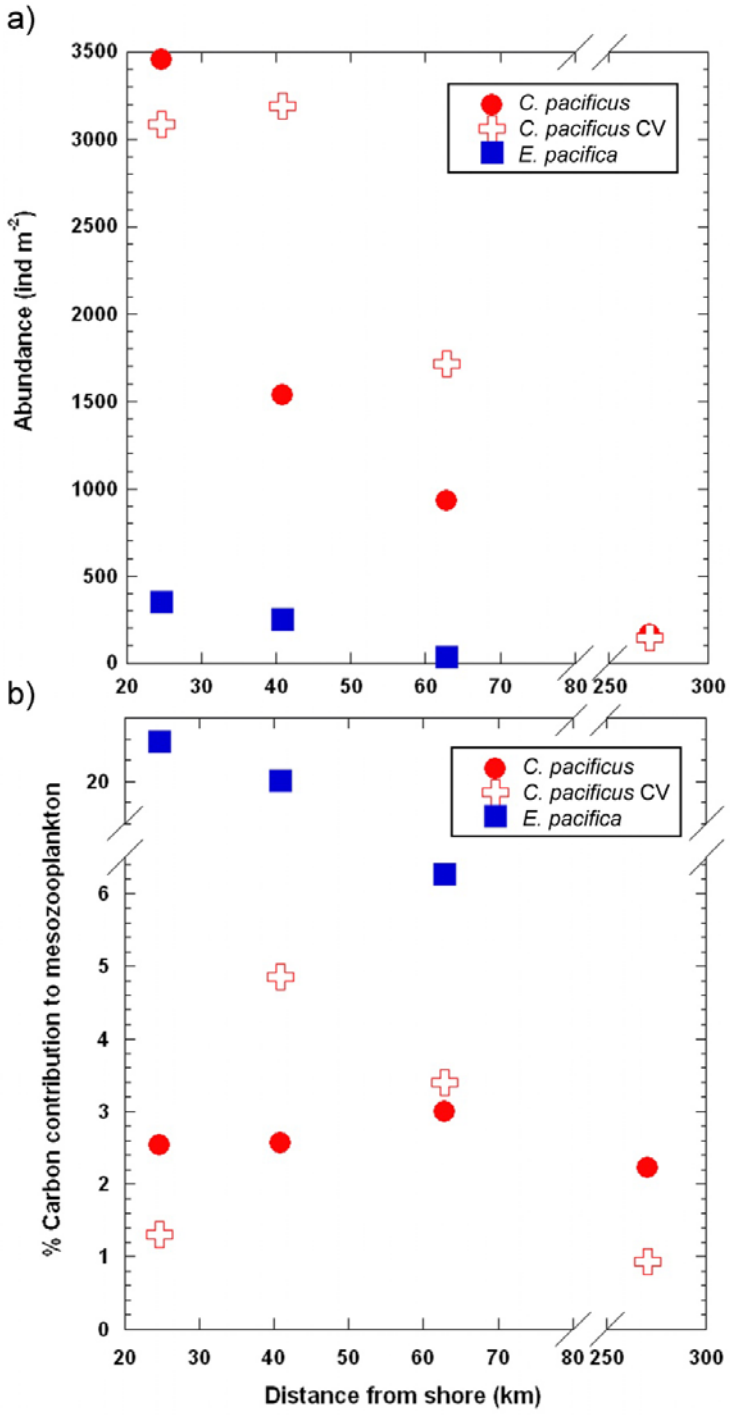

Figure 3.6. a) Abundance of *C. pacificus* (females and stage CV) and adult *E. pacifica* during the four experimental cycles of P0704. Note the break on the *x* axis. b) % carbon contribution of the two species to total mesozooplankton biomass. Note break on both *y* and *x* axis.

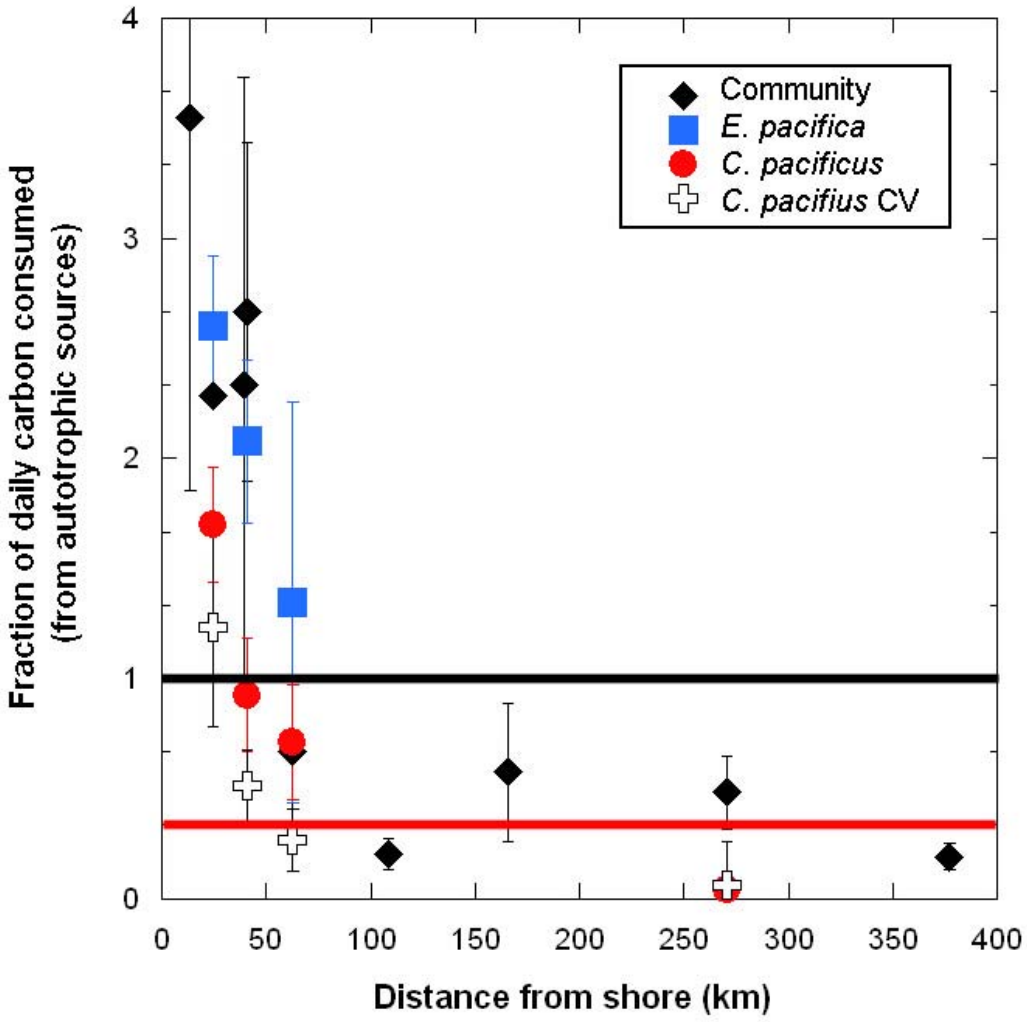

Figure 3.7. Fraction of daily carbon requirement obtained from phytoplankton alone, as estimated from gut pigments, for the entire mesozooplankton community, and for *C. pacificus* and *E. pacifica* separately (mean ± SD). Estimates below the black line correspond to instances when mesozooplankton consumption was insufficient to fulfill total carbon requirements. Estimates below the red line indicate times when respiratory requirements were not met.

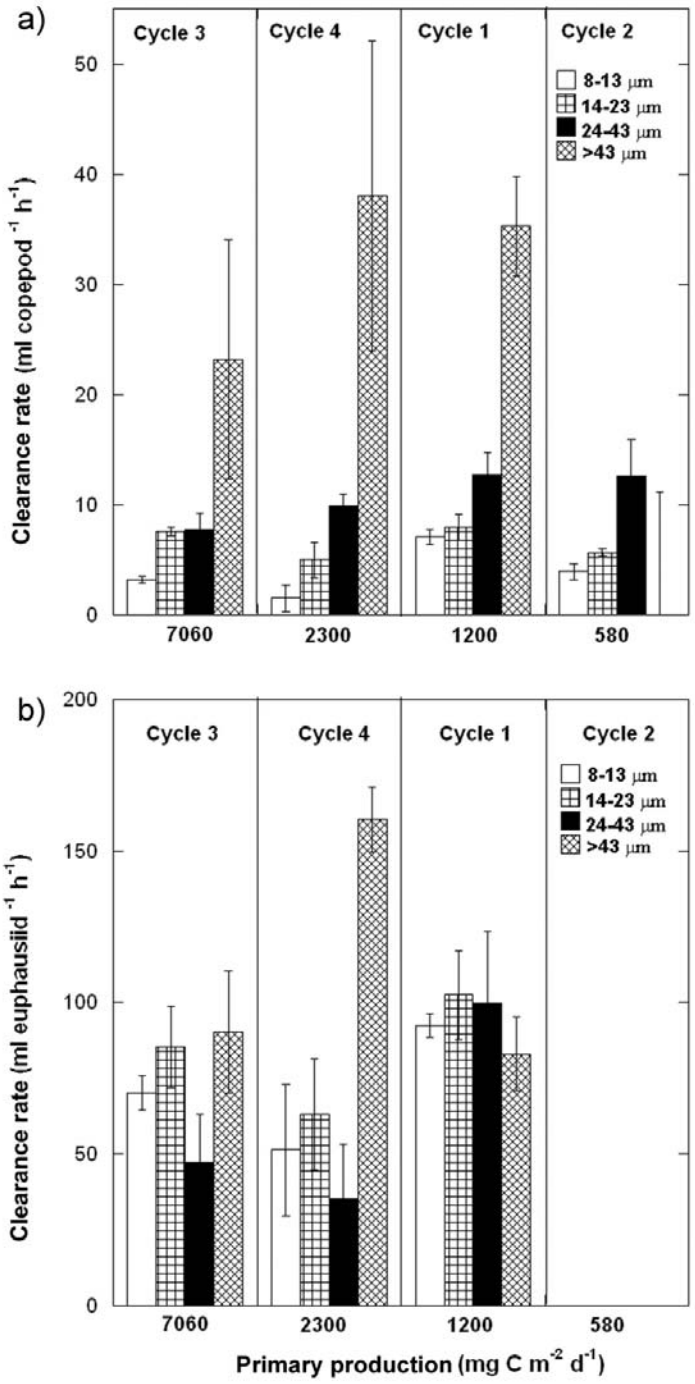

Figure 3.8. Clearance rates (mean ± SD) from incubations using individual species of zooplankton on four different types of particles sizes. a) Volume swept clear (F, ml copepod^{-1} h^{-1}) for female *C. pacificus*. b) Volume swept clear (F, ml euphausiid^{-1} h^{-1}) for adult individual *E. pacifica*. Cycles are organized in decreasing order of measured euphotic zone integrated rate of primary production.

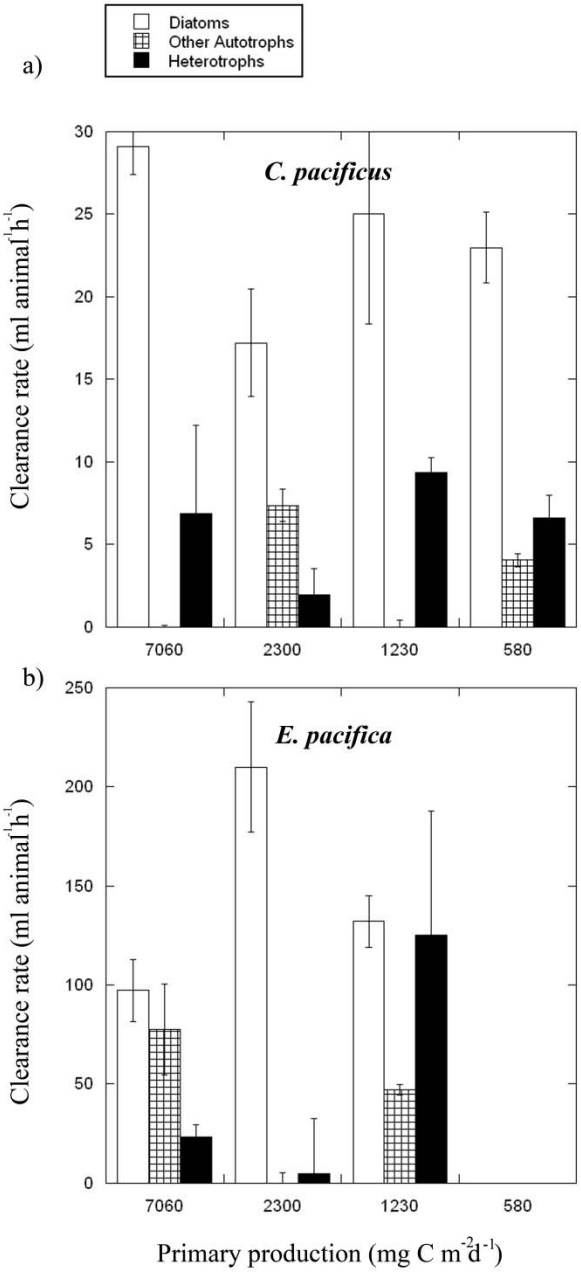

Figure 3.9. Clearance rates (mean ± SD) from incubations using individual species of zooplankton on 3 particle types: Diatoms, other autotrophs and heterotrophs. a) Volume swept clear (F, ml copepod^{-1} h^{-1}) for female *C. pacificus*. b) Volume swept clear (F, ml euphausiid^{-1} h^{-1}) for adult individual *E. pacifica*. Cycles are organized in decreasing order of measured euphotic zone integrated rate of primary production.

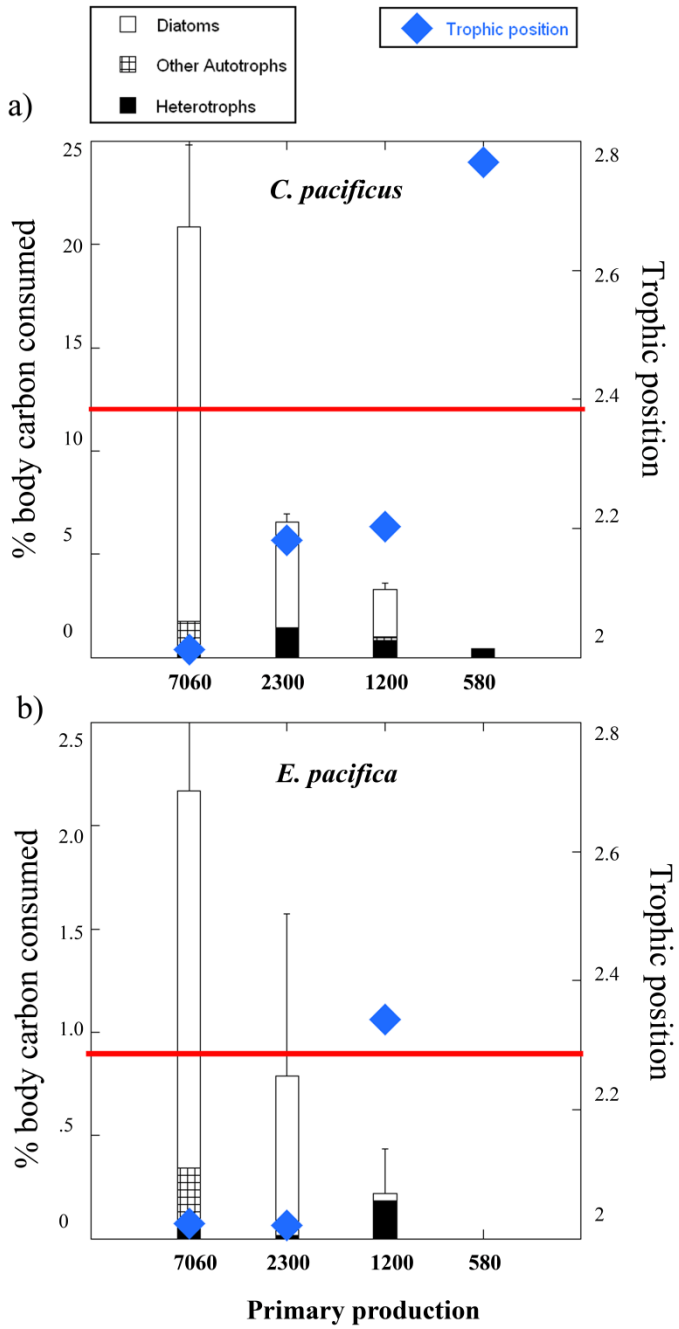

Figure 3.10. Experimental estimates of trophic position and % body carbon consumed (note different *y* axis) by two dominant species of zooplankton in the CCE region (mean ± SD). a) *C. pacificus* was present throughout the study region, during all four experimental cycles. b) *E. pacifica* was restricted to cool, recently upwelled waters nearshore, and had a negligible abundance during cycle 0704-2. Dietary contribution of different groups of microplankton is detailed in legend. Red line indicates % daily carbon necessary for respiration.

References

Al-Mutairi, H., and M. R. Landry. 2001. Active export of carbon and nitrogen at Station ALOHA by diel migrant zooplankton. Deep-Sea Res. II **48:** 2083-2103.

Bonnet, D., J. Titelman, and R. Harris. 2004. Calanus the cannibal. J. of Plankton Res. **26:** 937-948.

Brinton, E. 1960. Changes in the distribution of euphausiid crustaceans in the region of the California current. In: The Changing Pacific Ocean in 1957 and 1958. California Coop Oceanic Fish Invest Repts **7:** 137-146.

Brinton, E. 1976. Population biology of *Euphausia pacifica* off southern California. Fish. Bull. **74:** 733-762.

Brinton, E., and A. Townsend. 2003. Decadal variability in abundances of the dominant euphausiid species in southern sectors of the California Current. Deep-Sea Res. II **50:** 2449-2472.

Buitenhuis, E., C. Le Quere, O. Aumont, G. Beaugrand, A. Bunker, A. Hirst, T. Ikeda, T. O'Brien, S. Piontkovski, and D. Straile. 2006. Biogeochemical fluxes through mesozooplankton. Glob. Biogeochem. Cycle **20:** 18.

Calbet, A. 2001. Mesozooplankton grazing effect on primary production: A global comparative analysis in marine ecosystems. Limnol. Oceanogr. **46:** 1824-1830.

Calbet, A., D. Atienza, C. I. Henriksen, E. Saiz, and T. R. Adey. 2009. Zooplankton grazing in the Atlantic Ocean: A latitudinal study. Deep-Sea Res. II **56:** 954-963.

Calbet, A., and M. R. Landry. 1999. Mesozooplankton influences on the microbial food web: Direct and indirect trophic interactions in the oligotrophic open ocean. Limnol. Oceanogr. **44:** 1370-1380.

Calbet, A., and Y. T. Prairie. 2003. Mesozooplankton grazing and primary production: Reply to the comment by Laws. Limnol. Oceanogr. **48:** 1359-1362.

Calbet, A., and E. Saiz. 2005. The ciliate-copepod link in marine ecosystems. Aquat. Microb. Ecol. **38:** 157-167.

Conover, R. J., R. Durvasula, S. Roy, and R. Wang. 1986. Probable loss of chlorophyll-derived pigments during passage through the gut of zooplankton, and some of the consequences. Limnol. Oceanogr. **31:** 878-887.

Cushing, D. H. 1989. A difference in structure between ecosystems in strongly stratified waters and in those that are only weakly stratified. J. of Plankton Res. **11:** 1-13.

Davis, R. E., M. D. Ohman, D. L. Rudnick, J. T. Sherman, and B. Hodges. 2008. Glider surveillance of physics and biology in the southern California Current System. Limnol. Oceanogr. **53:** 2151-2168.

Dam, H. G., C. A. Miller, and S. H. Jonasdottir. 1993. The trophic role of mesozooplankton at 47°N, 20°W during the North Atlantic bloom experiment. Deep-Sea Res. II **40:** 197-212.

Dam, H. G., and W. T. Peterson. 1988. The Effect of Temperature on the Gut Clearance Rate-Constant of Planktonic Copepods. J. Exp. Mar. Biol. Ecol. **123:** 1-14.

Dam, H. G., X. S. Zhang, M. Butler, and M. R. Roman. 1995. Mesozooplankton grazing and metabolism at the equator in the central Pacific: Implications for carbon and nitrogen fluxes. Deep-Sea Res. II **42:** 735-756.

del Giorgio, P. A., and C. M. Duarte. 2002. Respiration in the open ocean. Nature **420:** 379-384.

Durbin, E. G., and R. G. Campbell. 2007. Reassessment of the gut pigment method for estimating in situ zooplankton ingestion. Mar. Ecol. Prog. Ser. **331:** 305-307.

Eppley, R. W. 1968. An incubation method for estimating carbon content of phytoplankton in natural samples. Limnol. Oceanogr. **13:** 574-582.

Eppley, R. W., F. M. H. Reid, and J. D. H. Strickland. 1970. The ecology of the plankton off La Jolla, California, in the period April through September, 1967. Part 3. Estimates of phytoplankton crop size, growth rate and primary production. Bull. Scripps Instn Oceanogr. tech. Ser. **17:** 33-42.

Fessenden, L., and T. J. Cowles. 1994. Copepod predation on phagotrophic ciliates in Oregon coastal waters. Mar. Ecol. Prog. Ser. **107:** 103-111.

Frost, B. W. 1972. Effects of size and concentration of food particles on feeding behavior of marine planktonic copepod *Calanus pacificus*. Limnol. Oceanogr. **17:** 805-815.

Hayward, T. L., and E. L. Venrick. 1998. Nearsurface pattern in the California Current: coupling between physical and biological structure. Deep-Sea Res. II **45:** 1617-1638.

Hernandez-Leon, S., and T. Ikeda. 2005. A global assessment of mesozooplankton respiration in the ocean. J. of Plankton Res. **27:** 153-158.

Huntley, M. E., and M. D. G. Lopez. 1992. Temperature-dependent production of marine copepods: A global synthesis. Am. Nat. **140:** 201-242.

Ikeda, T. 1985. Metabolic rates of epipelagic marine zooplankton as a function of body-mass and temperature. Mar. Biol. **85:** 1-11.

Kahru, M., and B. G. Mitchell. 2000. Influence of the 1997-98 El Nino on the surface chlorophyll in the California Current. Geophysical Research Letters **27:** 2937-2940.

Kleppel, G. S., and R. E. Pieper. 1984. Phytoplankton pigments in the gut contents of planktonic copepods from coastal waters off southern California. Mar. Biol. **78:** 193-198.

Landry, M. R. 1980. Detection of prey by *Calanus pacificus*: Implications of the 1st antennae. Limnol. Oceanogr. **25:** 545-549.

Landry, M. R. 1981. Switching between herbivory and carnivory by the planktonic marine copepod *Calanus pacificus*. Mar. Biol. **65:** 77-82.

Landry, M. R., H. Al-Mutairi, K. E. Selph, S. Christensen, and S. Nunnery. 2001. Seasonal patterns of mesozooplankton abundance and biomass at Station ALOHA. Deep-Sea Res. II **48:** 2037-2061.

Landry, M. R., M. Décima, M. P. Simmons, C. C. S. Hannides, and E. Daniels. 2008. Mesozooplankton biomass and grazing responses to Cyclone Opal, a subtropical mesoscale eddy. Deep-Sea Res. II **55:** 1378-1388.

Landry, M. R., and R. P. Hassett. 1982. Estimating the grazing impact of marine microzooplankton. Mar. Biol. **67:** 283-288.

Landry, M. R., M. D. Ohman, R. Goericke, M. R. Stukel, and K. Tsyrklevich. 2009. Lagrangian studies of phytoplankton growth and grazing relationships in a coastal upwelling ecosystem off Southern California. Prog. Oceanogr. **83:** 208-216.

Lavaniegos, B. E., and M. D. Ohman. 2007. Coherence of long-term variations of zooplankton in two sectors of the California Current System. Prog. Oceanogr. **75:** 42-69.

Laws, E. A. 2003. Mesozooplankton grazing and primary production: An alternative assessment. Limnol. Oceanogr. **48:** 1357-1359.

Legendre, L., and F. Rassoulzadegan. 1995. Plankton and nutrient dynamics in marine waters. Ophelia **41:** 153-172.

Lorenzen, C. J. 1967. Determination of chlorophyll and pheo-pigments: Spectrophotometric equations. Limnol. Oceanogr. **12:** 343-346.

Mackas, D., and R. Bohrer. 1976. Fluorescence Analysis of Zooplankton Gut Contents and an Investigation of Diel Feeding Patterns. J. Exp. Mar. Biol. Ecol. **25:** 77-85.

Martin, E. S., X. Irigoien, R. P. Harris, A. Lopez-Urrutia, M. V. Zubkov, and J. L. Heywood. 2006. Variation in the transfer of energy in marine plankton along a productivity gradient in the Atlantic Ocean. Limnol. Oceanogr. **51:** 2084-2091.

McArdle, B. H. 2003. Lines, models, and errors: Regression in the field. Limnol. Oceanogr. **48:** 1363-1366.

McManus, M. A., A. L. Alldredge, A. H. Barnard, E. Boss, J. F. Case, T. J. Cowles, P. L. Donaghay, L. B. Eisner, D. J. Gifford, C. F. Greenlaw, C. M. Herren, D. V. Holliday, D. Johnson, S. MacIntyre, D. M. McGehee, T. R. Osborn, M. J. Perry, R. E. Pieper, J. E. B. Rines, D. C. Smith, J. M. Sullivan, M. K. Talbot, M. S. Twardowski, A. Weidemann, and Zaneveld, Jr. 2003. Characteristics, distribution and persistence of thin layers over a 48 hour period. Mar. Ecol. Prog. Ser. **261:** 1-19.

Mullin, M. M., and E. R. Brooks. 1976. Some consequences of distributional heterogeneity of phytoplankton and zooplankton. Limnol. Oceanogr. **21:** 784-796.

Nakagawa, Y., Y. Endo, and K. Taki. 2001. Diet of *Euphausia pacifica* Hansen in Sanriku waters off northeastern Japan. Plankton Biology and Ecology **48:** 68-77.

Nejstgaard, J. C., L. J. Naustvoll, and A. Sazhin. 2001. Correcting for underestimation of microzooplankton grazing in bottle incubation experiments with mesozooplankton. Mar. Ecol. Prog. Ser. **221:** 59-75.

Ohman, M. D., and J. A. Runge. 1994. Sustained fecundity when phytoplankton resources are in short supply - omnivory by *Calanus finmarchicus* in the Gulf of St-Lawrence. Limnol. Oceanogr. **39:** 21-36.

Ohman, M. D., and H. J. Hirche. 2001. Density-dependent mortality in an oceanic copepod population. Nature **412:** 638-641.

Omori, M., and T. Ikeda. 1984. Methods in marine zooplankton ecology, p. i-xiii, 1-332. Methods in marine zooplankton ecology. John Wiley & Sons, New York, Chichester etc.

Peterson, B., R. Emmett, R. Goericke, E. Venrick, A. Mantyla, S. J. Bograd, F. B. Schwing, S. Ralston, K. A. Forney, R. Hewitt, N. Lo, W. Watson, J. Barlow, M. Lowry, B. E. Lavaniegos, F. Chavez, W. J. Sydeman, D. Hyrenbach, R. W. Bradley, P. Warzybok, K. Hunter, S. Benson, M. Weise, and J. Harvey. 2006. The state of the California current, 2005-2006: Warm in the north, cool in the south. Calif. Coop. Ocean. Fish. Invest. Rep. **47:** 30-74.

Rebstock, G. A. 2002. Climatic regime shifts and decadal-scale variability in calanoid copepod populations off southern California. Glob. Change Biol. **8:** 71-89.

Ricker, W. E. 1975. Linear Regressions in Fishery Research - Note. Journal of the Fisheries Research Board of Canada **32:** 1494-1498.

Roesler, C. S., and D. B. Chelton. 1987. Zooplankton variability in the California current, USA, 1951-1982. Calif. Coop. Ocean. Fish. Invest. Rep. **28:** 59-97.

Ross, R. M. 1982. Energetics of *Euphausia pacifica*. 2. Complete carbon and nitrogen budgets at 8°C and 12°C throughout the life-span. Mar. Biol. **68:** 15-23.

Runge, J. A. 1980. Effects of hunger and season on the feeding behavior of *Calanus pacificus*. Limnol. Oceanogr. **25:** 134-145.

Rykaczewski, R. R., and D. M. Checkley. 2008. Influence of ocean winds on the pelagic ecosystem in, upwelling regions. Proceedings of the National Academy of Sciences, United States of America **105:** 1965-1970.

Sevadjian, J. C., M. A. McManus, and G. Pawlak. 2010. Effects of physical structure and processes on thin zooplankton layers in Mamala Bay, Hawaii. Mar. Ecol. Prog. Ser. **409:** 95-106.

Sherr, E. B., and B. F. Sherr. 1993. Preservation and storage of samples for enumeration of heterotrophic protists, p. 207–212. *In* P. K. Kemp [ed.], Hand book of Methods in Aquatic Microbial Ecology. CRC Press.

Straile, D. 1997. Gross growth efficiencies of protozoan and metazoan zooplankton and their dependence on food concentration, predator-prey weight ratio, and taxonomic group. Limnol. Oceanogr. **42:** 1375-1385.

Strathmann, R. R. 1967. Estimating organic carbon content of phytoplankton from cell volume or plasma volume. Limnol. Oceanogr. **12:** 411- 418.

Stromberg, K. H. P., T. J. Smyth, J. I. Allen, S. Pitois, and T. D. O'Brien. 2009. Estimation of global zooplankton biomass from satellite ocean colour. J. Mar. Syst. **78:** 18-27.

Stukel, M. R., M. R. Landry, C. R. Benitez-Nelson, and R. Goericke. in press. Trophic cycling and carbon export relationships in the California Current Ecosystem. Limnol. Oceanogr.

Stukel, M. R., M. R. Landry, and K. E. Selph. 2011. Nanoplankton mixotrophy in the eastern equatorial Pacific. Deep-Sea Res. II **58:** 378-386.

Venrick, E. L. 2002. Floral patterns in the California current system off southern California: 1990-1996. J. Mar. Res. **60:** 171-189.

CHAPTER 4

The 1998/1999 El Niño Southern Oscillation event and the isotopic content of amino acids in California Current zooplankton: effects on baseline ^{15}N and trophic structure

By Moira Décima, Michael R. Landry and Brian N. Popp

Abstract

The effects of El Niño Southern Oscillation (ENSO) conditions on the marine pelagic food web were investigated for two regionally important zooplankton species in the California Current System (CCS): *Calanus pacificus* (females and copepodid V) and *Euphausia pacifica* (juveniles).

Previous studies have demonstrated changes in the bulk nitrogen (N) stable isotopes of zooplankton associated with El Niño years. However, they could not differentiate between three hypothesized mechanisms to explain the observed changes: changes in nitrate utilization leading to changes in the isotopic content of phytoplankton due to Rayleigh distillation; different ^{15}N content in the source waters during ENSO events also leading to changes in the $\delta^{15}N$ of phytoplankton at the base of the food web; and finally, altered trophic position (TP) of consumers relative to phytoplankton. We used Compound-Specific Isotope Analysis (CSIA) of Amino Acids (AA) to investigate temporal changes in trophic structure, specifically during the 1998/1999 ENSO event.

This method only allows for the differentiation between changes in the isotopic content of phytoplankton at the base of the food web and changes in trophic steps between phytoplankton and consumers. The distinction of the mechanism via which the phytoplankton can enrich during ENSO events cannot be made with this method. We used CSIA to distinguish between these two mechanisms of isotopic enrichment, using specimens collected off Point Conception, California, during the contrasting 1998 El Niño and 1999 La Niña events. In addition to the traditional approach to test these two hypotheses, using phenylalanine as indicative of changes in the N source and the difference in $\delta^{15}N$ of glutamic acid and phenylalanine ($\delta^{15}N$ glu - phe) as a proxy for trophic position, we use $\delta^{15}N$ data for all AAs in a linear mixed-effects (LME) model. Phenylalanine $\delta^{15}N$ values were lower during the 1999 La Niña for all zooplankton groups, although this difference was significant only for the younger zooplankton stages: *C. pacificus* CVs and *E. pacifica* juveniles. There were no significant between-year differences in TP estimates from $\delta^{15}N$ glu – phe for any zooplankton group. The result of the LME model indicated statistically significant higher $\delta^{15}N$ values for all AAs during 1998 compared to 1999, confirming the baseline ^{15}N enrichment hypothesis. TPs for both stages of *C. pacificus* were similar and not statistically different between years. However, the LME model indicated that *E. pacifica* fed at a higher trophic level during 1998 than 1999. Rather than feeding higher in the food chain during the 1998 El Niño, additional evidence suggests that the anomaly was enhanced herbivory of *E. pacifica* in response to higher phytoplankton concentrations in 1999.

In testing these hypotheses, individual AAs allowed the exploration of spatial and temporal patterns, but the use of all AA data in the LME model showed more statistical power in distinguishing mechanisms.

Introduction

Zooplankton studies in many marine ecosystems have documented community changes associated with climatic forcing at various time scales, including long-term, decadal and interannual trends (see Mackas and Beaugrand 2010). While elucidating the underlying mechanisms of community responses to climate forcing is challenging, it is of paramount importance for understanding the future directions of ocean food web responses to climate change.

The California Current System (CCS) has been monitored nearly continuously since 1949 as part of the *California Cooperative Oceanic Fisheries Investigations* (CalCOFI). The detection of community responses to short and long-term scales of forcing has been possible due to the length of the time-series and the breath of measurements undertaken. The community changes include long-term secular trends, e.g. decreases in zooplankton biovolume and pelagic tunicate biomass (Lavaniegos and Ohman 2007), multidecadal oscillations, e.g. abundance fluctuations in some euphausiid and tunicate taxa (Ohman and Venrick 2003), and interannual variability related to El Niño Southern Oscillation (ENSO) conditions (e.g. Kahru and Mitchell 2002; Brinton and Townsend 2003).

Zooplankton community changes in response to ENSO-associated conditions in the CCS have been documented for a variety of species. The major El Niño's have consistently depressed zooplankton biomass as well as many of the main taxa in the region, although these effects have been transitory (Lavaniegos and Ohman 2007). Anomalies in calanoid species composition have increased after 1976/77, often coinciding with strong El Niño events (Rebstock 2002). The abundance of the dominant

euphausiid, *Euphausia pacifica*, has shown high fluctuations coincident with strong El Niño/La Niña events (Brinton and Townsend 2003).

Studies investigating the nitrogen stable isotope content of zooplankton bulk tissue have revealed ^{15}N enrichment in three of four species in northern California (Rau et al. 2003), and two species in southern California (Ohman et al. submitted) associated with El Niño events. This enrichment could arise via two mechanisms, which are not mutually exclusive. The first is that the phytoplankton community may become enriched in ^{15}N during ENSO years. Such baseline enrichment can occur if increased nitrate utilization, in response to decreased nutrient supply, leads to greater Rayleigh fractionation. Alternatively, the ^{15}N content of dissolved nitrogen in source waters can become higher due to increased importance of denitrified water flowing from the Eastern Tropical Pacific (Rau et al. 2003; Ohman et al. submitted).

The second mechanism that could result in higher ^{15}N content in zooplankton tissue is a lengthening of the planktonic food chain in response to decreased nutrient or phytoplankton supply. If the mean size of phytoplankton becomes significantly smaller due to increased competition for diminished nutrients, additional trophic steps or alternate trophic pathways (Landry 1977) may be needed to transfer energy to consumers of equal size. Alternatively, given diminished phytoplankton resources, plankton consumers may draw a larger share of their diets from carnivory (Landry 1981; Ohman et al. submitted). Zooplankton have been shown to exhibit higher degrees of omnivory/carnivory when phytoplankton is in short supply (e.g. Fessenden and Cowles 1994; Dam et al. 1995).

One way to test these two hypotheses is by Compound-Specific Isotope Analysis (CSIA) of amino acids (AAs). The strength of this method is that different AAs are

metabolized differently in the food web, and thus exhibit different degrees of ^{15}N enrichment with trophic step. Some AAs, categorized as 'source', show very low fractionation with each step, while others, termed 'trophic' AAs, become highly enriched in ^{15}N (McClelland and Montoya 2002). This method has been used in a number of studies investigating trophic structure in the marine ecosystem because it provides an internal reference to the $\delta^{15}N$ of the primary producers. In contrast, determining trophic position (TP) using the bulk method requires knowledge of the $\delta^{15}N$ of the baseline autotrophs. Marine pelagic autotrophs, phytoplankton, have very high turnover rates. Difficulties in determining the $\delta^{15}N$ of the prey consumed by a zooplankter arise due to temporal mismatches in the characteristics of the food consumed relative to the time-integrated accumulated biomass (N) of the zooplankton. Since the CSIA method does not require sampling of the primary producers, inferences can be made about the time-averaged TP of the consumer based solely on its tissue composition (see McClelland and Montoya 2002; Chikaraishi et al. 2009; Hannides et al. 2009)

In the present study, we used the CSIA method to test the hypotheses of baseline ^{15}N enrichment and trophic elongation in the CCS during ENSO years, focusing on the El Niño/ La Niña events of 1998 and 1999 in the southern California region. We analyzed two dominant species of zooplankton in the CCS: the copepod *Calanus pacificus* and the euphausiid *Euphausia pacifica*. Both of these regionally important species have shown previous evidence of response to ENSO conditions (Brinton and Townsend 2003; Rau et al. 2003; Ohman et al. submitted), but neither has been specifically assessed with regard to impact on trophic positions. Observations and model results indicate that much of the variability in the Pacific is accounted for by El Niño/ La Niña events (Overland et al.

2010). Understanding the mechanisms that connect physical forcing and biological community responses is a first step towards prediction of ecosystem changes from climate variability.

Material and Methods

Zooplankton collection and water column conditions

Samples for CSIA were collected in the vicinity of Point Conception (California) as part of the CalCOFI time-series program (Fig. 1). Routine sampling of zooplankton has been conducted at least quarterly in the southern region of the California Current since 1949 and standard CalCOFI protocols can be found online (www.calcofi.org). Briefly, zooplankton tows are conducted using 0.71-m diameter Bongo frames equipped with 505-µm Nitex mesh. The Bongo net is lowered to depth at 50 m min^{-1}, allowed to settle for 30 seconds, and retrieved at 20 m min^{-1}. To achieve the target tow depth of 210 m, 300 m of wire are let out, adjusted accordingly at shallower locations. Vessel speed is usually 1-2 knots to keep the wire angle at 45° (±8), and the angle is noted every 10 m to estimate actual depth of tow. Once the net is retrieved, cod end contents are collected and zooplankton samples are preserved in 1.8% buffered formaldehyde.

We used samples collected during spring 1998 and 1999, at three near-shore stations on CalCOFI line 80: stations 80.55, 80.60 and 80.70 (Fig. 1). These stations were sampled on 15 April 1998 and 13 April 1999 (Fig. 1a, b). Formalin-preserved samples were sorted to obtain specimens of the two target species: the copepod *C. pacificus* and the euphausiid *E. pacifica*. We analyzed female and copepodite V (CV) life history stages of *C. pacificus* separately. We restricted our euphausiid analysis to

juveniles, which presumably had N tissue contents that better reflected contemporaneous food conditions than larger adults. Typically, 20 *C. pacificus* females, 100 *C. pacificus* CV, and 5-10 *E. pacifica* juveniles were removed from each sample, rinsed three times in Milli-Q water and dried at 60 °C for 24 h, for later analysis. All specimens were gently handled and transferred using ethanol-cleaned forceps.

Upper ocean profiles of temperature, salinity, nitrate and Chl *a* were obtained from the CalCOFI website (www.calcofi.org). These measurements come from CTD casts conducted during the same spring survey cruises and stations as the collected zooplankton. Briefly, each station involved a CTD/rosette cast with sensors for pressure, temperature, salinity, dissolved oxygen, photosynthetically active radiation, fluorescence and transmissivity. Water samples were collected at 20-24 depths in the upper 500 m to determine salinity, dissolved oxygen, nutrients and phytoplankton pigments. Nutrient samples were drawn into 40-ml polypropylene screw-capped centrifuge tubes and samples were analyzed with a Seal Analytical continuous-flow AutoAnalyzer 3, within 2-16 hours after sample collection, allowing sufficient time for all samples to reach room temperature (details in Hager et al. 1972; Gordon et al. 1993). For phytoplankton pigments, seawater samples of known volume (50-250 ml) were filtered onto GF/F filters, and extracted in the dark at -20 °C for 24-48h in 10-ml screw-top culture tubes containing 8 ml of 90% acetone (Venrick and Hayward 1984). Fluorescence readings (Turner 10AU Fluorometer) are taken prior to and after acidification to calculate concentrations of Chl *a* and phaeopigments (Lorenzen 1967).

Sample preparation for CSIA – hydrolysis and derivatization

Samples were prepared as detailed in previous studies (see Popp et al. 2007; Hannides et al. 2009; Dale et al. 2011). Prior to AA analysis, zooplankton specimens were subject to acid hydrolysis, esterification of the carboxyl terminus, and trifluoroacetylation of the amine group (Macko et al. 1997; Popp et al. 2007). Samples were hydrolyzed by adding Sequanal grade 6 N HCl to each sample vial (containing 1-2 mg of zooplankton). Each vial was then flushed with N_2, capped with a Teflon-lined cap, and boiled at 150 °C for 70 min. Acid hydrolysis destroys tryptophan and cystine, and converts asparagine to aspartic acid and glutamine to glutamic acid. The resulting hydrolysate was evaporated to dryness under N_2 at 55 °C, redissolved in 1 ml 0.01 N HCl, purified by filtration (0.45-µm hydrophilic filter), and washed with 1 ml of 0.01 N HCL. The hydrolysate was further purified using cation-exchange chromatography with a 5 cm column of resin (Dowex 50WX8-400) prepared in a glass Pasteur pipette (Metges et al. 1996). AAs were eluted with 4 ml of 2 N NH_4OH and evaporated to dryness under a stream of N_2 at 80 °C. Samples were then reacidified with 0.5 ml of 0.2 N HCl, flushed with N_2 and heated to 110 °C for 5 min. Finally, samples were evaporated to dryness under N_2 at 55 °C. Hydrolyzed samples were esterified with 2 ml of 4:1 isopropanol:acetyl chloride, flushed with N_2 and heated to 110 °C for 60 min. Samples were dried at 60 °C under N_2, after which samples were acylated by adding 1 ml of 3:1 methylene chloride:trifluoracetic anhydride (TFAA) and heated to 100 °C for 15 min. The derivatized AAs were further purified by solvent extraction following Ueda et al. (1989). The acylated AA esters were evaporated at room temperature under N_2 and redissolved in 3 ml of 1:2 chloroform:P-buffer (KH_2PO_4 + Na_2HPO_4 in Milli-Q water, pH 7). Vigorous shaking ensured that the derivitized AAs were partitioned into

chloroform and that contaminants remained in the P-buffer. The solvents were separated by centrifugation (10 min at 600 g), the chloroform was transferred to a clean vial, and the solvent extraction process repeated. Finally, to ensure derivatization, the acylation step was repeated. Samples were stored at –20 °C in 3:1 methylene chloride:TFAA for up to 6 months until isotope analysis.

Compound specific isotope analysis (CSIA)

The nitrogen isotopic compositions of TFAA derivatives of amino acids were analyzed by isotope ratio monitoring gas chromatography-mass spectrometry. We used a Delta XP Plus mass spectrometer interfaced to a Trace GC gas chromatograph through a GC-C III combustion furnace (980 °C), reduction furnace (650 °C), and liquid nitrogen cold trap. The samples (1 to 2 μl) were injected (split/splitless injector, 10:1 split ratio) onto a *forte* BPx5 capillary column (30 m × 0.32 mm × 1.0 μm film thickness) at an injector temperature of 180 °C with a constant helium flow rate of 1.4 ml min^{-1}. The column was initially held at 50 °C for 2 min and then increased to 190 °C at a rate of 8 °C min^{-1}. Once at 190 °C, the temperature was increased at a rate of 10 °C min^{-1} to 300 °C, where it was held for 7.5 min. Internal reference compounds, aminoadipic acid and norleucine of known nitrogen isotopic composition, were co-injected with samples and used to normalize the measured $\delta^{15}N$ values of unknown amino acids. All samples were analyzed at least in triplicate. The average standard deviation of the multiple runs per amino acid was 0.69‰, ranging from 0.01‰ to 2.5‰.

Statistical analysis: individual amino acids

The sampling design of this study is unbalanced and multileveled. Replicate zooplankton samples were not uniformly available for species and locations, and the number of machine runs also varied by sample and AA (ranging from 3-6 runs per sample, but some values for certain AAs were removed due to peak co-elution). In order to account for both the different sources of variability and the unbalanced design we used linear mixed-effects (LME) models for our analysis (Pinheiro and Bates 2000; West et al. 2007). These include both fixed and random effects, the mix of the two giving these models their name. They differ from the common generalized linear models (GLMs) by including random- in addition to fixed-effects parameters associated with one or more covariates. In addition, LME models are well suited for dealing with correlated and unbalanced study designs and have been used previously to combine analytical (machine) and replicate errors to obtain species population estimates (e.g. Lorrain et al. 2009).

We used this approach to combine our replicate observations (when available) to obtain species/stage estimates for each year and location. Estimates were obtained by analyzing the results as a two-level clustered data set, where level 1 comprised the different measurement runs, clustered by sample (level 2). We obtained best estimates (± SE when replicates were available, otherwise ± SD) with this approach for phenylalanine and glutamic acid. We focused on these two AAs because they have been presented as canonical source and trophic AAs, respectively, in previous studies (e.g. Chikaraishi et al. 2009; Hannides et al. 2009; Lorrain et al. 2009). Parameter estimation used the restricted-maximum likelihood method (REML), which has a lower bias than the maximum likelihood method when dealing with random effects (West et al. 2007).

However, replicates were plotted individually to illustrate both the source and replicate error within the study.

We calculated trophic position (TP), using the difference in $\delta^{15}N$ of glutamic acid and phenylalanine ($\Delta\delta^{15}N$), as:

$$TP = \frac{(\Delta\delta^{15}N_{consumer} - \Delta\delta^{15}N_{phyto})}{TEF} + 1$$

where $\Delta\delta^{15}N_{consumer}$ denotes this difference in the consumers and $\Delta\delta^{15}N_{phyto}$ in the primary producers. *TEF* is the ^{15}N enrichment that occurs in glutamic acid with each trophic step, called the trophic enrichment factor. The two parameters necessary for this calculation are $\Delta\delta^{15}N_{phyto}$ and *TEF*, while $\Delta\delta^{15}N_{consumer}$ is the measured variable. These two parameters were originally estimated to be 4‰ and 7‰, respectively (McClelland and Montoya 2002) to calculate trophic positions of zooplankton (Schmidt et al. 2004; Hannides et al. 2009). More recently, Chikaraishi et al. (2009) estimated $\Delta\delta^{15}N_{phyto}$ as 3.4‰ (β in their study) and *TEF* as 7.6‰ (Δ) from an analysis of 17 photoautotrophs and four laboratory studies. We used the latter parameter estimates for the trophic position calculations in this study.

Differences in phenylalanine, glutamic acid, and trophic position for the fixed effects of this model (year and station) were tested using likelihood ratio tests. We used the 'step-up' model strategy, building our model by adding covariates one at a time, and conducting likelihood ratio tests at each step to determine fit improvements of the

reference vs. nested models. For details on LME model building and diagnostics, see West et al. (2007).

Statistical analysis: all amino acids

The two hypotheses explored in this study were tested in two ways: by investigating the patterns in the source (phenylalanine) and trophic (glutamic acid) AAs, and by using all amino acids within a sample. We developed this second form of analysis as an alternative to the traditional practice of relying solely on differences in individual amino acid for hypothesis testing. Taking simple averages of trophic and source groupings would be inappropriate given the multiple levels of data and the unbalanced design of the present study. Therefore, we developed a three-level model for clustered data to determine the main predictors of $\delta^{15}N$ measurements in each stage/species group.

Data were clustered in three levels as: runs within each AA (level 1), AAs within each sample (level 2), and samples separated by stage/species (level 3). Separate runs were considered random effects around the AA mean (level 1), such that no fixed effects (covariates) were incorporated at this level. One fixed effect was included for the AA cluster (level 2), corresponding to the trophic and source categorical grouping. Finally, we considered fixed-effects associated with the years and stations sampled. As for the statistical analysis for the individual AAs, we used the 'step-up' model strategy, building our model by adding level 2, then level 3 covariates at a time, and conducting likelihood ratio tests at each step to determined the improved fits of the reference vs. nested models (West et al. 2007).

Final diagnostics were conducted on each species/stage model. Random effects and model residuals were checked for normality. All statistical computations were carried out in R (http://www.r-project.org), using the nlme package.

Results

Oceanographic conditions

Detailed accounts of the regional oceanographic conditions during 1998 (El Niño) and 1999 (La Niña) have been discussed at length elsewhere (see Lynn et al. 1998; Hayward et al. 1999; Hayward 2000), and are only briefly presented here. Contrasting ENSO conditions during spring 1998 and 1999 were strongly evident in the areal extent of sea surface Chl *a* concentrations in the Southern California Current (Fig. 1). Prevailing El Niño conditions during spring of 1998 restricted high surface Chl *a* concentrations to a narrow coastal zone. The relative inactivity of mesoscale features advecting high Chl *a* waters offshore contributed to the strong spatial pattern in sea surface Chl *a* (Fig. 1). Very different conditions characterized spring of 1999, when mesotrophic conditions (Chl *a* concentrations of ~1 μg L^{-1}) were generally present at distances greater than 250 km from the coastline (Fig. 1). Mesoscale features were particularly active in advecting filaments of high concentrations of Chl *a* (~ 2-5 μg L^{-1}) far offshore, contributing to elevated but patchy Chl *a* concentrations throughout most of the CalCOFI sampling grid.

Depth profiles taken during spring ENSO conditions revealed high temperatures and low salinities throughout the upper water column leading to strong surface stratification to a depth of ~60 m (Fig. 2a). Temperature and salinity patterns were very

different during the 1999 La Niña, with lower surface temperatures (11-12 °C), high salinities (33.6 - 33.8), and weaker stratification (Fig. 2b). The 1999 profiles suggest a strong upwelling signature at all sampling locations (Fig. 2b). As a consequence, nitrate and Chl *a* concentrations differed dramatically between the two spring seasons. Nitrate during 1998 was very low at the surface, slowly increasing at ~20 m at the station closest to shore, but concentrations at Stns. 80.60 and 80.70 remained close to zero to about 60 m, coincident with the depth of the pycnocline (Fig. 2a). Chl *a* was generally low throughout the water column for stations further from shore, and higher values were only present at Stn. 80.55, with a subsurface maxima at 35 m. The La Niña conditions led to high Chl *a* concentrations at all sampling locations, with Stn. 80.60 being most strongly linked to upwelling source waters based on temperature, salinity, nutrients and Chl *a* (>10 μg L^{-1}) profiles.

Patterns in individual amino acids

We first tested the hypotheses of ^{15}N enrichment at the base of the food web vs. trophic length variations by looking at patterns in the individual source and trophic AAs: phenylalanine and glutamic acid, respectively. Low abundance of female *C. pacificus* and machine problems precluded AA $\delta^{15}N$ estimates at Stn. 80.60 during 1998 for comparison at the same location during 1999. The phenylalanine $\delta^{15}N$ in female *C. pacificus* was visibly lower during 1999, but not statistically different between the two years (Fig. 3a), due to high replicate variability. Replicate variability was not as high for either *C. pacificus* CVs or *E. pacifica* juveniles (Fig. 3). *C. pacificus* CV stages had a very different pattern than the females during both years. During spring 1998, *C.*

pacificus CVs displayed a pattern of decreasing ^{15}N enrichment with distance from shore, but the opposite was true in spring 1999 (Fig. 3b). Phenylalanine $\delta^{15}N$ values, indicative of the N source, were significantly different between years (One-way ANOVA, p = 0.007). Juvenile *E. pacifica* showed almost identical somewhat similar patterns in the $\delta^{15}N$ of phenylalanine during both years (Fig. 3c). The ^{15}N content of the source AA was low at Stn. 80.55, while organisms sampled at stations 80.60 and 80.70 had similar phenylalanine $\delta^{15}N$ values (Fig. 3c). Similarly to *C. pacificus* CV, we found a statistically significant difference between years (One-way ANOVA, $p = 0.003$).

Enrichment patterns of glutamic acid are shown in Figure 4. Female *C. pacificus* had visibly different spatial patterns between years (Fig. 4a), but no statistical difference was detected. An estimate of glutamic acid $\delta^{15}N$ from female *C. pacificus* sampled at Stn. 80.55 in 1999 was not available due to peak co-elution. For *C. pacificus* CVs, spatial patterns in glutamic acid $\delta^{15}N$ values were similar to those for phenylalanine (Fig. 4b). During spring of 1998, the highest ^{15}N content was at the station closest to shore (17‰), the other two stations with similar values of 15‰ (Fig. 4b). Values for 1999 showed the same linear increase observed for phenylalanine, the ^{15}N isotopic content increasing with distance from shore (Fig. 4b). For juvenile euphausiids, spatial patterns of glutamic acid $\delta^{15}N$ were different between years, in addition to having significantly higher values during spring 1998 (Fig. 4c). Both year (One-way ANOVA, $p = 0.04$) and station (One-way ANOVA, $p = 0.03$) differences were statistically significant. The spatial pattern for glutamic acid during 1999 was nearly identical to that observed in phenylalanine, with higher values in organisms sampled at Stns. 80.60 and 80.70 (Fig. 4c). $\delta^{15}N$ values in glutamic acid increased monotonically with distance from shore

during the 1998 El Niño. The N content of glutamic acid in euphausiids sampled at Stn. 80.70 had the highest ^{15}N content of all samples analyzed in this study (Fig. 4).

Spatial and temporal patterns in calculated TP, based on differences in glutamic acid and phenylalanine $\delta^{15}N$, were quite different among the three groups (Fig. 5). In general, we observed that ¾ of the positions fell below 2, the minimum value for any consumer, for all animals analyzed (Fig. 5). We discuss these unrealistic absolute estimates below, but focus here on the relative differences among test organisms, stations and years.

Estimates for *C. pacificus* female TPs were more spatially variable during 1999 (Fig. 5a). Females collected during spring 1998 had similar estimates, ~2.0 at the 2 sampled stations (Fig. 5a). For *C. pacificus* CVs, TPs were generally similar among years and stations (Fig. 5b). Some spatial variability was observable during 1998, with the highest TP at Stn. 80.70 (Fig. 5b). For *E. pacifica* juveniles, TPs were similar at Stn. 80.55, but higher during 1998 than 1999 at Stns. 80.60 and 80.70 (Fig. 5c). An increasing trend with distance from shore was observed only during spring 1998, where we found the highest TP estimate of 2.4 (Fig. 5c). Finally, we tested the difference between the $\delta^{15}N$ of glutamic acid and phenylalanine and found no statistical difference between years for any of the analyzed zooplankton groups. Only *E. pacifica* showed a marginal statistical difference ($p = 0.1$) for the combined Stn./year effect.

Patterns using all amino acids

The $\delta^{15}N$ of AAs in our region cluster roughly into the two trophic groups previously described in the literature (McClelland and Montoya 2002; Hannides et al.

2009). The isotopic values are visibly higher during 1998 than 1999 in all amino acids, regardless of the trophic/source distinction, a pattern consistent with the baseline enrichment hypothesis (Fig. 6). For the LME model using all AAs, we did not include Threonine, which was originally grouped with source AAs (McClelland and Montoya 2002). However, it constitutes an outlier with more negative values (Fig. 6) and displays a unique behavior among the AAs (Styring et al. 2010; Sherwood et al. 2011).

The parameter estimates from the LME models using all AAs are shown in Table 1. The significant fixed-effects shared by all groups were: year sampled (β_1) and AA trophic/source grouping (β_2). The trophic/year interaction effect (β_3) was significant only for the juvenile euphausiids (Table 1), and fixed effects associated with station sampled were not significant for any group.

The final model was:

$$\delta^{15}N_{ijk} = \beta_o + \beta_1 \times year_k + \beta_2 \times trophic_j + \beta_3 \times trophic_j \times year_k + u_k + u_{j|k} + \varepsilon_{ijk}$$

The β parameters are the statistically significant fixed-effect covariates. They include the intercept (β_o), the parameter β_1 corresponding to the categorical year variable (1998 = 0, 1999 = 1), β_2 multiplies the categorical variable 'trophic' (source AAs = 0, trophic AAs = 1), and the β_3 parameter associated with the interaction term year/trophic (Table 1). The *i, j* and *k* subscripts refer to each level of clustering. The u_k and $u_{j|k}$ represent the random effects in the model, and ε_{ijk} are the residuals.

The intercept parameters are similar among the three groups, although β_o for *C. pacificus* CVs is slightly higher (Table 1). The negative parameter associated with the sampled year (β_1) indicates that all AAs were significantly depleted in ^{15}N during 1999 versus 1998, in all zooplankton groups. The highly significant parameter associated with the AA grouping (β_2) confirms the empirical observation of differential AA enrichment. Interestingly, model β_2 estimates for the copepods (~ 7) are almost identical for both stages (Table 1). This parameter is similar to the trophic enrichment factor used in the TP calculation (7 or 7.6‰, depending on the study), derived by using only the difference between glutamic acid and phenylalanine (Chikaraishi et al. 2009; Hannides et al. 2009). The fact that an interaction parameter of year/trophic (β_3) did not improve the model fit for *C. pacificus* indicates that there was no significant enrichment in the trophic AAs during 1998. Consequently, no trophic shift between years is evident from the N isotopic content.

The main difference between copepod and euphausiid LMEs was the significance of β_3 (Table 1). The LME β_2 parameter for *E. pacifica* was also higher when compared to *C. pacificus*. These two parameters indicated that the euphausiids had significantly higher trophic AA ^{15}N enrichment during 1998 (~10.3 ‰; Table 1). However, during the 1999 La Niña conditions, *E. pacifica* TPs would be comparable to *C. pacificus*. The combined effect of β_2 and $\beta_3$indicate that trophic AAs were enriched by ~ 7.9‰ in *E. pacifica*, compared to 7.1‰ in *C. pacificus* (Table 1).

The standard deviations (σ^2) at each level of data clustering are compared in Table 2. The only standard deviation that differed noticeably among groups was σ^2_{sample},

the measure of variance at the sample level, which was 1 five-fold greater for *C. pacificus* females than CVs, and 3 orders of magnitude lower for *E. pacifica* (Table 2). This parameter reflects the random effects of $\delta^{15}N$ at the sample level. This means that there is still a lot of variability that remains unexplained for *C. pacificus* (particularly the females) even after the incorporation of the year fixed-effect into the LME model.

Finally, we investigated the random effects (u_k and $u_{j|k}$) and residuals (ε_{ijk}) for normality. A Q-Q plot showed that most effects were normally distributed (not shown). However, a few observations were identified as outliers. The outliers were Alanine and Glycine for *C. pacificus* females; Alanine, Leucine and Isoleucine for *C. pacificus* CVs; Alanine, Isoleucine and Glycine for *E. pacifica*. Outliers for all groups were < 2.5% of observations, and did not significantly affect the model results.

Discussion

Baseline ^{15}N enrichment versus trophic shifts

Based on the results from isotope analysis of the three tested zooplankton groups, we confirm the hypothesis of baseline ^{15}N enrichment during the 1998 El Niño. This hypothesis is supported by statistically higher $\delta^{15}N$ values in the source AA phenylalanine in the young zooplankton stages, *C. pacificus* CV and *E. pacifica* juveniles (Fig. 3b, c). Further confirmation is found from the results of the LME models indicating that, although the AAs in female *C. pacificus* displayed higher variability (Table 2), obscuring the phenylalanine significance, the pattern was consistent for all zooplankton groups and for all AAs (Fig. 6, Table 1).

Conclusions regarding the trophic shift hypothesis are species-dependent. For both life history stages of *C. pacificus*, we reject the hypothesis of a regional trophic shift during the 1998 El Niño. This conclusion is supported by results from both the analysis using individual amino acids (Fig. 5) as well as from the LME model (Table 1). For juvenile *E. pacifica*, however, the LME model evinced a statistically significant difference in trophic positions during 1998 versus 1999, reflected in the interaction of trophic grouping and year (β3; Table 1). The analysis using individual AAs did not show this result, although the combined effect of year/station was marginally significant (p = 0.1) for the difference in $\delta^{15}N$ of glutamic acid and phenylalanine (Fig. 5c).

Results from previous regional studies, showing enrichments in bulk ^{15}N of three zooplankton groups during ENSO years, including female *C. pacificus* (e.g. Rau et al. 2003; Ohman et al. in press), are explained by ^{15}N enrichment of the primary producers, as opposed to trophic increases in response to reduced food supply. The mechanisms described by Rau et al (2003) and Ohman et al (in press) that can lead to the enrichment of phytoplankton, either changes in source ^{15}N or increased uptake of ^{15}N due to Rayleigh utilization, however, cannot be determined by this method.

The difference in AA patterns as well as isotopic content between the *C. pacificus* female and CV stages was initially surprising. Females were chosen for the study because previous studies had originally been done with this stage (Rau et al. 2003). However, we found no statistical differences in phenylalanine $\delta^{15}N$ for *C. pacificus* females (Fig. 3a), in contrast to the significant 1-2‰ bulk enrichments detected in both Northern and Southern California female populations (Rau et al. 2003; Ohman et al. submitted). Previous studies of *C. pacificus* in Southern California waters have found it

to have a biphasic life history, with one segment of the population active in surface waters during the winter while the CV stage is dormant with depressed metabolic enzymatic activity in subsurface waters (Ohman et al. 1998). High aggregations of diapausing CVs have been detected in the Santa Barbara Basin during the winter and fall (Osgood and Checkley 1997b; Osgood and Checkley 1997a), and previous studies have shown that upwelling at Pt. Conception can bring these organisms to the surface (Smith et al. 1986). Finally, Ohman et al (1988) suggested that a small fraction of deep-dwelling CVs molt to adult at depth. It is very possible that our samples of *C. pacificus* females from the Pt. Conception area were composed of a mixture of surface-dwelling females and those recently molted from diapausing CVs. The relative contribution of these different component populations may also have varied substantially between years and stations.

That female *C. pacificus* had the highest variability among samples in the AA $\delta^{15}N$ (Table 2) may also reflect metabolic changes resulting from reproduction. A study in alpine lake zooplankton found significant changes in both elemental and AA composition associated with reproduction (Ventura and Catalan 2005; Ventura and Catalan 2010). Southern Ocean krill have been found to have large fractionation differences in the $\delta^{15}N$ of trophic amino acids between males and females (Schmidt et al. 2004), again hinting to important biochemical changes associated with reproductive maturity. The effects of reproduction on AA composition or AA $\delta^{15}N$ content have not been studied for *C. pacificus*. However, we can hypothesize that the variability (spatially and between replicates) in the female AA $\delta^{15}N$ was likely caused by reproduction-

associated changes in individual organisms, combined with a lack of synchronization in these changes due to mixed sampled populations.

C. pacificus CVs and juvenile *E. pacifica* were chosen for this analysis with the expectation that the younger, actively growing stages would more closely track concurrent environmental conditions compared to adults. Both actively growing zooplankton were characterized by lower sample variability (Table 2) and statistically distinct phenylalanine ^{15}N enrichment by year (Fig. 3b, c). However, *C. pacificus* CVs shared noticeable replicate variability (although five-fold less) and the same trophic parameters with female *C. pacificus*, showing that they fed at the same trophic level with no shift between years (Fig. 5a, b; Table 1).

Similar spatial patterns of phenylalanine $\delta^{15}N$ for *E. pacifica* juveniles, with different values, showed the clearest evidence of baseline ^{15}N enrichment (Fig. 3c). The 'year' parameter from the LME model also showed the highest significance of all groups (Table 1). *E. pacifica* juveniles were the only zooplankton group of those analyzed here that fed at different trophic levels between years. The spatial pattern observed during 1998, with higher TPs farther from shore during (Fig. 5c), and the significance of LME parameter β_3 (Table 1) support this hypothesis. It is possible, however, that *E. pacifica* displayed enhanced herbivory during the 1999 La Niña, rather than a trophic shift up the food chain during the 1998 El Niño. TPs from *E. pacifica* juveniles collected at station 80.60 during the years 1997 and 2000 were ~ 2.2 (based on $\delta^{15}N$ glu-phe), which is about 0.4 TP higher than 1999 (Décima, unpublished). Oceanographic conditions in Southern California were closer to normal conditions during these two years compared to 1998 or 1999 (Schwing et al. 1997; Bograd et al. 2000), which suggests that the results from 1999

are more the anomaly than the rule. Very high phytoplankton concentrations (suggested by high surface and upper water column Chl *a*) at all stations during the 1999 La Niña likely contributed to lower TPs throughout the region (Fig. 1, 2b).

Absolute trophic position estimates

Previous studies have suggested that TP values may be underestimated when laboratory-derived parameters are used for the expected offset of trophic and source AAs (e.g. Lorrain et al. 2009; Dale et al. 2011). These studies concluded that the *TEF* parameter of 7 or 7.6 ‰ (McClelland and Montoya 2002; Chikaraishi et al. 2009) consistently underestimates TPs by one third to a half. We did neither stomach content analysis nor bulk isotope analysis to independently obtain TP estimates, but the simple fact that most estimates were < 2 clearly indicates that they are unrealistically low. What are the possible reasons for this discrepancy between laboratory results and field samples? A study of several zooplankton in the North Pacific Subtropical Gyre (NPSG) oligotrophic open ocean found TPs between 2 and 3, corresponding well with the herbivore and carnivore classifications of individual species (Hannides et al. 2009). However, considering that the dominant phytoplankton species in this region are generally too small for direct consumption by mesozooplankton and that protozooplankton are the primary grazers in open-ocean waters, this was a very surprising result. In fact, copepods are expected to have a omnivorous diet (Kleppel 1993), and to depend nutritionally on microzooplankton as food in water where phytoplankton concentrations are low (e.g. Fessenden and Cowles 1994; Dam et al. 1995;

Calbet et al. 2009). In addition, the need for different *TEF*'s for different consumer types has been argued by studies of higher predators (Lorrain et al. 2009; Dale et al. 2011).

In our study, the TP estimate variability is not symmetrical around 2 (Fig. 5) suggesting that analytical and parameter errors are not sufficient to explain the pattern. Rather, there may be processes occurring in the field that did not appear in the controlled laboratory experiments that generated the parameter values for the TP calculations. It has been argued, for example, that nitrogen fractionation is inversely correlated to food quality in vertebrates, with lower quality protein leading to higher fractionation, independent of the absolute concentration of nitrogen (Robbins et al. 2005). Ventura and Catalan (2010) showed that $\delta^{15}N$ fractionation in alpine lake zooplankton was inversely related to the similarity of AA composition between prey and consumer, suggesting that homeostasis between predators and prey is important in determining the degree of fractionation. Given that the laboratory studies used to derive parameter estimates are based on prey monocultures (by definition unnatural diets) with potentially higher AA dissimilarity to consumers, it is possible that fractionation is higher in the laboratory than in the field.

Finally, since nitrogen sources are not constant in the field (varying seasonally with upwelling, nitrogen fixation, denitrification, etc), variation in phytoplankton supply and demand suggest that both concentration and isotopic content should be variable. The different turnover rates of AAs could potentially play an important role, contradicting the assumed constant *TEF* between glutamic acid and phenylalanine. Glutamic acid (glutamine + glutamic acid) is the main contributor to the AA pool in crustacean zooplankton, comprising 13% of the total (Ventura and Catalan 2010). Glutamic acid is

involved in a number of deamination processes (Macko et al. 1987; Chikaraishi et al. 2007; Bender 2008) and is a precursor for purines and pyrimidines (Bender 2008). Phenylalanine is an essential AA that contributes only ~4% to the total AA pool (Ventura and Catalan 2010). It is therefore quite likely that the turnover times of these two AA would be different, and metabolism dependent. This argument does not, however, explain why TPs might be consistently underestimated in nature unless there are systematic differences in AA metabolisms of predators and prey under lab and field conditions.

Statistical tests using LME models

The LME models are a very useful tool for combining replicate samples in order to draw conclusions regarding spatial and temporal patterns of zooplankton groups. They also demonstrated very conclusively the baseline changes in ^{15}N content in all AAs and all zooplankton groups between sampling years (Fig. 6, Table 1). The use of all AAs avoids the problems associated with relying on any one amino acid, especially when the variability among samples is high as we observed for *C. pacificus* females (Fig. 3a, Table 2).

The LME models allowed a greater exploration of the data, indicating differences and commonalities among different zooplankton groups in the different parameters and in the variability at different cluster levels. Metabolic pathways and general AA biogeochemistry is highly complex as well as taxonomically variable, hence patterns in individual AAs are likely to vary. The approach also circumvents the multiplicity of

tedious tests that would be involved in comparing each amino acid individually with different study variables.

The conclusions drawn for the juvenile euphausiids differ depending on whether they are based on the LME model or TP estimated using the difference in $\delta^{15}N$ of glutamic acid and phenylalanine. The LME approach allowed the statistical detection of a pattern that was suggested, yet not statistically significant, by individual source and trophic AAs patterns. However, the LME model interaction parameter β_3 was significant and indicated statistically higher trophic positions during 1998 versus 1999 (Table 1). The parameters in this model suggest that *E. pacifica* fed slightly higher in the food chain during 1999 than *C. pacificus*, and significantly higher in the food chain during 1998.

In conclusion, CSIA of AAs for three groups of dominant mesozooplankton in the CCS supports the hypothesis of baseline ^{15}N enrichment during the 1998 El Niño event, in accord with the results of Ohman et al. (in press). The hypothesis that the mean TP of mesozooplankton increased due to depressed phytoplankton biomass or dietary switching during ENSO conditions is rejected. However, the possibility of a shift down in trophic position during the 1999 La Niña is suggested for *E. pacifica*. Patterns of AA ^{15}N enrichment were different for each zooplankton group examined, demonstrating the importance of species and life history stage distinctions. Finally, LME models are introduced as an approach to utilize information from all AAs in addressing ecological questions, in addition to the traditional focus on single source and trophic AAs.

Acknowledgements

This chapter would not have been possible without the efforts of the highly qualified CalCOFI seagoing technicians. Samples were provided by the Pelagic Invertebrates Collection of Scripps Institution of Oceanography. I especially thank Annie Townsend for sample delivery. I am particularly indebted to Mary McCormick for help with zooplankton sorting and sample preparation, Elizabeth Gier for sample processing at the University of Hawaii, and Christina Bradley for her constant and untiring help with data processing, quality control and moral support. I also thank Lihini Aluwihare, Jeff Moore, and Mark Ohman for general comments and statistical advice.

Chapter 4, in full, is currently in preparation for submission: Décima, M., Landry, M. R., Popp, B. N., "The 1998/1999 El Niño Southern Oscillation event and the isotopic content of amino acids in California Current zooplankton: effects on baseline ^{15}N and trophic structure". The dissertation author was the primary investigator and author on this paper.

Table 4.1. LME model results for each groups of zooplankton analyzed. Parameter estimates (± SE) are presented along with significance levels. The β parameters are for the fixed-effects within the model. Year sampled was represented as a categorical value: 1998=0, 1999 =1. Trophic and source AAs were represented in the same manner: Source = 0, Trophic = 1. NS indicates non-significant terms.

	C. pacificus ♀		***C. pacificus* CV**		***E. pacifica***	
	value ± SE	*p-value*	value ± SE	*p-value*	value ± SE	*p-value*
β_o (intercept)	7.65 ± 0.92	<0.001	8.4 ± 0.49	<0.001	5.9 ± 0.64	<0.001
β_1 (year)	- 2.8 ± 1.13	0.04	- 2.62 ± 0.56	0.005	- 1.66 ± 0.9	0.0004
β_2 (trophic)	7.1 ± 0.58	<0.001	7.14 ± 0.52	<0.001	10.3 ± 0.84	<0.001
β_3 (year*trophic)	-	NS	-	NS	-2.4 ± 1.1	0.03

Table 4.2. Standard deviations for random effects at different levels of clustering, for each zooplankton group. $\sigma_{residual}$ indicates random effects due to analytical precision, σ_{AA} refers to variation in $\delta^{15}N$ of AAs not due to trophic enrichment, and σ_{sample} represents random effects at the sample level, unexplained by year effects.

	C. pacificus ♀	***C. pacificus* CV**	***E. pacifica***
σ_{sample}	1.47	0.3	0.0004
σ_{AA}	2.73	2.16	2.14
$\sigma_{residual}$	0.96	0.72	0.86

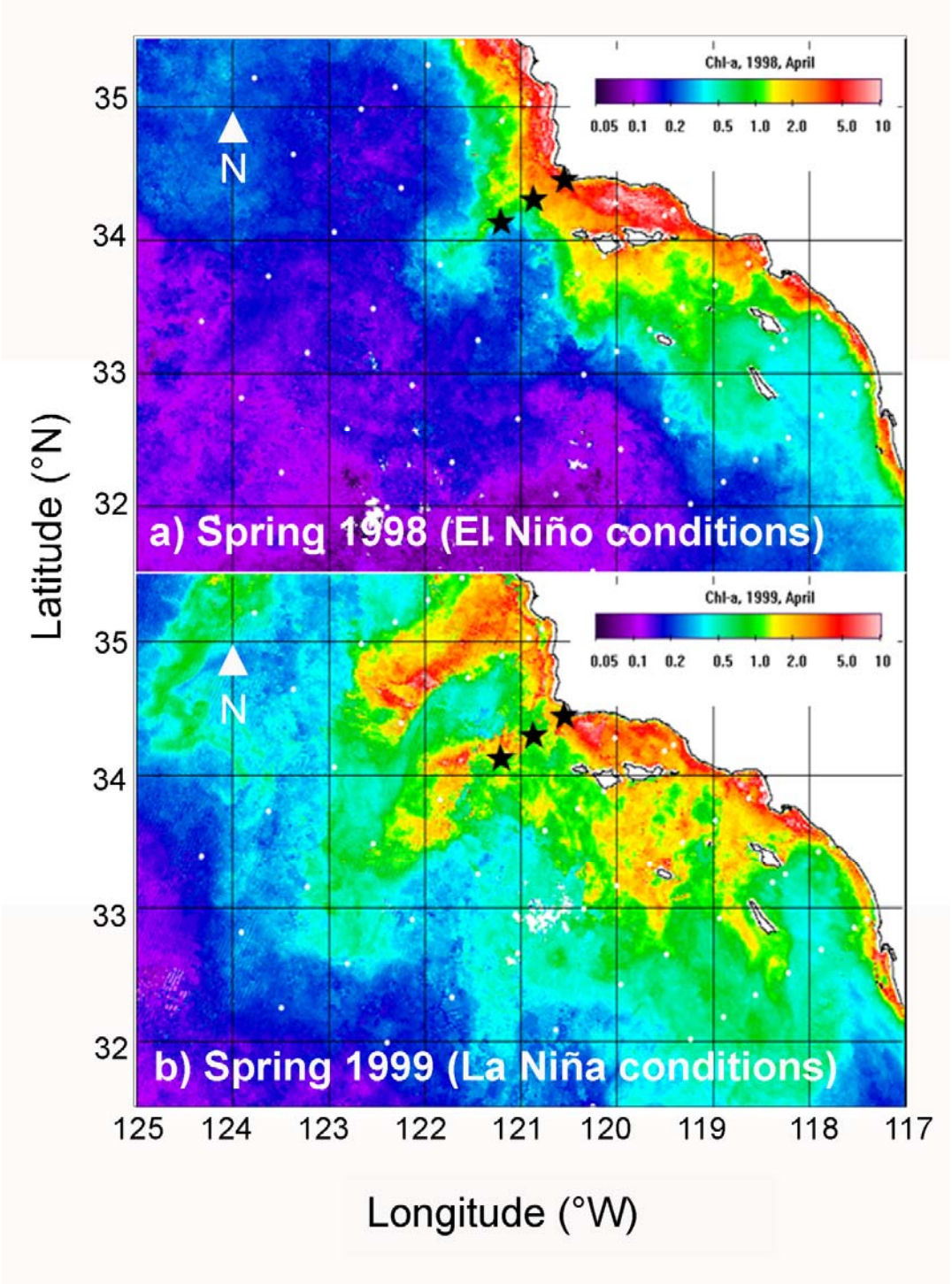

Figure 4.1. MODIS-Aqua monthly averaged maps of surface Chl *a* for a) April 1998, and b) April 1999. Black stars indicate stations sampled, and white dots show the Southern California CalCOFI sampling grid. Figure courtesy of Mathi Kahru.

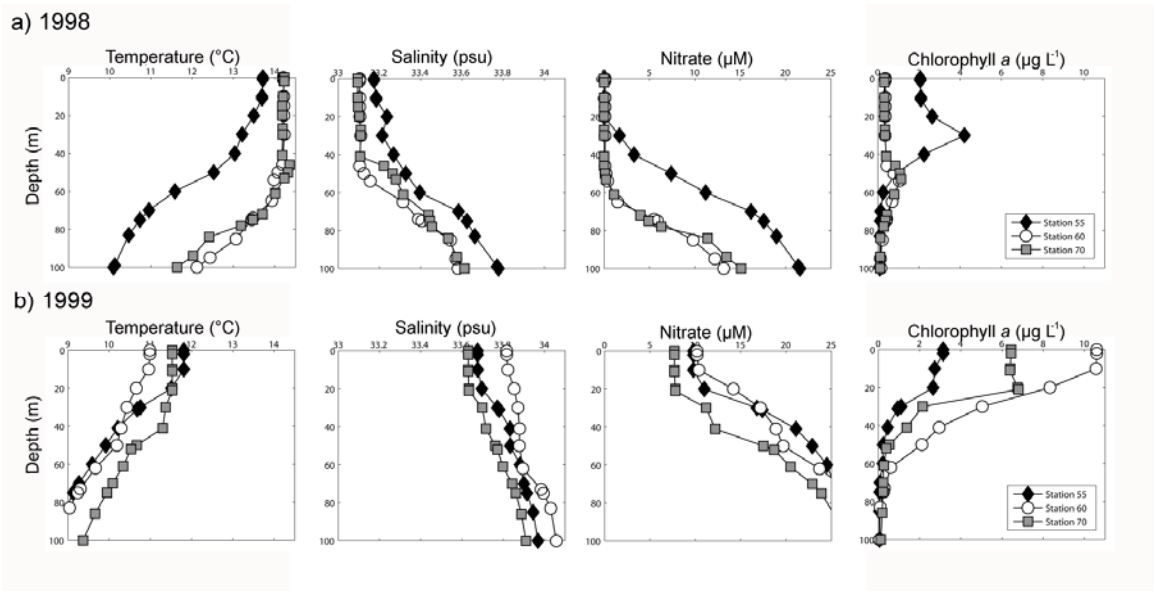

Figure 4.2. Profiles of Temperature (°C), Salinity (psu), Nitrate (µM), and Chl *a* (µg L^{-1}) with depth. Measurements were collected during a) April 15 1998 and, b) April 13 1999. Boxes on the right indicate the symbols for each of the three stations sampled each year.

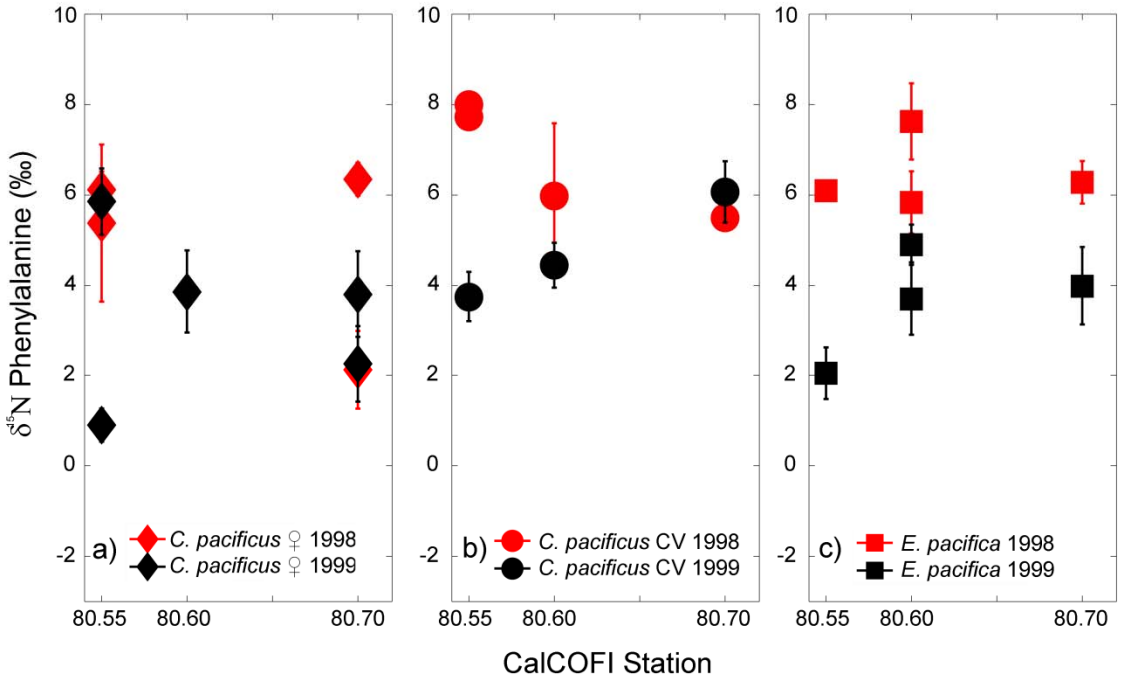

Figure 4.3. Phenylalanine $\delta^{15}N$ (‰) values (mean ± SD) for organisms collected at Stns 80.55, 80.60 and 80.70. a) *C. pacificus* females, b) *C. pacificus* CVs and c) *E. pacifica* juveniles. Red indicates estimates from 1998, in black are 1999 estimates.

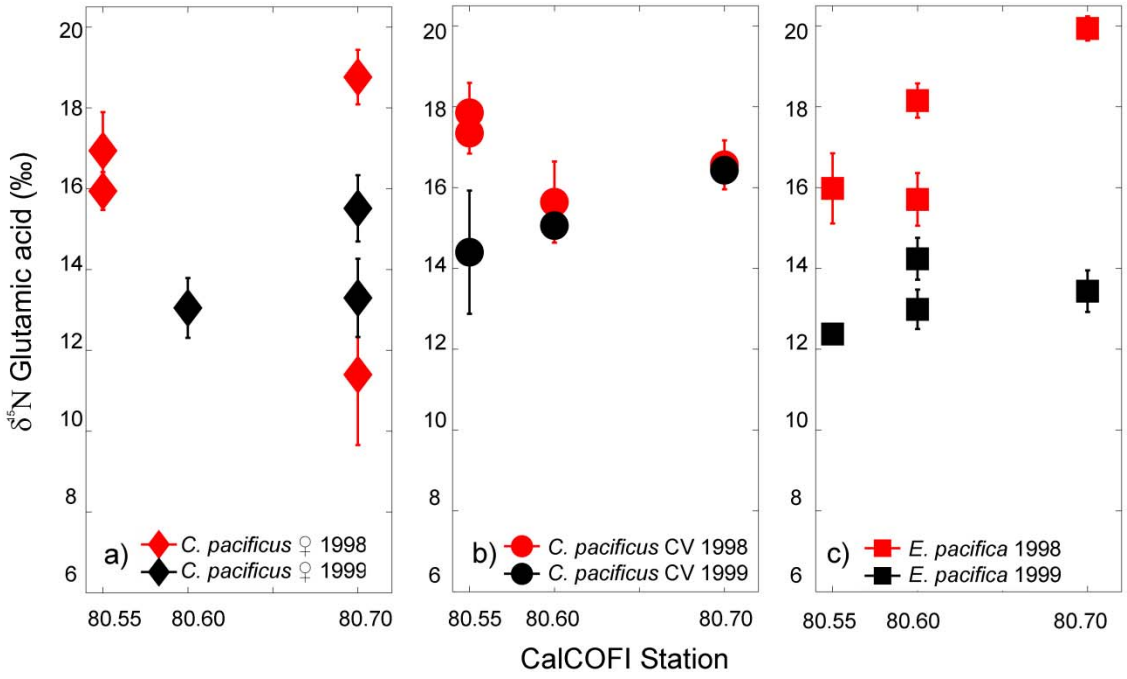

Figure 4.4. Glutamic acid $\delta^{15}N$ (‰) values (mean ± SD) for organisms collected at Stns. 80.55, 80.60 and 80.70. a) *C. pacificus* females, b) *C. pacificus* CVs and c) *E. pacifica* juveniles. Red indicates estimates from 1998, in black are 1999 estimates.

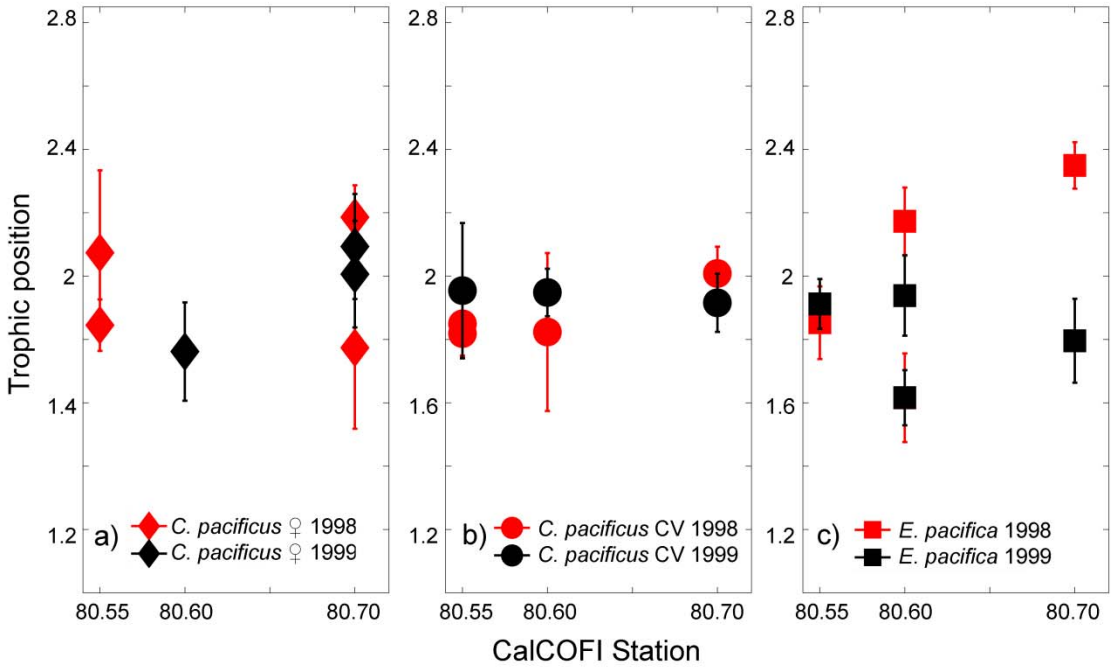

Figure 4.5. Trophic positions (mean ± SD) calculated after Chikaraishi et al. (2009). a) *C. pacificus* females, b) *C. pacificus* CVs and c) *E. pacifica* juveniles. Red indicates estimates are from 1998, in black are 1999 estimates.

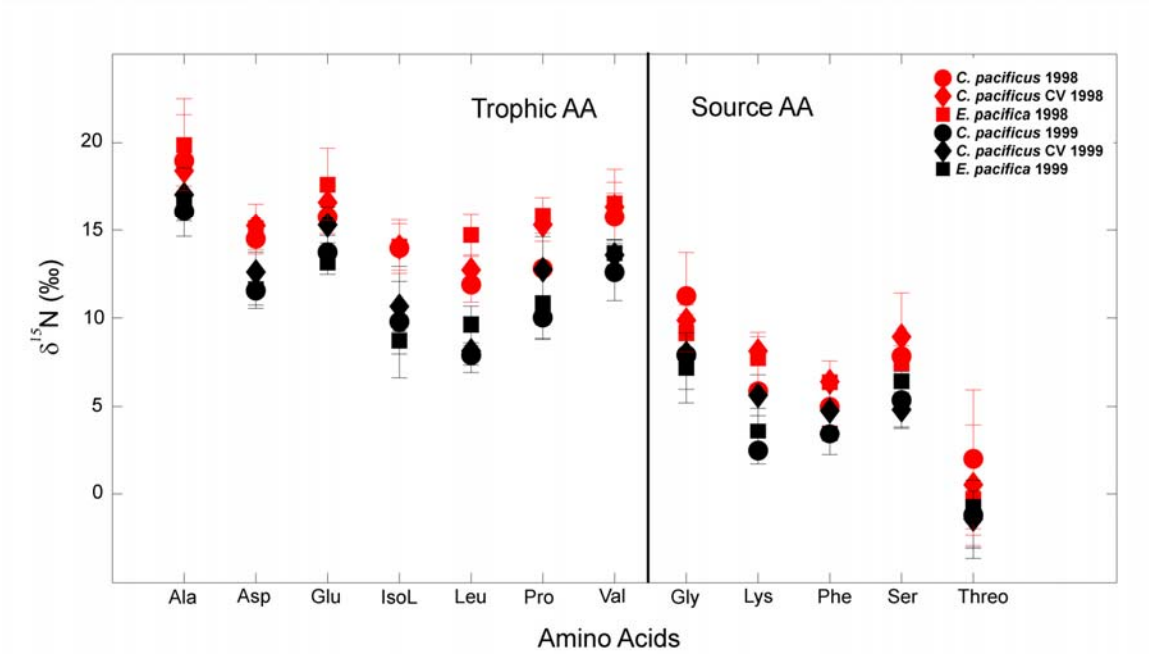

Figure 4.6. Average $\delta^{15}N$ of all AAs for each zooplankton group. Estimates in red are from 1998 and in black are from 1999. AAs are grouped into trophic and source amino acids. Note that Threonine is more depleted than other source AAs. Error bars are SD of all replicates.

References

Bender, D. A. 2008. Introduction to Metabolism, Fourth ed. CRC Press p 416.

Bograd, S. J., P. M. Digiacomo, R. Durazo, T. L. Hayward, K. D. Hyrenbach, R. J. Lynn, A. W. Mantyla, F. B. Schwing, W. J. Sydeman, T. Baumgartner, B. Lavaniegos, and C. S. Moore. 2000. The state of the California Current, 1999-2000: Forward to a new regime? Calif. Coop. Ocean. Fish. Invest. Rep. **41:** 26-52.

Brinton, E., and A. Townsend. 2003. Decadal variability in abundances of the dominant euphausiid species in southern sectors of the California Current. Deep-Sea Res. II **50:** 2449-2472.

Calbet, A., D. Atienza, C. I. Henriksen, E. Saiz, and T. R. Adey. 2009. Zooplankton grazing in the Atlantic Ocean: A latitudinal study. Deep-Sea Res. II **56:** 954-963.

Chikaraishi, Y., Y. Kashiyamal, N. O. Ogawa, H. Kitazato, and N. Ohkouchi. 2007. Metabolic control of nitrogen isotope composition of amino acids in macroalgae and gastropods: implications for aquatic food web studies. Mar. Ecol. Prog. Ser. **342:** 85-90.

Chikaraishi, Y., N. O. Ogawa, Y. Kashiyama, Y. Takano, H. Suga, A. Tomitani, H. Miyashita, H. Kitazato, and N. Ohkouchi. 2009. Determination of aquatic food-web structure based on compound-specific nitrogen isotopic composition of amino acids. Limnol. Oceanogr. Meth. **7:** 740-750.

Dale, J. J., N. J. Wallsgrove, B. N. Popp, and K. N. Holland. 2011. Nursery habitat use and foraging ecology of the brown stingray *Dasyatis lata* determined from stomach contents, bulk and amino acid stable isotopes. Mar. Ecol. Prog. Ser. **433:** 221-236.

Dam, H. G., X. S. Zhang, M. Butler, and M. R. Roman. 1995. Mesozooplankton grazing and metabolism at the equator in the central Pacific: Implications for carbon and nitrogen fluxes. Deep-Sea Res. II **42:** 735-756.

Fessenden, L., and T. J. Cowles. 1994. Copepod predation on phagotrophic ciliates in Oregon coastal waters. Mar. Ecol. Prog. Ser. **107:** 103-111.

Gordon, L. I., J. C. Jennings, A. A. Ross, and J. M. Krest. 1993. A Suggested Protocol for Continuous Flow Automated Analysis of Seawater Nutrients (Phosphate, Nitrate, Nitrite and Silicic Acid) in the WOCE Hydrographic Program and the Joint Global Ocean Fluxes Study, p. 1-52. *In* W. O. Manual [ed.], WHP Office Report. Oregon State University.

Hager, S. W., E. L. Atlas, L. I. Gordon, A. W. Mantyla, and P. K. Park. 1972. Comparison at Sea of Manual and Autoanalyzer Analyses of Phosphate, Nitrate, and Silicate. Limnol. Oceanogr. **17:** 931-937.

Hannides, C. C. S., B. N. Popp, M. R. Landry, and B. S. Graham. 2009. Quantification of zooplankton trophic position in the North Pacific Subtropical Gyre using stable nitrogen isotopes. Limnol. Oceanogr. **54:** 50-61.

Hayward, T. L. 2000. El Nino 1997-98 in the coastal waters of Southern California: A timeline of events. Calif. Coop. Ocean. Fish. Invest. Rep. **41:** 98-116.

Hayward, T. L., T. R. Baumgartner, D. M. Checkley, R. Durazo, G. Gaxiola-Castro, K. D. Hyrenbach, A. W. Mantyla, M. M. Mullin, T. Murphree, F. B. Schwing, P. E. Smith, and M. J. Tegner. 1999. The state of the California Current in 1998-1999: Transition to cool-water conditions. Calif. Coop. Ocean. Fish. Invest. Rep. **40:** 29-62.

Kahru, M., and B. G. Mitchell. 2002. Influence of the El Niño-La Niña cycle on satellite-derived primary production in the California Current. Geophysical Research Letters **29:** 4.

Kleppel, G. S. 1993. On the diets of calanoid copepods. Mar. Ecol. Prog. Ser. **99:** 183-195.

Landry, M. R. 1977. Review of Important Concepts in Trophic Organization of Pelagic Ecosystems. Helgolander Wissenschaftliche Meeresuntersuchungen **30:** 8-17.

Landry, M. R. 1981. Switching between herbivory and carnivory by the planktonic marine copepod *Calanus pacificus*. Mar. Biol. **65:** 77-82.

Lavaniegos, B. E., and M. D. Ohman. 2007. Coherence of long-term variations of zooplankton in two sectors of the California Current System. Prog. Oceanogr. **75:** 42-69.

Lorenzen, C. J. 1967. Determination of chlorophyll and pheo-pigments: Spectrophotometric equations. Limnol. Oceanogr. **12:** 343-346.

Lorrain, A., B. Graham, F. Menard, B. Popp, S. Bouillon, P. van Breugel, and Y. Cherel. 2009. Nitrogen and carbon isotope values of individual amino acids: a tool to study foraging ecology of penguins in the Southern Ocean. Mar. Ecol. Prog. Ser. **391:** 293-306.

Lynn, R. J., T. Baumgartner, J. Garcia, C. A. Collins, T. L. Hayward, K. D. Hyrenbach, A. W. Mantyla, T. Murphree, A. Shankle, F. B. Schwing, K. M. Sakuma, and M. J. Tegner. 1998. The state of the California current, 1997-1998: Transition to El Niño conditions. Calif. Coop. Ocean. Fish. Invest. Rep. **39:** 25-49.

Mackas, D. L., and G. Beaugrand. 2010. Comparisons of zooplankton time series. J. Mar. Syst. **79:** 286-304.

Macko, S. A., M. L. Fogel, P. E. Hare, and T. C. Hoering. 1987. Isotopic fractionation of nitrogen and carbon in the synthesis of amino acids by microorganisms. Chem. Geol. **65:** 79-92.

Macko, S. A., M. E. Uhle, M. H. Engel, and V. Andrusevich. 1997. Stable nitrogen isotope analysis of amino acid enantiomers by gas chromatography combustion/isotope ratio mass spectrometry. Anal. Chem. **69:** 926-929.

McClelland, J. W., and J. P. Montoya. 2002. Trophic relationships and the nitrogen isotopic composition of amino acids in plankton. Ecology **83:** 2173-2180.

Metges, C. C., K. J. Petzke, and U. Hennig. 1996. Gas chromatography combustion isotope ratio mass spectrometric comparison of N-acetyl- and N-pivaloyl amino acid esters to measure N-15 isotopic abundances in physiological samples: A pilot study on amino acid synthesis in the upper gastro-intestinal tract of minipigs. J. Mass Spectrom. **31:** 367-376.

Ohman, M. D., A. V. Drits, M. E. Clarke, and S. Plourde. 1998. Differential dormancy of co-occurring copepods. Deep-Sea Res. II **45:** 1709-1740.

Ohman, M. D., G. Rau, and P. Hull. in press. Multi-decadal variations in stable N isotopes of California Current zooplankton. Deep-Sea Res. I

Ohman, M. D., and E. Venrick. 2003. CalCOFI in a changing ocean. Oceanography **16:** 76-85.

Osgood, K. E., and D. M. Checkley. 1997a. Observations of a deep aggregation of *Calanus pacificus* in the Santa Barbara Basin. Limnol. Oceanogr. **42:** 997-1001.

Osgood, K. E., and D. M. Checkley. 1997b. Seasonal variations in a deep aggregation of *Calanus pacificus* in the Santa Barbara Basin. Mar. Ecol. Prog. Ser. **148:** 59-69.

Overland, J. E., J. Alheit, A. Bakun, J. W. Hurrell, D. L. Mackas, and A. J. Miller. 2010. Climate controls on marine ecosystems and fish populations. J. Mar. Syst. **79:** 305-315.

Pinheiro, J. C., and D. M. Bates. 2000. Mixed-effects models in S and S-PLUS Springer p.

Popp, B. N., B. S. Graham, R. J. Olson, C. C. S. Hannides, M. J. Lott, G. A. Lopez-Ibarra, F. Galvan-Magana, and B. Fry. 2007. Insight into the trophic ecology of yellowfin tuna, *Thunnus albacares*, from compound-specific nitrogen isotope analysis of proteinaceous amino acids, p. 173-190. *In* T. E. Dawson and R. T. W.

Siegwolf [eds.], Stable isotopes as indicators of ecological change. [Terrestrial Ecology Series.]. Elsevier Academic Press.

Rau, G. H., M. D. Ohman, and A. Pierrot-Bults. 2003. Linking nitrogen dynamics to climate variability off central California: a 51 year record based on $^{15}N/^{14}N$ in CalCOFI zooplankton. Deep-Sea Res. II **50:** 2431-2447.

Rebstock, G. A. 2002. Climatic regime shifts and decadal-scale variability in calanoid copepod populations off southern California. Glob. Change Biol. **8:** 71-89.

Robbins, C. T., L. A. Felicetti, and M. Sponheimer. 2005. The effect of dietary protein quality on nitrogen isotope discrimination in mammals and birds. Oecologia **144:** 534-540.

Schmidt, K., J. W. McClelland, E. Mente, J. P. Montoya, A. Atkinson, and M. Voss. 2004. Trophic-level interpretation based on $\delta^{15}N$ values: implications of tissue-specific fractionation and amino acid composition. Mar. Ecol. Prog. Ser. **266:** 43-58.

Schwing, F. B., T. L. Hayward, K. M. Sakuma, T. Murphree, A. S. Mascarenas, S. I. L. Castillo, A. W. Mantyla, S. L. Cummings, F. P. Chavez, K. Baltz, and D. G. Ainley. 1997. The state of the California Current, 1996-1997: Mixed signals from the tropics. Calif. Coop. Ocean. Fish. Invest. Rep. **38:** 22-47.

Sherwood, O. A., M. F. Lehmann, C. J. Schubert, D. B. Scott, and M. D. McCarthy. 2011. Nutrient regime shift in the western North Atlantic indicated by compound-specific $\delta^{15}N$ of deep-sea gorgonian corals. Proceedings of the National Academy of Sciences, United States of America **108:** 1011-1015.

Smith, S. L., B. H. Jones, L. P. Atkinson, and K. H. Brink. 1986. Zooplankton in the upwelling fronts off Pt. Conception, California. Elsevier Oceanography Series **42:** 195-213.

Styring, A. K., J. C. Sealy, and R. P. Evershed. 2010. Resolving the bulk $\delta^{15}N$ values of ancient human and animal bone collagen via compound-specific nitrogen isotope analysis of constituent amino acids. Geochim. Cosmochim. Acta **74:** 241-251.

Ueda, K., S. L. Morgan, A. Fox, J. Gilbart, A. Sonesson, L. Larsson, and G. Odham. 1989. D-Alanine as a Chemical Marker for the Determination of Streptococcal Cell Wall Levels in Mammalian Tissues by Gas Chromatography/Negative Ion Chemical Ionization Mass-Spectrometry. Anal. Chem. **61:** 265-270.

Venrick, E., and T. L. Hayward. 1984. Determining chlorophyll on the 1984 CalCOFI survey. Calif. Coop. Ocean. Fish. Invest. Rep. **XXV:** 74-79.

Ventura, M., and J. Catalan. 2005. Reproduction as one of the main causes of temporal variability in the elemental composition of zooplankton. Limnol. Oceanogr. **50:** 2043-2056.

Ventura, M., and J. Catalan. 2010. Variability in amino acid composition of alpine crustacean zooplankton and its relationship with nitrogen-15 fractionation. J. of Plankton Res. **32:** 1583-1597.

West, B. T., K. B. Welch, and A. T. Gałecki. 2007. Linear Mixed Models. A Practical Guide Using Statistical Software Chapman and Hall/CRC p 353.

CONCLUSIONS

Factors determining trophic structure

As part of my dissertation research, I used different methods to address the portion of the mesozooplankton diet that comes from non-pigmented organisms. Each of these methods has limitations. The experimental incubation approach (assessing diet from measured disappearance of prey) underestimates ciliate consumption (due to preservation methods) and maybe total carbon ingestion in general. The empirical regressions of metabolic rates versus body size from Ikeda (1985) have substantial scatter, and my inferences on trophic structure assume that mesozooplankton consume the entirety of microzooplankton production. In addition, these calculations do not tell me the amount of heterotrophic prey consumed, but rather how much they would have to consume in order to fulfill energetic requirements. Finally, stable isotopes might not adequately detect ^{15}N enrichments due to protozoan pathways. While all these caveats should be kept in mind, my results have generally given a consistent depiction of mesozooplankton trophic dynamics, adding robustness to the conclusions based on any single method.

So what determines trophic structure within an ecosystem? In Chapter 3 I found that in the offshore areas of the CCE, where PP was relatively low and less variable, the number of trophic steps separating the phyto- and mesozooplankton communities was higher than in the inshore region. This conclusion, based on *C. pacificus* feeding experiments and nutritional calculations for the entire community, is consistent with expectations for environments characterized by stable water columns and oligotrophic conditions. What about the highly productive, dynamic, inshore CCE region? The two

zooplankton species that I focused on are shown to be primarily herbivorous in this area, and had higher TPs when PP was lower. However, their feeding behaviors were fundamentally different. Contrary to my expectations (see Paffenhofer and Knowles 1980; Kleppel 1993; Fessenden and Cowles 1994), I found the feeding behavior of *C. pacificus* to be relatively predictable and independent of microplankton community composition within the range sampled in the field. *C. pacificus* consistently preferred larger particles and diatoms. *E. pacifica*, in contrast, generally consumed all size classes in proportion to their abundance, and had no clear pattern in type or size selectivity. That two dominant herbivores in the same region displayed different feeding responses to spatial variability of prey assemblages means that species/taxon composition must be taken into consideration in order to predict the response of the 'herbivorous' portion of the mesozooplankton community to varying conditions.

However, trophic structure is not only determined by taxonomic composition and selective responses to prey composition. It was in the region closest to shore (< 50 km from shore) where I encountered the highest variability in mesozooplankton biomass and PP. In addition, it was in this region where high mesozooplankton biomass led to negative net phytoplankton growth despite high nutrient conditions (Landry et al. 2009), and where *E. pacifica* shifted to a more omnivorous diet, presumably in response to decreased phytoplankton concentration. It follows that, in the nearshore CCE region, biological accumulation or aggregation processes can significantly alter trophic structure. The ability to predict such occurrences will nonetheless require better understanding of the mechanisms leading to high mesozooplankton concentrations.

In Chapter 2, I found that aggregation of large euphausiids was consistent with predator avoidance behavior and that patchiness of euphausiids was greater in conditions of higher production. The picture that emerges from the combined results of Chapter 2 and 3 is that in the productive inshore zone of the CCE region high mesozooplankton biomass can result in excess grazing pressure, depressing the phytoplankton community even during favorable growth conditions, and causing variability in trophic position. Mesozooplankton biomass and trophic structure are therefore determined by a delicate interplay of bottom up and top down controls.

Trophic structure in a changing ocean

The marine pelagic ecosystem is rapidly changing in response to climate change in multiple ways, with secular increases in stratification (Sarmiento et al. 2004), decadal changes in advection patterns (e.g. Feely et al. 2006), and various interannual and multi-decadal fluctuations superimposed (e.g. Aksnes and Ohman 2009; Schwing et al. 2010; Keister et al. 2011). How these changes will affect marine biological communities, and particularly mesozooplankton, is unclear.

In Chapter 1 I found higher mesozooplankton biomass in the equatorial Pacific with respect to the JGOFS EqPac studies conducted a decade previously, in 1992. I was cautious in hypothesizing that this could constitute a decadal shift in zooplankton biomass, similar to that observed in the Subtropical Pacific (Sheridan and Landry 2004), due to the lack of sampling between the two studies. However, model results from a coupled physical-biological model in the equatorial Pacific have also revealed small changes in PP but much larger changes in secondary production (up to a 50% increase)

between the periods of 1988-1998 and 1999-2007 (Wang et al. 2010), and support this hypothesis. The underlying mechanism could be a decadal trade wind strengthening (Feely et al. 2006) which could result in a higher proportion of larger primary producers. If PP magnitude alone was driving the pattern observed for zooplankton, production rates would have had approximately double, a pattern not observed between the temporally and spatially robust PP estimates during the two study periods (Barber et al. 1996; Balch et al. 2011). The nonlinearity of the disproportionate change of zooplankton relative to phytoplankton highlight the importance of mechanisms that channel more of the available production to mesozooplankton under the more recent ecological conditions.

In Chapter 4 I tested the prediction that the temporal perturbation of the 1998/1999 El Niño/La Niña event resulted in *C. pacificus* and *E. pacifica* shifting their trophic positions in response to decreased phytoplankton concentration. This expectation stemmed from ecological paradigms and previous copepod dietary studies (e.g. Landry 1981; Kleppel 1993; Fessenden and Cowles 1994; Bonnet et al. 2004). While both *E. pacifica* and *C. pacificus* exhibited spatial patterns of higher TPs with lower PPs in Chapter 3, their responses to temporal perturbations were different. The spatial patterns in feeding behavior from Chapter 3, where *C. pacificus* had relatively invariable prey preference and *E. pacifica* was a more generalist consumer, could explain why we detected that *E. pacifica* altered its trophic position, and failed to do so with *C. pacificus*. The spatial increase in trophic position shown in Chapter 3 for *C. pacificus* arose as a consequence of relatively higher heterotrophic concentrations, rather than a variable feeding behavior. CSIA-AA results suggested that *E. pacifica* shifted its trophic position during the more favorable nutrient conditions. The sensitivity of this method has yet to

be shown in the field, but given the observed replicate variability (see Fig. 4.5) we can speculate that a difference of at least 0.3 TP is necessary for detection. It is possible that the diet of *C. pacificus* changed in response to the prey field, but because of stronger dietary preferences, the shift was less pronounced as that exhibited by *E. pacifica*, and hence not detected by the CSIA-AA method.

The greater ability of *E. pacifica* to exploit more favorable conditions might stem from the demonstrated generalist feeding behavior of *E. pacifica* in Chapter 3. The diet of *E. pacifica* might simply reflects the relative proportions of what is currently available as food resources (as opposed to a selective behavior). That changes in trophic position during 1999 coincided with peaks in population abundance (Brinton and Townsend 2003) are consistent either with higher biomass yields resulting from feeding lower in the food chain or greater food availability in 1999.

Perhaps the largest surprise were my results for *C. pacificus*, an organism known to be omnivorous (e.g. Fessenden and Cowles 1994) and to display switching between feeding on phytoplankton and copepod nauplii depending on their relative proportions in laboratory settings (Landry 1981). It is possible that while the contribution of carbon from heterotrophic prey (protozoans and/or crustaceans) might at times exceed that of phytoplankton in relative terms, it is small compared to the total carbon contribution of phytoplankton prey, at least during the spring bloom when I conducted these studies. In addition, as discussed above, small shifts in TP are not detectable by CSIA-AA, and hence, if only ~20-30 % of the diet is heterotrophic in origin, we might not be able to detect it with this method. Still, these results are interesting given that both omnivorous copepods in general (Ohman and Runge, 1994) and *C. pacificus* in particular

(e.g. Landry 1981; Fessenden and Cowles, 1994) have been shown to exhibit exclusive heterotrophic diets when phytoplankton is in low supply.

The extent to which different mesozooplankton species display flexibility in TP in nature might be strongly related to where they fall on the behavioral spectrum from generalist to selective feeding. Trophic flexibility is, however, a characteristic of mesozooplankton communities as well as some individual species. The ecological and biogeochemical implications, as well as the time scales involved in these two processes are dramatically different, but both are suggested to strongly influence mesozooplankton biomass yield. Finally, this flexibility can be reflected in both space and time, and is likely to be a determining factor in how climate change affects mesozooplankton communities and the marine pelagic ecosystem.

References

Aksnes, D. L., and M. D. Ohman. 2009. Multi-decadal shoaling of the euphotic zone in the southern sector of the California Current System. Limnol. Oceanogr. **54:** 1272-1281.

Balch, W. M., A. J. Poulton, D. T. Drapeau, B. C. Bowler, L. A. Windecker, and E. S. Booth. 2011. Zonal and meridional patterns of phytoplankton biomass and carbon fixation in the Equatorial Pacific Ocean, between 110°W and 140°W. Deep-Sea Res. II **58:** 400-416.

Barber, R. T., M. P. Sanderson, S. T. Lindley, F. Chai, J. Newton, C. C. Trees, D. G. Foley, and F. P. Chavez. 1996. Primary productivity and its regulation in the equatorial Pacific during and following the 1991-1992 El Niño. Deep-Sea Res. II **43:** 933-969.

Bonnet, D., J. Titelman, and R. Harris. 2004. Calanus the cannibal. J. of Plankton Res. **26:** 937-948.

Brinton, E., and A. Townsend. 2003. Decadal variability in abundances of the dominant euphausiid species in southern sectors of the California Current. Deep-Sea Res. II **50:** 2449-2472.

Feely, R. A., T. Takahashi, R. H. Wanninkhof, M. J. McPhaden, C. E. Cosca, S. C. Sutherland, and M.-E. Carr. 2006. Decadal variability of the air-sea CO_2 fluxes in the equatorial Pacific Ocean. Journal of Geophysical Research, Oceans **111:** doi:10.1029/2005JC003129.

Fessenden, L., and T. J. Cowles. 1994. Copepod predation on phagotrophic ciliates in Oregon coastal waters. Mar. Ecol. Prog. Ser. **107:** 103-111.

Ikeda, T. 1985. Metabolic rates of epipelagic marine zooplankton as a function of body-mass and temperature. Mar. Biol. **85:** 1-11.

Keister, J. E., E. Di Lorenzo, C. A. Morgan, V. Combes, and W. T. Peterson. 2011. Zooplankton species composition is linked to ocean transport in the Northern California Current. Glob. Change Biol. **17:** 2498-2511.

Kleppel, G. S. 1993. On the diets of calanoid copepods. Mar. Ecol. Prog. Ser. **99:** 183-195.

Landry, M. R. 1981. Switching between herbivory and carnivory by the planktonic marine copepod *Calanus pacificus*. Mar. Biol. **65:** 77-82.

Landry, M. R., M. D. Ohman, R. Goericke, M. R. Stukel, and K. Tsyrklevich. 2009. Lagrangian studies of phytoplankton growth and grazing relationships in a coastal upwelling ecosystem off Southern California. Prog. Oceanogr. **83:** 208-216.

Ohman, M. D., and J. A. Runge. 1994. Sustained fecundity when phytoplankton resources are in short supply - omnivory by *Calanus finmarchicus* in the Gulf of St-Lawrence. Limnol. Oceanogr. **39:** 21-36.

Paffenhofer, G. A., and S. C. Knowles. 1980. Omnivorousness in marine planktonic copepods. J. of Plankton Res. **2:** 355-366.

Sarmiento, J. L., R. Slater, R. Barber, L. Bopp, S. C. Doney, A. C. Hirst, J. Kleypas, R. Matear, U. Mikolajewicz, P. Monfray, V. Soldatov, S. A. Spall, and R. Stouffer. 2004. Response of ocean ecosystems to climate warming. Glob. Biogeochem. Cycle **18:** 35.

Schwing, F. B., R. Mendelssohn, S. J. Bograd, J. E. Overland, M. Y. Wang, and S. Ito. 2010. Climate change, teleconnection patterns, and regional processes forcing marine populations in the Pacific. J. Mar. Syst. **79:** 245-257.

Sheridan, C. C., and M. R. Landry. 2004. A 9-year increasing trend in mesozooplankton biomass at the Hawaii Ocean Time-Series Station ALOHA. ICES J. Mar. Sci. **61:** 457-463.

Wang, X. J., R. Murtugudde, and R. Le Borgne. 2010. Climate driven decadal variations of biological production and plankton biomass in the equatorial Pacific Ocean: is this a regime shift? Biogeosciences Discuss. **7:** 2169-2193.